

Universality classes in nonequilibrium lattice systems

Géza Ódor*

*Research Institute for Technical Physics and Materials Science,
H-1525 Budapest, P.O.Box 49, Hungary*

In the first section I summarize the most important critical exponents, relations and the field theoretical formalism used in this work. In the second section I briefly address the question of scaling behavior at first order phase transitions. In section three I review dynamical extensions of basic static classes, show the effect of mixing dynamics and percolation behavior. The main body of this work is given in section four where genuine, dynamical universality classes specific to nonequilibrium systems are introduced. In section five I continue overviewing such nonequilibrium classes but in coupled, multi-component systems. Most of known transitions in low dimensional systems are between active and absorbing states of reaction-diffusion type systems, but I shall briefly introduce related classes that appear in interface growth models in section six. Some of them are related to critical behavior of coupled, multi-component systems. Finally in section seven I summarize families of absorbing state system classes, mean-field classes and give an outlook for further directions of research.

*Electronic address: odor@mfa.kfki.hu

Contents

I. Introduction	3
A. Critical exponents of equilibrium systems	4
B. Static percolation cluster exponents	5
C. Dynamical critical exponents	5
D. Critical exponents of spreading processes	6
1. Damage spreading exponents	6
E. Field theoretical approach to reaction-diffusion systems	7
II. Scaling at first order phase transitions	7
III. Out of equilibrium classes	8
A. Ising classes	9
1. Correlated percolation clusters at T_C	9
2. Dynamical Ising classes	9
3. Competing dynamics added to spin-flip	10
4. Competing dynamics added to spin-exchange	11
5. Long-range interactions and correlations	12
6. Damage spreading behavior	12
B. Potts classes	12
1. Correlated percolation at T_c	13
2. The vector Potts model	13
3. Dynamical Potts classes	13
4. Long-range interactions	14
C. XY model classes	14
1. Long-range correlations	14
2. Self-propelled particles	14
D. $O(N)$ symmetric model classes	15
1. Correlated percolation at T_c	15
IV. Genuine, basic nonequilibrium classes	16
A. Directed percolation classes	16
1. The Contact process	18

2. DP-class stochastic cellular automata	19
3. Branching and annihilating random walks with odd number of offspring	20
4. DP with spatial boundary conditions	20
5. DP with mixed (parabolic) boundary condition scaling	21
6. Lévy flight anomalous diffusion in DP	21
7. Long-range correlated initial conditions in DP	22
8. Quench disordered DP systems	23
B. Dynamical percolation (DyP) classes	24
1. Isotropic percolation universality classes	24
2. DyP with spatial boundary conditions	25
3. Lévy flight anomalous diffusion in DyP	25
C. Voter model (VM) classes	25
1. The $2A \rightarrow \emptyset$ (ARW) and the $2A \rightarrow A$ models	26
2. Compact DP (CDP) with spatial boundary conditions	26
3. CDP with parabolic boundary conditions	26
4. Lévy flight anomalous diffusion in ARW-s	27
D. Parity conserving (PC) classes	27
1. Grassberger's A and B model	27
2. Branching and annihilating random walks with even number of offspring	28
3. The NEKIM model	29
4. The generalized Domany-Kinzel model (GDK)	31
5. PC class surface catalytic models	32
6. NEKIM with long-range correlated initial conditions	33
7. GDK with spatial boundary conditions	33
E. Branching with $kA \rightarrow \emptyset$ annihilation	34
F. General $nA \rightarrow (n+k)A$, $mA \rightarrow (m-l)A$ processes	34
1. The $n = m$ symmetric case	35
2. The $n > m$ symmetric case	35
3. The $n < m$ case	35
V. Universality classes of multi-component systems	35
A. The $A + B \rightarrow \emptyset$ classes	35
B. $AA \rightarrow \emptyset$, $BB \rightarrow \emptyset$ with hard-core repulsion	36
C. Multi-species $A_i + A_j \rightarrow \emptyset$ classes	36
D. Unidirectionally coupled ARW classes	37
E. DP coupled to frozen field classes	37
1. The pair contact process model	38
2. The threshold transfer process (TTP)	39
F. DP with coupled diffusive field classes	39
1. The PCPD model	40
2. The annihilation-coagulation model	41
3. Cyclically coupled spreading with pair annihilation	42
4. The parity conserving AF model	42
G. BARWe with coupled non-diffusive field class	42
H. DP with diffusive conserved slave field classes	43
I. DP with frozen conserved slave field classes	43
J. Coupled N-component DP classes	44
K. Coupled N-component BARW2 classes	44
1. Generalized contact processes with $n > 2$ absorbing states in 1d	45
2. The NEKIMA model	45
L. Hard-core 2-BARW2 classes in 1d	46
1. Hard-core 2-BARWo models in 1d	46
2. Coupled binary spreading processes	47
VI. Interface growth classes	47
A. The random deposition class	49
B. Edwards-Wilkinson (EW) classes	49
C. Quenched EW classes	49

D. Kardar-Parisi-Zhang (KPZ) classes	49
1. Multiplicative noise systems	50
E. Quenched KPZ classes	50
F. Other continuum growth classes	50
G. Classes of mass adsorption-desorption, aggregation and chipping models	51
H. Unidirectionally coupled DP classes	52
1. Monomer adsorption-desorption at terraces models	53
2. Polynuclear growth models	53
I. Unidirectionally coupled PC classes	53
1. Dimer adsorption-desorption at terraces models	54
2. Parity conserving polynuclear growth	55
VII. Summary	56
Acknowledgements	57
Abbreviations	58
References	59

I. INTRODUCTION

Universal scaling behavior is an attractive feature in statistical physics because a wide range of models can be classified purely in terms of their collective behavior. Scaling phenomenon has been observed in many branches of physics, chemistry, biology, economy ... etc., most frequently by critical phase transitions. Nonequilibrium phase transitions may appear in models of population [1], epidemics [2, 3], catalysis [4], cooperative transport [5, 6], enzyme biology [7] and markets [8] for example.

Dynamical extensions of static universality classes — established in equilibrium — are the simplest nonequilibrium models systems, but beyond that critical phenomena, with a series of new classes have been explored so far [9, 10]. While the theory of phase transitions is quite well understood in thermodynamic equilibrium its research in nonequilibrium is rather new. In general phase transitions, scaling and universality retain most of the fundamental concepts of equilibrium models. The basic ingredients affecting universality classes are again the collective behavior of systems, the symmetries, the conservation laws and the spatial dimensions as described by renormalization group theory. Besides them several new factors have also been identified recently [11]. Low dimensional systems are of primary interest because the fluctuation effects are relevant, hence the mean-field type of description is not valid. In the past decades this field of research was growing very quickly and now we are faced with a zoo of models, universality classes, strange notations and abbreviations. This article aims to help newcomers as well as researchers to navigate in the literature by systematically reviewing most of the explored universality classes. I define models by their field theory (when it is available), show their symmetries or other important features and list the critical exponents and scaling relations.

Nonequilibrium systems can be classified into two cat-

egories: (a) Systems which do have a hermitian Hamiltonian and whose stationary states are given by the proper Gibbs-Boltzmann distribution. However, they are prepared in an initial condition which is far from the stationary state and sometimes, in the thermodynamic limit, the system may never reach the true equilibrium. These nonequilibrium systems include, for example, phase ordering systems, spin glasses, glasses etc. I begin the review of classes by showing the scaling behavior of the simplest prototypes of such systems in section III. These are defined by adding simple dynamics to static models. (b) Systems without a hermitian Hamiltonian defined by transition rates, which do not satisfy the detailed balance condition (the local time reversal symmetry is broken). They may or may not have a steady state and even if they have one, it is not a Gibbs state. Such models can be created by combining different dynamics or by generating currents in them externally. The critical phenomena of these systems are referred here as “Out of equilibrium classes” and discussed in section III. There are also systems, which are not related to equilibrium models, in the simplest case these are lattice Markov processes of interacting particle systems [2]. These are referred here as “Genuinely non-equilibrium systems” and are discussed in the rest of the work. The discussion of the latter type of systems is splitted to three parts: In section IV phase transition classes of simplest such models is presented. These are usually reaction-diffusion (RD) type of models exhibiting phase transition to absorbing states. In section V I list the known classes which occur by combinations of basic genuine class processes. These models are coupled multi-component RD systems. While the former two sections are related to critical phenomena near extinction in section VI I discuss universality classes in systems, where site variables are non-vanishing, in surface growth models. The bosonic field theoretical description is applicable for them as well. I point out mapping between growth and RD systems when it is possible.

In section II I briefly touch the point of discontinuous nonequilibrium phase transitions especially because dynamical scaling may occur at such points.

I define a critical universality class by the complete set of exponents at the phase transition. Therefore different dynamics split up the basic static classes of homogeneous systems. I emphasize the role of symmetries, boundary conditions which affect these classes. I also point out very recent evidence according to which in low dimensional systems symmetries are not necessarily the most relevant factors of universality classes. Although the systems covered here might prove to be artificial to experimentalists or to application oriented people they constitute the fundamental blocks of understanding of nonequilibrium critical phenomena. Note that the understanding of even so simple models runs into tremendous difficulties very often.

I shall not discuss the critical behavior of quantum systems [413], self-organized critical phenomena [396] and neither show experimental realizations. The discussion of the applied methods is also omitted due to the lack of space, although in section (IE) I give a brief introduction of the field theoretical approach. This section shows the formalism for defining nonequilibrium models. This is necessary to express the symmetry relations affecting critical behavior. Researchers from other branches of science are provided a kind of catalog of classes in which they can identify their models and find corresponding theories. To help navigating in the text and in the literature I provided a list of the most common abbreviations at the end of the text.

Besides scaling exponents and scaling relations there are many other interesting features of universality classes like scaling distribution, extremal statistics, finite size effects, statistics of fluctuations in surface growth models etc., which I do not discuss in this review. Still I believe the shown material provides a useful frame for orientation in this huge field. There is no general theory of nonequilibrium phase transitions, hence a widespread overview of known classes can help theorists deducing the relevant factors determining universality classes.

There are two recent, similar reviews available. One of them is by Marro and Dickman [9] (1999), which gives a pedagogical introduction to driven lattice gas systems and to fundamental particle systems with absorbing states. The other one is by Hinrichsen [11] (2000), which focuses more on basic absorbing state phase transitions, methods and experimental realizations. However the field evolves rapidly and since the publication of this two remarkable introductory works a series of new developments have come up. The present work aims to give a comprehensive overview of known nonequilibrium dynamical classes, incorporating surface growth classes, classes of spin models, percolation and multi-component system classes, their relations and mappings to each other. The effects of boundary conditions, long-range interactions and disorder are shown systematically for each class where it is known. Since a debate on the conditions

of the parity conserving class has not been settled yet I provide a discussion on it through some surface catalytic model examples. Naturally this review can not be complete and I apologize for the omitted references.

A. Critical exponents of equilibrium systems

In this section I briefly summarize the definition of well known critical exponents of homogeneous equilibrium systems and show some scaling relations [12, 13, 14, 15, 16]. The basic exponents are defined via the scaling laws:

$$c_H \propto \alpha_H^{-1} \left((|T - T_c|/T_c)^{-\alpha_H} - 1 \right), \quad (1)$$

$$m \propto (T_c - T)^\beta, \quad (2)$$

$$\chi \propto |T - T_c|^{-\gamma}, \quad (3)$$

$$m \propto H^{1/\delta_H}, \quad (4)$$

$$G_c^{(2)}(r) \propto r^{2-d-\eta_a}, \quad (5)$$

$$\xi \propto |T - T_c|^{-\nu_\perp}. \quad (6)$$

Here c_H denotes the specific heat, m the order parameter, χ the susceptibility and ξ the correlation length. The presence of another degree of freedom besides the temperature T , like a (small) external field (labeled by H), leads to other interesting power laws when $H \rightarrow 0$. The d present in the expression of two-point correlation function $G_c^{(2)}(r)$ is the space dimension of the system.

Some laws are valid both to the right and to the left of the critical point; the values of the relative proportionality constants, or *amplitudes*, are in general different for the two branches of the functions, whereas the exponent is the same. However there are universal amplitude relations among them. We can see that there are altogether six basic exponents. Nevertheless they are not independent of each other, but related by some simple scaling relations:

$$\begin{aligned} \alpha_H + 2\beta + \gamma &= 2, \quad \alpha_H + \beta(\delta_H + 1) = 2, \\ (2 - \eta_a)\nu_\perp &= \gamma, \quad \nu_\perp d = 2 - \alpha_H. \end{aligned} \quad (7)$$

The last relation is a so-called hyper-scaling law, which depends on the spatial dimension d and is not valid above the upper critical dimension d_c , for example by the Gaussian theory. Therefore below d_c there are only two independent exponents in equilibrium. One of the most interesting aspects of second order phase transitions is the so-called **universality**, i.e., the fact that systems which can be very different from each other share the same set of critical indices (exponents and some amplitude ratios). One can therefore hope to assign all systems to **classes** each of them being identified by a set of critical indices.

B. Static percolation cluster exponents

Percolation [17, 18] is a geometrical phenomenon that describes the occurrence of infinitely large connected clusters in lattice models. The definition of connected clusters is not unambiguous. It may mean the set of sites or bonds with variables in the same state, or connected by bonds with probability $b = 1 - \exp(-2J/kT)$.

By changing the system control parameters ($p \rightarrow p_p$) (that usually is the temperature in equilibrium systems) the coherence length between sites may diverge as

$$\xi(p) \propto |p - p_p|^{-\nu_\perp}, \quad (8)$$

hence percolation at p_p like standard critical phenomena exhibits renormalizability and universality of critical exponents. At p_p the cluster size (s) distribution follows the scaling law:

$$n_s \propto s^{-\tau} f(|p - p_p|s^\sigma). \quad (9)$$

while moments of this distribution exhibit singular behavior the exponents:

$$\sum_s s n_s(p) \propto |p - p_p|^{\beta_p}, \quad (10)$$

$$\sum_s s^2 n_s(p) \propto |p - p_p|^{-\gamma_p}. \quad (11)$$

Further critical exponents and scaling relations among them are shown in [17]. In case of completely random placement of (sites, bonds, etc) variables (with probability p) on lattices we find **random isotropic (ordinary) percolation** (see Sect. IV B 1). Percolating clusters may arise at critical, thermal transitions or by nonequilibrium processes. If the critical point (p_c) of the order parameter does not coincide with p_p than at the percolation transition the order parameter coherence length is finite and does not influence the percolation properties. We observe random percolation in that case. In contrast if $p_p = p_c$ percolation is influenced by the order parameter behavior and we find different, **correlated percolation** universality [17, 19, 20] whose exponents may coincide with those of the order parameter.

According to the Fortuin-Kasteleyn construction of clusters [19] two nearest-neighbor spins of the same state belong to the same cluster with probability $b = 1 - \exp(-2J/kT)$. It was shown that using this prescription for Z_n and $O(n)$ and symmetric models [20, 21, 22, 23] the **thermal phase transition** point coincides with the percolation limits of such clusters. On the other hand in case of “pure-site clusters” ($b = 1$) different, universal cluster exponents are reported in two dimensional models [22] (see Sects. III A 1, III B 1, III D 1).

C. Dynamical critical exponents

Nonequilibrium systems were first introduced to study relaxation to equilibrium states [24] and phase ordering

kinetics [25, 26]. Power-law time dependences were investigated away from the critical point as well, example by the domain growth in a quench to $T = 0$. Later the combination of different heat-baths, different dynamics, external currents became popular investigation tools of fully nonequilibrium models. To describe the dynamical behavior of a critical system additional exponents were introduced. For example the relation of the divergences of the relaxation time τ and correlation length ξ is described by the dynamical exponent Z

$$\tau \propto \xi^Z. \quad (12)$$

Systems out of equilibrium may show anisotropic scaling of two (and n) point functions

$$G(\mathbf{r}, b^\zeta t) = b^{-2x} G(\mathbf{r}, t) \quad (13)$$

where \mathbf{r} and t denote spatial and temporal coordinates, x is the scaling dimension and ζ is the anisotropy exponent. As a consequence the temporal (ν_\parallel) and spatial (ν_\perp) correlation length exponents may be different, described by $\zeta = Z$.

$$Z = \zeta = \frac{\nu_\parallel}{\nu_\perp}. \quad (14)$$

For some years it was believed that dynamical critical phenomena are characterized by a set of three critical exponents, comprising two independent static exponents (other static exponents being related to these by scaling laws) and the dynamical exponent Z . Recently, it was discovered that there is another dynamical exponent, the ‘non-equilibrium’ or **short-time exponent** λ , needed to describe two-time correlations in a spin system ($\{s_i\}$) of size L relaxing to the critical state from a disordered initial condition [56, 57].

$$A(t, 0) = \frac{1}{L^d} < \sum_i s_i(0) s_i(t) > \propto t^{-\lambda/Z} \quad (15)$$

More recently the **persistence exponents** θ_l and θ_g were introduced by [27, 28]. These are associated with the probability, $p(t)$, that the local or global order parameter has not changed sign in time t following a quench to the critical point. In many systems of physical interest these exponents decay algebraically as

$$p(t) \propto t^{-\theta} \quad (16)$$

(see however example Sect. V A). It turned out that in systems where the scaling relation

$$\theta_g Z = \lambda - d + 1 - \eta_a/2 \quad (17)$$

is satisfied the dynamics of the global order parameter is a Markov process. In contrast in systems with non-Markovian global order parameter θ_g is in general a new, non-trivial critical exponent [28]. For example it was shown that while in the $d = 1$ Glauber Ising model the magnetization is Markovian and the scaling relation (17)

is fulfilled, at the critical point of the $d = 1$ NEKIM Ising model this is not satisfied and the persistence behavior there is characterized by a different, non-trivial θ_g exponent [29] (see discussion in section IV D 3). As we can see the *universality classes of static models are split by the dynamical exponents*.

D. Critical exponents of spreading processes

Here I define a basic set of critical exponents that occur in spreading processes and show the scaling relations among them. In such processes phase transition may exist to **absorbing state(s)** where the density of spreading entity (particle, agent, epidemic etc.) disappears. The order parameter is usually the density of active sites $\{s_i\}$

$$\rho(t) = \frac{1}{L^d} \langle \sum_i s_i(t) \rangle, \quad (18)$$

which in the supercritical phase vanishes as

$$\rho^\infty \propto |p - p_c|^\beta, \quad (19)$$

as the control parameter p is varied. The “dual” quantity is the ultimate survival probability P_∞ of an infinite cluster of active sites that scales in the active phase as

$$P_\infty \propto |p - p_c|^{\beta'} \quad (20)$$

with some critical exponent β' [285]. In field theoretical description of such processes β is associated with the particle annihilation, β' with the particle creation operator and in case of time reversal symmetry (see Eq. (89)) they are equal. The critical long-time behavior of these quantities are described by

$$\rho(t) \propto t^{-\alpha} f(\Delta t^{1/\nu_{||}}), \quad P(t) \propto t^{-\delta} g(\Delta t^{1/\nu_{||}}), \quad (21)$$

where α and δ are the critical exponents for decay and survival, $\Delta = |p - p_c|$, f and g are *universal scaling functions* [39, 40, 285]. The obvious scaling relations among them are

$$\alpha = \beta/\nu_{||}, \quad \delta = \beta'/\nu_{||}. \quad (22)$$

For finite systems (of size $N = L^d$) these quantities scale as

$$\rho(t) \propto t^{-\beta/\nu_{||}} f'(\Delta t^{1/\nu_{||}}, t^{d/Z}/N), \quad (23)$$

$$P(t) \propto t^{-\beta'/\nu_{||}} g'(\Delta t^{1/\nu_{||}}, t^{d/Z}/N). \quad (24)$$

For “relatively short times” or for initial conditions with a single active seed the the number of active sites $N(t)$ and its mean square of spreading distance $\langle x_i^2(t) \rangle$ from the origin

$$R^2(t) = \frac{1}{N(t)} \langle \sum_i x_i^2(t) \rangle \quad (25)$$

follow the “initial slip” scaling laws [285]

$$N(t) \propto t^\eta, \quad (26)$$

$$R^2(t) \propto t^z, \quad (27)$$

and usually the $z = 2/Z$ relation holds.

1. Damage spreading exponents

While damage spreading (DS) was first introduced in biology [58] it has become an interesting topic in physics as well [59, 60, 61]. The main question is if a damage introduced in a dynamical system survives or disappears. To investigate this the usual technique is to make replica(s) of the original system and let them evolve with the same dynamics and external noise. This method has been found to be very useful to measure accurately dynamical exponents of equilibrium systems [30]. It has turned out however, that DS properties do depend on the applied dynamics. An example is the case of the two-dimensional Ising model with heat-bath algorithm versus Glauber dynamics [31, 32, 33].

To avoid dependency on the dynamics Hinrichsen et al.[34] suggested a definition of “physical” family of DS dynamics according to the active phase may be divided to a sub-phase in which DS occurs for every member of the family, another sub-phase where the damage heals for every member of the family and a third possible sub-phase, where DS is possible for some members and the damage disappears for other members. The family of possible DS dynamics is defined to be consistent with the physics of the single replicas (symmetries, interaction ranges etc.).

Usually the order parameter of the damage is the Hamming distance between replicas

$$D(t) = \left\langle \frac{1}{L} \sum_{i=1}^L |s(i) - s'(i)| \right\rangle \quad (28)$$

where $s(i)$ and $s'(i)$ denote variables of the replicas. At continuous DS transitions D exhibits power-law singularities as physical quantities at the critical point. For example one can follow the fate of a single difference between two (or more) replicas and measure the spreading exponents:

$$D(t) \propto t^{\eta_d}, \quad (29)$$

Similarly the survival probability of damage variables behaves as:

$$P_D(t) \propto t^{-\delta_d} \quad (30)$$

and similarly to eq.(25) the average mean square spreading distance of damage variables from the center scales as:

$$R_D^2(t) \propto t^{z_d}. \quad (31)$$

Grassberger conjectured, that DS transitions should belong to DP class (see Sect.IV A) unless they coincide with other transition points and provided the probability for a locally damaged state to become healed is not zero [35]. This hypothesis has been confirmed by simulations of many different systems.

E. Field theoretical approach to reaction-diffusion systems

In this review I define nonequilibrium systems formally by their field theoretical action where it is possible. Therefore in this subsection I give a brief introduction to (bosonic) field theoretical formalism. This will be through the simplest example of reaction-diffusion systems, via the: $A + A \rightarrow \emptyset$ annihilating random walk (ARW) (see Sect.IV C 1). Similar stochastic differential equation formalism can also be set up for growth processes in most cases. For a more complete introduction see [36, 37, 38].

A proper field theoretical treatment should start from the master equation for the microscopic time evolution of probabilities $p(\alpha; t)$ of states α

$$\frac{dp(\alpha; t)}{dt} = \sum_{\beta} R_{\beta \rightarrow \alpha} p(\beta; t) - \sum_{\beta} R_{\alpha \rightarrow \beta} p(\alpha; t), \quad (32)$$

where $R_{\alpha \rightarrow \beta}$ denotes the transition matrix from state α to β . In field theory this can be expressed in Fock space formalism with annihilation (a_i) and creation (c_i) operators satisfying the commutation relation

$$[a_i, c_j] = \delta_{ij}. \quad (33)$$

The states are built up from the vacuum $|0\rangle$ as the linear superposition

$$\Psi(t) = \sum_{\alpha} p(n_1, n_2, \dots; t) c_1^{n_1} c_2^{n_2} \dots |0\rangle, \quad (34)$$

with occupation number coefficients $p(n_1, n_2, \dots; t)$. The evolution of states can be described by a Schrödinger-like equation

$$\frac{d\Psi(t)}{dt} = -H\Psi(t) \quad (35)$$

with a generally non-hermitian Hamiltonian, which in case of the ARW process looks like

$$H = D \sum_{ij} (c_i - c_j)(a_i - a_j) - \lambda \sum_j (a_j^2 - c_j^2 a_j^2), \quad (36)$$

here D denotes the diffusion strength and λ the annihilation rate. By going to the continuum limit this turns into

$$H = \int d^d x [D(\nabla\psi)(\nabla\phi) - \lambda(\phi^2 - \psi^2\phi^2)], \quad (37)$$

and in the path integral formalism over fields $\phi(x, t)$, $\psi(x, t)$ with weight $e^{-S(\phi, \psi)}$ one can define an action, that in case of ARW is

$$S = \int dt d^d x [\psi \partial_t \phi + D \nabla \psi \nabla \phi - \lambda(\phi^2 - \psi^2 \phi^2)]. \quad (38)$$

The action is analyzed by renormalization group (RG) methods at criticality [15, 16], usually by perturbative epsilon expansion below the upper critical dimension d_c — that is the lower limit of the validity of the mean-field (MF) behavior of the system. The symmetries of the model can be expressed in terms of the $\phi(x, t)$ field and $\psi(x, t)$ response field variables and the corresponding hyper-scaling relations can be derived [39, 40].

By a Gaussian transformation one may set up an alternative formalism — integrating out the response field — the Langevin equation, that in case of ARW is

$$\partial_t \phi = D \nabla^2 \phi - 2\lambda \phi^2 + \eta(x, t) \quad (39)$$

with a Gaussian noise, exhibiting correlations

$$\langle \eta(x, t) \eta(x', t') \rangle = -\lambda \phi^2 \delta(x - x') \delta(t - t'). \quad (40)$$

Here δ denotes the Dirac delta functional and λ is the noise amplitude. From the Langevin equation — if it exists — one can deduce a naive upper critical dimension (d_c) by power counting. However this estimate may be modified by fluctuations, which can be analyzed by the application of the RG method.

II. SCALING AT FIRST ORDER PHASE TRANSITIONS

In nonequilibrium systems dynamical scaling of variables may occur even when the order parameter jumps at the transition. We call such a transition first order, although the free energy is not defined. First order phase transitions have rarely been seen in low dimensions. This is due to the fact that in lower dimension the fluctuations are more relevant and may destabilize the ordered phase. Therefore fluctuation induced second ordered phase transitions are likely to appear. Hinrichsen advanced the hypothesis [41] that first-order transitions do not exist in 1+1 dimensional systems without extra symmetries, conservation laws, special boundary conditions or long-range interactions (which can be generated by macroscopic currents or anomalous diffusion in nonequilibrium systems for instance). Examples are the Glauber and the NEKIM Ising spin systems (see sections III A, IV D 3) possessing Z_2 symmetry in one dimension [42, 43], where the introduction of a “temperature like” flip inside of a domain or an external field (h) causes discontinuous jump in the magnetization order parameter (m). Interestingly enough the correlation length diverges at the transition point: $\xi \propto p_T^{-\nu_\perp}$ and static

$$m \propto \xi^{-\beta_s/\nu_\perp} g(h\xi^{\Delta/\nu_\perp}) \quad (41)$$

as well as cluster critical exponents can be defined:

$$P_s(t, h) \propto t^{-\delta_s} \quad (42)$$

$$R_s^2(t, h) \propto t^{z_s} \quad (43)$$

$$|m(t, h) - m(0)| \propto t^{\eta_s} \quad (44)$$

$$\lim_{t \rightarrow \infty} P_s(t, h) \propto h^{\beta_s} \quad (45)$$

Here s refers to the spin variables. The table II summarizes the results obtained for these transitions. Other examples for first order transition are known in

	β_s	ν_\perp	β_s'	Δ	η_s	δ_s	z_s
Glauber	0	1/2	.99(2)	1/2	.0006(4)	.500(5)	1
NEKIM	.00(2)	.444	.45(1)	.49(1)	.288(4)	.287(3)	1.14

TABLE I: Critical 1d Ising spin exponents at the Glauber and NEKIM transition points [43]

driven diffusive systems [44], in the 1d asymmetric exclusion process [45], in bosonic annihilation-fission models (Sect.VF), in asymmetric triplet and quadruplet models [354] (Sect.IV F) and DCF models for $D_A > D_B$ and $d > 1$ [265] (Sect.VH). By simulations it is quite difficult to decide whether a transition is really discontinuous. The order parameter of weak first order transitions – where the jump is small – may look very similar to continuous transitions. The hysteresis of the order parameter that is considered to be the indication of a first order transition is a demanding task to measure. There are some examples with debates over the order of the transition (see for example [41, 46, 47, 48, 49, 50]). In some cases the mean-field solution results in first order transition [51, 52]. In two dimensions there are certain stochastic cellular automata for which systematic cluster mean-field techniques combined with simulations made it possible to prove first order transitions [53] firmly (see table II).

n	$y = 1$	$y = 2$		$y = 3$	
	p_c	p_c	$\rho(p_c)$	p_c	$\rho(p_c)$
1	0.111	0.354	0.216	0.534	0.372
2	0.113	0.326	0.240	0.455	0.400
4	0.131	0.388	0.244	0.647	0.410
simulation	0.163	0.404	0.245	0.661	0.418

TABLE II: Convergence of the critical point estimates in various ($y = 1, 2, 3$) two dimensional SCA calculated by n-cluster (GMF) approximation (see section IV A 2). First order transitions are denoted by boldface numbers. The gap sizes ($\rho(p_c)$) of the order parameter shown for $y = 2, 3$ increase with n , approximating the simulation value [53].

III. OUT OF EQUILIBRIUM CLASSES

In this section I begin introducing basic nonequilibrium classes starting with the simplest dynamical extensions of equilibrium models. These dynamical systems exhibit hermitian Hamiltonian and starting from a nonequilibrium state they evolve into a Gibbs state. Such nonequilibrium models include, for example, phase ordering systems, spin glasses, glasses etc. In these cases one is usually interested in the ‘nonequilibrium dynamics’ at the equilibrium critical point. It is an important and new universal phenomenon that scaling behavior can be observed far away from criticality as well. In quenches to zero temperature of **model A** systems (which do not conserve the order parameter) the characteristic length in the late time regime grows with an universal power-law $\xi \propto t^{1/2}$, while in case of **model B** systems (which conserve the order parameter) $\xi \propto t^{1/3}$. Since percolation is a central topic of section IV I point out recently discovered connection of critical systems with percolation phenomena. Another novel feature of dynamic phase transitions is the emergence of a chaotic state, therefore I shall discuss damage spreading transitions and behavior in these systems.

Then I continue towards such nonequilibrium models which have no hermitian Hamiltonian and equilibrium Gibbs state. In this section I show cases when this is achieved by combining different competing dynamics (for example by connecting two reservoirs with different temperatures to the system) or by generating current from outside. Field theoretical investigations have revealed that **model A** systems are **robust** against the introduction of various competing dynamics, which are *local* and *do not conserve the order parameter* [82]. Furthermore it was shown, that this robustness of the critical behavior persists if the competing dynamics breaks the discrete symmetry of the system [83] or it comes from reversible mode coupling to a non-critical conserved field [84]. On the other hand if a competing dynamics is coupled to **model B** systems by an external drive [85] or by local, anisotropic order-parameter conserving process [86, 87, 88] long-range interactions are generated in the steady state with angular dependence. The universality class will be the same as that of the kinetic version of the equilibrium Ising model with **dipolar long-range interactions**.

As the number of neighboring interaction sites decreases by lowering the spatial dimensionality of a system with short-ranged interactions the relevance of fluctuations increases. In equilibrium models finite-range interactions cannot maintain long-range order in $d < 2$. This observation is known as the Landau-Peierls argument [54]. According to the Mermin-Wagner theorem [55], for systems with continuous symmetry long-range order do not exist even in $d = 2$. Hence in equilibrium models phase transition universality classes exist for $d \geq 2$ only. One of the main open questions to be answered is whether there exist a class of nonequilibrium

systems with restricted dynamical rules for which the Landau-Peierls or Mermin-Wagner theorem can be applied.

A. Ising classes

The equilibrium Ising model was introduced by [67] as the simplest model for an uniaxial magnet but it is used in different settings for example binary fluids or alloys as well. It is defined in terms of spin variables $s_i = \pm 1$ attached to sites i of some lattice with the Hamiltonian

$$H = -J \sum_{i,i'} s_i s_{i'} - B \sum_i s_i \quad (46)$$

where J is the coupling constant and B is the external field. In one and two dimensions it is solved exactly [68], hence it plays a fundamental test-ground for understanding phase transitions. The Hamiltonian of this model exhibits a global, so called Z_2 (up-down) symmetry of the state variables. While in one dimension a first order phase transition occurs at $T = 0$ only (see section II) in two dimensions there is a continuous phase transition where the system exhibits conformal symmetry [69] as well. The critical dimension is $d_c = 4$. The following table (III) summarizes some of the known critical exponents of the Ising model. The quantum version of the

exponent	$d = 2$	$d = 3$	$d = 4(\text{MF})$
α_H	$0(\log)$	0.1097(6)	0
β	$1/8$	0.3265(7)	$1/2$
γ	$7/4$	1.3272(3)	1
ν_\perp	1	0.6301(2)	$1/2$

TABLE III: Static critical exponents of the Ising model

Ising model, which in the simplest cases might take the form (in 1d)

$$H = -J \sum_i (t \sigma_i^x + \sigma_i^z \sigma_{i+1}^z + h \sigma_i^z), \quad (47)$$

– where $\sigma^{x,z}$ are Pauli matrices and t and h are couplings – for $T > 0$ has been shown to exhibit the same critical behavior as the classical one (in the same dimension). For $T = 0$ however quantum effects become important and the quantum Ising chain can be associated with the two dimensional classical Ising model such that the transverse field t plays the role of the temperature. In general a mapping can be constructed between classical $d + 1$ dimensional statistical systems and d dimensional quantum systems without changing the universal properties, which has been widely utilized [70, 71]. The effects of disorder and boundary conditions are not discussed here (for recent reviews see [72, 315]).

1. Correlated percolation clusters at T_c

If we generate clusters in such a way that we join nearest neighbor spins of the same sign we can observe percolation at T_c in 2d. While the order parameter percolation exponents β_p and γ_p of this percolation (defined in section IV B 1) were found to be different from the exponents of the magnetization (β, γ) the correlation length exponent is the same: $\nu = \nu_p$. For 2d models with Z_2 symmetry the universal percolation exponents are [22]:

$$\beta_p = 0.049(4), \quad \gamma_p = 1.908(16). \quad (48)$$

These exponents are clearly different from those of the ordinary percolation classes (Table XV) or from Ising class magnetic exponents.

On the other hand by Fortuin-Kasteleyn cluster construction [19] the percolation exponents of the Ising model at T_c coincide with those of the magnetization of the model.

2. Dynamical Ising classes

Kinetic Ising models such as the spin-flip Glauber Ising model [42] and the spin-exchange Kawasaki Ising model [73] were originally intended to study relaxational processes near equilibrium states. In order to assure the arrival to an equilibrium state the detailed balance condition for transition rates ($w_{i \rightarrow j}$) and probability distributions ($P(s)$) are required to satisfy

$$w_{i \rightarrow j} P(s(i)) = w_{j \rightarrow i} P(s(j)) \quad (49)$$

Knowing that $P_{eq}(s) \propto \exp(-H(s)/(k_B T))$ this entails the

$$\frac{w_{i \rightarrow j}}{w_{j \rightarrow i}} = \exp(-\Delta H(s)/(k_B T)) \quad (50)$$

condition which can be satisfied in many different ways. Assuming **spin-flips** (which do not conserve the magnetization (**model A**)) Glauber formulated the most general form in a magnetic field (h)

$$w_i^h = w_i (1 - \tanh h s_i) \approx w_i (1 - h s_i) \quad (51)$$

$$w_i = \frac{\Gamma}{2} (1 + \tilde{\delta} s_{i-1} s_{i+1}) \left(1 - \frac{\gamma}{2} s_i (s_{i-1} + s_{i+1}) \right) \quad (52)$$

where $\gamma = \tanh 2J/kT$, Γ and $\tilde{\delta}$ are further parameters. The $d = 1$ Ising model with Glauber kinetics is exactly solvable. In this case the critical temperature is at $T = 0$ and the transition is of first order. We recall that $p_T = e^{-\frac{4J}{kT}}$ plays the role of $\frac{T - T_c}{T_c}$ in 1d and in the vicinity of $T = 0$ critical exponents can be defined as powers of p_T , thus e.g. that of the coherence length, ν_\perp , via $\xi \propto p_T^{-\nu_\perp}$ (see Section II). In the presence of a magnetic field B , the magnetization is known exactly. At $T = 0$

$$m(T = 0, B) = \text{sgn}(B). \quad (53)$$

Moreover, for $\xi \gg 1$ and $B/kT \ll 1$ the exact solution reduces to

$$m \sim 2h\xi; \quad h = B/k_B T. \quad (54)$$

In scaling form one writes:

$$m \sim \xi^{-\frac{\beta_s}{\nu_\perp}} g(h\xi^{\frac{\Delta}{\nu_\perp}}) \quad (55)$$

where Δ is the static magnetic critical exponent. Comparison of eqs. (54) and (55) results in $\beta_s = 0$ and $\Delta = \nu_\perp$. These values are well known for the 1d Ising model. It is clear that the transition is discontinuous at $B = 0$, also when changing B from positive to negative values, see eq.(53). The order of limits are meant as: $B \rightarrow 0$ and then $T \rightarrow 0$. The $\tilde{\delta} = 0$, $\Gamma = 1$ case is usually referred as the Glauber-Ising model. The dynamical exponents are [28, 42]:

$$Z_{1d \text{ Glauber}} = 2, \quad \theta_{g,1d \text{ Glauber}} = 1/4 \quad (56)$$

Applying **spin-exchange** Kawasaki dynamics, which conserves the magnetization (**model B**)

$$w_i = \frac{1}{2\tau} \left[1 - \frac{\gamma_2}{2} (s_{i-1}s_i + s_{i+1}s_i + 2) \right] \quad (57)$$

where $\gamma_2 = \tanh(2J/k_B T)$, the dynamical exponent is different. According to linear response theory [74] in one dimension, at the critical point ($T_c = 0$) it is:

$$Z_{1d \text{ Kaw}} = 5 \quad (58)$$

Note however, that in case of fast quenches to $T = 0$ coarsening with scaling exponent $1/3$ is reported [75]. Hence another dynamic Ising universality class appears with the same static but different dynamical exponents.

Interestingly while the two dimensional equilibrium Ising model is solved the exact values of the dynamical exponents are not known. Table IV summarizes the known dynamical exponents of the Ising model in $d = 1, 2, 3, 4$. The $d = 4$ results are mean-field values. In

	$d = 1$		$d = 2$		$d = 3$	$d = 4$	
	A	B	A	B	A	A	B
Z	2	5[74]	2.165(10)[76]	2.325(10)[78]	2.032(4)[30]	2	4
λ	1		0.737(1)[76]	0.667(8)[78]	1.362(19)[79]	4	
θ_g	1/4		0.225(10)		0.41(2)[77]	1/2	

TABLE IV: Critical dynamical exponents in the Ising model. Columns denoted by (A) and (B) refer, model A and model B dynamics

Section IV D 3 I shall discuss an another fully nonequilibrium critical point of the $d = 1$ Ising model with competing dynamics (the NEKIM), where the dynamical exponents break the scaling relation (17) and therefore the

magnetization is a non-Markovian process. For $d > 3$ there is no non-Markovian effect (hence θ is not independent) but for $d = 2, 3$ the situation is still not completely clear [76].

In one dimension the domain walls (kinks) between up and down regions can be considered as particles. The spin-flip dynamics can be mapped onto particle movement

$$\uparrow\downarrow\downarrow\rightleftharpoons\uparrow\uparrow\downarrow \sim \bullet\circ\rightleftharpoons\circ\bullet \quad (59)$$

or to the creation or annihilation of neighboring particles

$$\uparrow\uparrow\uparrow\rightleftharpoons\uparrow\downarrow\uparrow \sim \circ\circ\rightleftharpoons\bullet\bullet \quad (60)$$

Therefore the $T = 0$ Glauber dynamics is equivalent to the diffusion limited annihilation (ARW) mentioned already in Section. II. By mapping the spin-exchange dynamics in the same way more complicated particle dynamics emerges, example:

$$\uparrow\uparrow\downarrow\rightleftharpoons\uparrow\downarrow\uparrow \sim \circ\bullet\circ\rightleftharpoons\bullet\bullet\bullet \quad (61)$$

one particle may give birth of two others or three particle may coagulate to one. Therefore these models are equivalent to branching and annihilating random walks to be discussed in Section IV D 2.

3. Competing dynamics added to spin-flip

Competing dynamics in general break the detailed balance symmetry (49) and make the kinetic Ising model to relax to a nonequilibrium steady state (if it exists). Generally these models become unsolvable, for an overview see [81]. Grinstein et al. [82] argued in 1985, that stochastic **spin-flip** models with two states per site and updating rules of a short-range nature with Z_2 symmetry should belong to the (kinetic) Ising model universality class. Their argument rests on the stability of the dynamic Ising fixed point in $d = 4 - \epsilon$ dimensions with respect to perturbations preserving both the spin inversion and the lattice symmetries. This hypothesis has received extensive confirmation by Monte Carlo simulations [184]–[93], [97, 98, 100] as well as from analytic calculations [94, 95, 96]. The models investigated include Ising models with a competition of two (or three [98]) Glauber-like rates at different temperatures [91, 92, 94, 96], or a combination of spin-flip and spin-exchange dynamics [99], majority vote models [100, 184] and other types of transition rules with the restrictions mentioned above [93].

Note that in all of the above cases the ordered state is fluctuating and non-absorbing. By relaxation processes this allows fluctuations in the bulk of a domain. It is also possible (and in 1d it is the only choice) to generate nonequilibrium two-state spin models (with short ranged interactions) where the ordered states are frozen (absorbing), hence by the relaxation to the steady state

fluctuations occur at the boundaries only. In this case non-Ising universality appears which is called the voter model (VM) universality class (see Sect. IV C).

In two dimensions **general Z_2 symmetric update rules** were investigated by [93, 101, 102, 103]. The essence of this – following [101] – is described below. Let us consider a two dimensional lattice of spins $s_i = \pm 1$, evolving with the following dynamical rule. At each evolution step, the spin to be updated flips with the heat bath rule: the probability that the spin s_i takes the value +1 is $P(s_i = 1) = p(h_i)$, where the local field h_i is the sum over neighboring sites $\sum_j s_j$ and

$$p(h) = \frac{1}{2} (1 + \tanh[\beta(h)h]). \quad (62)$$

The functions $p(h)$ and $\beta(h)$ are defined over integral values of h . For a square lattice, h takes the values 4, 2, 0, -2, -4. We require that $p(-h) = 1 - p(h)$, in order to keep the up down symmetry, hence $\beta(-h) = \beta(h)$ and this fixes $p(0) = 1/2$. The dynamics therefore depends on two parameters

$$p_1 = p(2), \quad p_2 = p(4), \quad (63)$$

or equivalently on two effective temperatures

$$T_1 = \frac{1}{\beta(2)}, \quad T_2 = \frac{1}{\beta(4)}. \quad (64)$$

Defining the coordinate system

$$t_1 = \tanh \frac{2}{T_1}, \quad t_2 = \tanh \frac{2}{T_2} \quad (65)$$

with $0 \leq t_1, t_2 \leq 1$ this yields

$$p_1 = \frac{1}{2} (1 + t_1), \quad p_2 = \frac{1}{2} \left(1 + \frac{2t_2}{1 + t_2^2} \right), \quad (66)$$

with $1/2 \leq p_1, p_2 \leq 1$. One can call T_1 and T_2 as two temperatures, respectively associated with *interfacial noise*, and to *bulk noise*. Each point in the parameter plane (p_1, p_2) , or alternatively in the temperature plane (t_1, t_2) , corresponds to a particular model. The class of models thus defined comprises as special cases the Ising model, the voter and anti-voter models [2], as well as the majority vote [2, 184] model (see Fig. 1). The $p_2 = 1$ line corresponds to models with no bulk noise ($T_2 = 0$), hence the dynamics is only driven by interfacial noise, defined above. The $p_1 = 1$ line corresponds to models with no interfacial noise ($T_1 = 0$), hence the dynamics is only driven by bulk noise. In both cases effects due to the curvature of the interfaces is always present. For these last models, the local spin aligns in the direction of the majority of its neighbors with probability one, if the local field is $h = 2$, i.e. if there is no consensus amongst the neighbors. If there is consensus amongst them, i.e. if $h = 4$, the local spin aligns with its neighbors with a probability $p_2 < 1$.

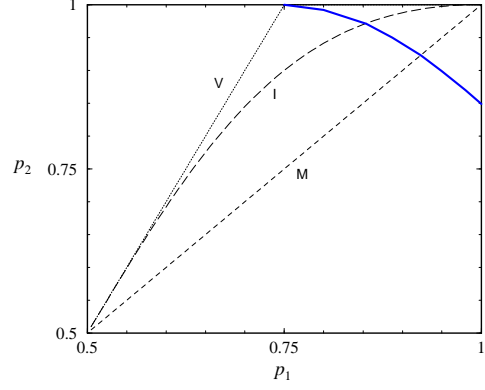


FIG. 1: Phase diagram of 2d, Z_2 symmetric nonequilibrium spin models from [101]. Broken lines correspond to the noisy voter model (V), the Ising model (I) and the majority vote model (M). The low temperature phase is located in the upper right corner, above the transition line (full line).

Simulations [93] revealed that the transition line between the low and high temperature regions is Ising type except for the endpoint $(p_1 = 1, p_2 = 0.75)$, that is first-order and corresponds to the voter model class. The local persistence exponent was also found to be constant along the line $\theta_l \sim 0.22$ [101] in agreement with that of the A-model (see Table IV) except for the VM point. The dynamics of this class of models may be described formally in terms of reaction diffusion processes for a set of coalescing, annihilating, and branching random walkers [101]. There are simulation results for other models exhibiting absorbing ordered state indicating VM critical behavior [104, 221].

It is important that nontrivial, nonequilibrium phase transition may occur even in one dimension if spin-exchange is added to spin-flip dynamics, the details will be discussed in Section IV D 3.

4. Competing dynamics added to spin-exchange

As mentioned in Section III **model-B** systems are more sensitive to competing dynamics. *Local and anisotropic* order parameter conserving processes generate critical behavior that coincides with that of the kinetic dipolar-interaction Ising model. In two dimensions both simulations and field theory [111] predicts the critical exponents. The critical dimension is $d_c = 3$. It

β	γ	η_a	ν_\perp
0.33(2)	1.16(6)	0.13(4)	0.62(3)

TABLE V: Critical exponents of the $d = 2$ randomly driven lattice gas

is shown that the Langevin equation (and therefore the critical behavior) of the anisotropic diffusive system coincides with that of the randomly driven lattice gas system as well. Other systems in this universality class are the two-temperature model [112], the ALGA model [113] and the infinitely fast driven lattice gas model [114]. In the randomly driven lattice gas model particle current does not occur but an anisotropy can be found, therefore Achacbar et al. argue [114] that the particle current is not a relevant feature for this class. This argument gives the possibility to understand why some set of simulations of driven lattice systems [115] leads to different critical behavior than that of the canonical coarse-grained representative of this class, in which an explicit particle current $j\hat{x}$ is added to the continuous, model-B Ising model Hamiltonian:

$$\frac{\partial\phi(\mathbf{r},t)}{\partial t} = -\nabla \left[\eta \frac{\delta H}{\delta\phi} + j\hat{x} \right] + \nabla\zeta \quad (67)$$

[9] (here η is a parameter, ζ is a Gaussian noise). In this model one obtains mean-field exponents for $2 \geq d \geq 5$ (with weak logarithmic corrections at $d = 2$) with $\beta = 1/2$ exactly. To resolve contradictions between simulation results [115, 116] Zia et al. [117] raised the possibility of the existence of another, extraordinary, “stringy” ordered phase in Ising type driven lattice gases that may be stable in *square* systems.

5. Long-range interactions and correlations

If the Glauber Ising model (with non-conserving dynamics) changed to a nonequilibrium one in such a way that one couples a **nonlocal dynamics** [118] to it long-range isotropic interactions are generated and mean-field critical behavior emerges. For example if the nonlocal dynamics is a random Levy flight with spin exchange probability distribution

$$P(r) \propto \frac{1}{r^{d+\sigma}} \quad (68)$$

effective long range interactions of the form $V_{eff} \propto r^{-d-\sigma}$ are generated and the critical exponents change continuously as the function σ and d [120]. Similar conclusions for other nonequilibrium classes will be discussed later (Sect.IV A 6).

The effect of power-law correlated initial conditions $\langle\phi(0)\phi(r)\rangle \sim r^{-(d-\sigma)}$ in case of a **quench to the ordered phase in systems with non-conserved order parameter** was investigated by Bray et al. [119]. An important example is the (2+1)-dimensional Glauber-Ising model quenched to zero temperature. It was observed that long-range correlations are relevant if σ exceeds a critical value σ_c . Furthermore, it was shown that the relevant regime is characterized by a continuously changing exponent in the autocorrelation function $A(t) = [\phi(r,t)\phi(r,0)] \sim t^{-(d-\sigma)/4}$, whereas the usual

short-range scaling exponents could be recovered below the threshold. These are in agreement with the simulations of the two-dimensional Ising model quenched from $T = T_c$ to $T = 0$.

6. Damage spreading behavior

The dynamics dependent DS critical behavior in different Ising models is in agreement with Grassberger’s conjecture [35]. Dynamical simulations with heat-bath algorithm in 2 and 3 dimensions [30, 62, 63] resulted in $T_d = T_c$ with a DS dynamical exponent coinciding with that of the Z-s of the replicas. In this case the DS transition picks up the Ising class universality of its replicas. With Glauber dynamics in 2d $T_d < T_c$ and DP class DS exponents were found [33]. With Kawasaki dynamics in 2d on the other hand the damage always spreads [64]. With Swendsen-Wang dynamics in 2d $T_d > T_c$ and DP class DS behavior was observed [65].

In 1d it is possible to design dynamics showing either PC or DP class DS behavior depending on the DS transition coincides or not with the critical point. In the PC class DS case damage variables follow BARW2 dynamics (see Sects.IV D 2 and IV D 3) and Z_2 symmetric absorbing states occur [66, 281].

B. Potts classes

The generalization of the two-state equilibrium Ising model was introduced by Potts [121], for an overview see [122]. In the q -state Potts model the state variables can take q different values $s_i \in (0, 1, 2, \dots, q)$ and the Hamiltonian is a sum of Kronecker delta function of states over nearest neighbors

$$H = -J \sum_{\langle i,i' \rangle} \delta(s_i - s_{i'}) \quad (69)$$

This hamiltonian exhibits a global symmetry described by the permutation group of q elements (S_q). The Ising model is recovered in the $q = 2$ case (discussed in Section III A). The q -state Potts model exhibits a disordered high-temperature phase and an ordered low-temperature phase. The transition is first-order, mean-field-like for q -s above the $q_c(d)$ curve (shown in Figure 2) (and for $q > 2$ in high dimensions). The $q = 1$ limit can be shown [19] to be equivalent to the isotropic percolation (see Section IV B 1) that is known to exhibit a continuous phase transition with $d_c = 6$. The problem of finding the effective resistance between two node points of a network of linear resistors was solved by Kirchhoff in 1847. Fortuin and Kasteleyn [19] showed that Kirchhoff’s solution can be expressed as a $q = 0$ limit of the Potts partition function. Further mappings were discovered between the spin glass [123] and the $q = 1/2$ Potts model and the two dimensional $q = 3, 4$ cases to vertex models (see [124]).

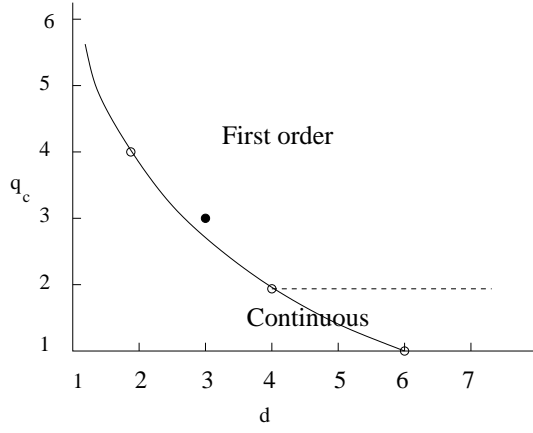


FIG. 2: Schematic plot from [122] for $q_c(d)$ (solid line). Open symbols correspond to continuous phase transition, filled symbol to a known first order transition. Below the dashed line the transition is continuous too.

From this figure we can see that for $q > 2$ Potts models continuous transitions occur in two dimensions only ($q = 3, 4$). Fortunately these models are exactly solvable (see [124]) and exhibit conformal symmetry as well as topological, Yang-Baxter invariance. The static exponents in two dimensions are known exactly (Table VI)

exponent	$q = 0$	$q = 1$	$q = 2$	$q = 3$	$q = 4$
α_H	$-\infty$	$-2/3$	$0(\log)$	$1/3$	$2/3$
β	$1/6$	$5/36$	$1/8$	$1/9$	$1/12$
γ	∞	$43/18$	$7/4$	$13/9$	$7/6$
ν_{\perp}	∞	$4/3$	1	$5/6$	$2/3$

TABLE VI: Static exponents of the q states Potts model in two dimension

1. Correlated percolation at T_c

In 2d models with Z_3 symmetry the critical point coincides with the percolation of site connected clusters and the following percolation exponents are reported [22]:

$$\beta_p = 0.075(14), \quad \gamma_p = 1.53(21) \quad . \quad (70)$$

In case of Fortuin-Kasteleyn cluster construction [19] the percolation exponents of the q state Potts model at T_c coincide with those of the magnetization of the model.

2. The vector Potts model

A variant of the q -state Potts model is the vector Potts model (or clock model), which exhibits a Z_q cyclic

symmetry (a subgroup of S_q) of the variables $\Theta = (2\pi/q)r$, $r = 0, \dots, q-1$. Its Hamiltonian is

$$H = -J \sum_{i,i'} \cos(\Theta_i - \Theta_{i'}) \quad . \quad (71)$$

Note that for $q = 2, 3$ it is equivalent to the ordinary Potts model. In two dimensions for $q \leq 4$ it exhibits second order phase transition but for $q > 4$ it has several distinct critical points. These separate a high temperature disordered phase from an intermediate phase with a conventional second-order transition and the intermediate phase from a low-temperature vortex phase with an XY type transition (see Section III C).

3. Dynamical Potts classes

The **model-A** dynamical exponents are determined in two dimensions for $q = 3, 4$ by short-time Monte Carlo simulations [125] (Table VII). The exponents were found to be the same for heat-bath and Metropolis algorithms. For the zero temperature **local persistence** exponent in

exponent	$q = 3$	$q = 4$
Z	2.198(2)	2.290(3)
λ	0.836(2)	
θ_g	0.350(8)	

TABLE VII: Known dynamical exponents of the q states Potts model in two dimensions

one dimension exact formulas have been determined. For sequential dynamics [126]

$$\theta_{l,s} = -\frac{1}{8} + \frac{2}{\pi^2} \left[\cos^{-1} \left(\frac{2-q}{\sqrt{2q}} \right) \right]^2 \quad (72)$$

while for parallel dynamics $\theta_{l,p} = 2\theta_{l,s}$ [127]. In a deterministic coarsening it is again different (see [128, 129]. As we can see the *dynamical universality class characterized by the $\xi \propto t^{1/2}$ characteristic length growth is split by different dynamics, as reflected by the persistence exponent*.

Similarly to the Ising model case in nonequilibrium systems the Potts model symmetry turned out to be a relevant factor for determining the universal behavior of transitions to **fluctuating ordered states** [131, 132, 133]. On the other hand in case of nonequilibrium transitions to **absorbing states** a simulation study [104] suggests first order transition for all $q > 2$ state Potts models in $d > 1$ dimensions. The $q = 2$, $d = 2$ case corresponds to the Voter model class (Sect. IV C) and in 1d either PC class transition ($q = 2$) or N-BARW2 class transition ($q = 3$) (Sect. V K) occurs.

The **DS transition** of a $q = 3$, $d = 2$ Potts model with heat-bath dynamics was found to belong to the DP class (Sect. IV A) because $T_d > T_c$ [134].

4. Long-range interactions

The effect of long-range interaction has also been investigated in case of the one dimensional $q = 3$ Potts model [130] with the Hamiltonian

$$H = - \sum_{i < j} \frac{J}{|i - j|^{1+\sigma}} \delta(s_i, s_j) . \quad (73)$$

For $\sigma < \sigma_c \sim 0.65$ a crossover from second order to first order (mean-field) transition was located by simulations. Similarly to the Ising model here we can expect to see this crossover if we generate the long-range interactions by the addition of a Levy type Kawasaki dynamics.

C. XY model classes

The classical XY model is defined by the same Hamiltonian as the clock model

$$H = -J \sum_{i,i'} \cos(\Theta_i - \Theta_{i'}) . \quad (74)$$

but the state variables are continuous $\Theta_i \in [0, 2\pi]$ and therefore it can be considered as the $q \rightarrow \infty$ limit of the vector Potts model. This model has a global $U(1)$ symmetry. The critical behavior is similar to the vortex transition of the clock model. Alternatively the XY model can be defined as a special $N = 2$ case of $O(N)$ symmetric models such that the spin vectors are two dimensional \mathbf{S}_i with absolute value $\mathbf{S}_i^2 = 1$

$$H = -J \sum_{\langle i,i' \rangle} \mathbf{S}_i \mathbf{S}_{i'} . \quad (75)$$

In this continuous model in **two dimensions** no local order parameter can take zero value according to the Mermin-Wagner theorem [55]. The appearance of free vortexes (which are non-local) cause an unusual transition mechanism that implies that most of the thermodynamic quantities do not show power-law singularities. The singular behavior of the correlation length (ξ) and the susceptibility (χ) is described by the forms for $T > T_c$

$$\xi \propto \exp\left(C(T - T_c)^{-1/2}\right) , \quad \chi \propto \xi^{2-\eta_a} , \quad (76)$$

where C is a non-universal positive constant. Conventional critical exponents cannot be used, but one can define scaling dimensions. At T_c the two-point correlation function has the following long-distance behavior

$$G(r) \propto r^{-1/4} (\ln r)^{1/8} \quad (77)$$

implying $\eta_a = 1/4$, and in the entire low-temperature phase

$$G(r) \propto r^{-\eta_a(T)} \quad (78)$$

such that the exponent η_a is a continuous function of the temperature, i.e. the model has a line of critical points starting from T_c to $T = 0$. This is the so called Kosterlitz-Thouless critical behavior [135] and corresponds to the conformal field theory with $c = 1$ [136]. This kind of transition can experimentally observed in many effectively two-dimensional systems with $O(2)$ symmetry, such as thin films of superfluid helium and describes roughening transitions of SOS models at crystal interfaces. In

α_H	β	γ	ν_\perp	η_a
-0.011(4)	0.347(1)	1.317(2)	0.670(1)	0.035(2)

TABLE VIII: Static exponents of the XY model in three dimensions

three dimensions the critical exponents of the $O(N)$ ($N = 0, 1, 2, 3, 4$) symmetric field theory have been determined by perturbative expansions up to seventh loop order [137]. The Table VIII summarizes these results for the XY case (for a more detailed overview see [139]).

Exponents of **model A** dynamics in 2d have been determined by short-time simulations and logarithmic corrections to scaling were found [140]. Table IX summarizes the known dynamical exponents

Z	λ	η
2.04(1)	0.730(1)	0.250(2)

TABLE IX: Dynamical exponents of the XY model in two dimensions

1. Long-range correlations

For **model B** dynamics Bassler and R acz [141] studied the validity of the Mermin-Wagner theorem by transforming the two dimensional XY model to a non-equilibrium one with two-temperature dynamics. They found that the Mermin-Wagner theorem does not apply for this case because dipole type of long-range correlations are generated and the universality class of the phase transition of the model coincides with that of the two temperature driven Ising model (see Table V).

2. Self-propelled particles

An other XY-like nonequilibrium model that exhibits ordered state for $d \leq 2$ dimensions is motivated by the description of the ‘flocking’ behavior among living things, such as birds, slime molds and bacteria. In the simplest version of the self-propelled particle model by Vicsek et al. [142] each particle’s velocity is set to a fixed magnitude, v_0 . The interaction with the neighboring particles

changes only the direction of motion: the particles tend to align their orientation to the local average velocity. In one dimension it is defined on the lattice as

$$\begin{aligned} x_i(t+1) &= x_i(t) + v_0 u_i(t), \\ u_i(t+1) &= G(\langle u(t) \rangle_i) + \xi_i, \end{aligned} \quad (79)$$

where the particles are characterized by their coordinate x_i and dimensionless velocity u_i and the function G that incorporates both the propulsion and friction forces which set the velocity in average to a prescribed value v_0 : $G(u) > u$ for $u < 1$ and $G(u) < u$ for $u > 1$. The distribution function $P(x = \xi)$ of the noise ξ_i is uniform in the interval $[-\eta/2, \eta/2]$. Keeping v_0 constant, the adjustable control parameters of the model are the average density of the particles, ρ , and the noise amplitude η . The order parameter is the average velocity $\phi \equiv \langle u \rangle$ which vanishes as

$$\phi(\eta, \rho) \sim \begin{cases} \left(\frac{\eta_c(\rho) - \eta}{\eta_c(\rho)} \right)^\beta & \text{for } \eta < \eta_c(\rho) \\ 0 & \text{for } \eta > \eta_c(\rho) \end{cases}, \quad (80)$$

at a critical $\eta_c(\rho)$ value.

This model is similar to the XY model of classical magnetic spins because the velocity of the particles, like the local spin of the XY model, has fixed length and continuous rotational $U(1)$ symmetry. In the $v_0 = 0$ and low noise limit the model reduces *exactly* to a Monte-Carlo dynamics of the XY model.

Toner and Tu [143] proposed a field theory that included in a self-consistent way the non-equilibrium effects as well. They have shown that their model is different from the XY model for $d < 4$. The essential difference between the self-propelled particle model and the equilibrium XY model is that at different times, the "neighbors" of one particular "bird" will be different depending on the velocity field itself. Therefore, two originally distant "birds" can interact with each other at some later time. They found a critical dimension $d_c = 4$, below which linearized hydrodynamics breaks down, but owing to a Galilean invariance they could obtain exact scaling exponents in $d = 2$. For the dynamical exponent they got $Z = 6/5$. Numerical simulations [142, 144] indeed found a long range ordered state with a continuous transition characterized by $\beta = 0.42(3)$ in two dimensions.

In one dimension the field theory and simulations of Czirók et. al [145] provided evidence for a continuous phase transition with $\beta = 0.60(5)$, which is different from the mean-field value $1/2$ [14].

D. $O(N)$ symmetric model classes

As already mentioned in the previous section the $O(N)$ symmetric models are defined on spin vectors \mathbf{S}_i of unit length $\mathbf{S}_i^2 = 1$ with the Hamiltonian

$$H = -J \sum_{\langle i, i' \rangle} \mathbf{S}_i \mathbf{S}_{i'}. \quad (81)$$

The most well known of them is the classical Heisenberg model that corresponds to $N = 3$ being the simplest model of isotropic ferromagnets. The $N = 4$ case corresponds to the Higgs sector of the Standard Model at finite temperature. The $N = 0$ case is related to polymers and the $N = 1$ and $N = 2$ cases are the Ising and XY models respectively. The critical dimension is $d_c = 4$ and by the Mermin-Wagner theorem we cannot find finite temperature phase transition in the short range equilibrium models for $N > 2$ below $d = 3$. The static critical exponents have been determined by $\epsilon = 4 - d$ expansions up to five loop order [146], by exact RG methods (see [147] and the references therein), by simulations [148] and by series expansions in 3D (see [137] and the references there). In Table X I show the latest estimates from [137] in three dimensions for $N = 0, 3, 4$. The $N \rightarrow \infty$

N	α_H	β	γ	ν_\perp	η_a
0	0.235(3)	0.3024(1)	1.597(2)	0.588(1)	0.028(2)
3	-0.12(1)	0.366(2)	1.395(5)	0.707(3)	0.035(2)
4	-0.22(2)	0.383(4)	1.45(1)	0.741(6)	0.035(4)

TABLE X: Static exponents of the $O(N)$ model in three dimensions

limit is the exactly solvable spherical model [138]. For a detailed discussion of the static critical behavior of the $O(N)$ models see [139].

The dynamical exponents for **model A** are known exactly for the $(N \rightarrow \infty)$ spherical model [28, 56] case. For other cases $\epsilon = 4 - d$ expansions up to two loop order exist [28, 149]. For a discussion about the combination

N	Z	λ	θ_g
∞	2	5/2	1/4
3	2.032(4)	2.789(6)	0.38

TABLE XI: Known dynamical exponents of model A $O(N)$ model in three dimensions

of different dynamics see the general introduction Section III and [150].

1. Correlated percolation at T_c

In three dimensions for $O(2)$, $O(3)$ and $O(4)$ symmetric models the Fortuin-Kasteleyn cluster construction [19] results in percolation points and percolation exponents which coincide with the corresponding T_c -s and magnetization exponent values [23].

IV. GENUINE, BASIC NONEQUILIBRIUM CLASSES

In this section I introduce such “genuine nonequilibrium” universality classes that do not occur in dynamical generalizations of equilibrium systems. Naturally in these models there is no hermitian Hamiltonian and they are defined by transition rates not satisfying the detailed balance condition (49). They can be described by a master equation and the deduced stochastic action or Langevin equation if it exists. The most well known cases are reaction-diffusion systems with order-disorder transitions in which the ordered state may exhibit only small fluctuations, hence they trap a system falling in it (absorbing state). They may occur in models of population [1], epidemics [2, 3], catalysis [4] or enzyme biology [7] for example. There are also other nonequilibrium phase transitions for example in lattice gases with currents [151, 152, 153, 154] or in traffic models [6], but in these systems the critical universality classes have not been explored yet.

Phase transitions in such models may occur in low dimensions in contrast with equilibrium ones [9]. As it was already shown in Section III A 2 reaction-diffusion particle systems may be mapped onto spin-flip systems stochastic cellular automata [155] or interface growth models (see Sect. VI). The mapping however may lead to nonlocal systems that does not bear real physical relevance. The universality classes of the simple models presented in this section constitute the fundamental building blocks of more complex systems.

For a long time phase transitions with completely frozen absorbing states were investigated. A few universality classes of this kind were known [10],[11], the most prominent and the first one that was discovered is that of the directed percolation (DP) [210]. An early hypothesis [211] was confirmed by all examples up to now. This **DP hypothesis** claims that **in one component systems exhibiting continuous phase transitions to a single absorbing state (without extra symmetry and inhomogeneity or disorder) short ranged interactions can generate DP class transition only**. Despite the robustness of this class experimental observation is still lacking [10, 212] probably owing to the sensitivity to disorder that cannot be avoided in real materials.

A major problem of these models is that they are usually far from the critical dimension and critical fluctuations prohibit mean-field (MF) like behavior. Further complication is that bosonic field theoretical methods cannot describe particle exclusion that may obviously happen in $d = 1$. The success of the application of bosonic field theory in many cases is the consequence of the asymptotically low density of particles near the critical point. However in multi-component systems, where the exchange between different types is non-trivial, bosonic field theoretical descriptions may fail. In case of the binary production (BP) models (Sect. V F) bosonic

RG predicts diverging density in the active phase contrary to the lattice model version of hard-core particles [248, 249, 250, 251, 252, 254]. Fermionic field theories on the other hand have the disadvantage that they are non-local, hence results exist for very simple reaction-diffusion systems only [269, 270, 311]. Other techniques like independent interval approximation [271], empty interval method [272], series expansion [317] or density matrix renormalization (DMRG) are currently under development.

The universal scaling-law behavior in these models is described by the critical exponents in the neighborhood of a steady state, hence the generalization of dynamical exponents introduced for “Out of equilibrium classes” (Sect. III) (like Z , θ , λ ...etc.) is used. Besides that there are genuinely non-equilibrium dynamical exponents as well to characterize spreading behavior, defined in Sect. I D. For each class I discuss the damage spreading transitions, the effects of different boundary conditions, disorder and long-correlations generated by anomalous diffusion or by special initial states.

A. Directed percolation classes

The directed percolation (DP) introduced by [273] is an anisotropic percolation with a preferred direction t . This means that this problem should be $d \geq 2$ dimensional. If there is an object (bond, site etc.) at (x_i, y_j, \dots, t_k) it must have a nearest neighboring object at t_{k-1} unless $t_k = 0$ (see Figure 3). If we consider the preferred direc-

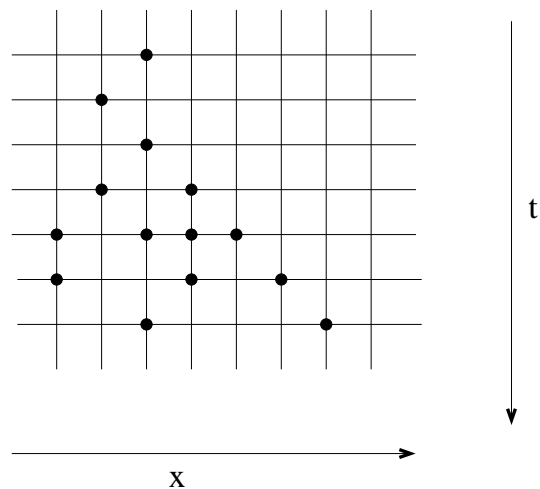
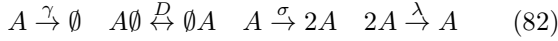


FIG. 3: Directed site percolation in $d = 1 + 1$ dimensions

tion as the time we recognize a spreading process of an agent A that can not have spontaneous source: $\emptyset \not\rightarrow A$. This results in the possibility of a completely frozen, so called *absorbing state* from which the system cannot escape if it has fallen into it. As a consequence these kinds of models may have phase transitions in $d = 1$ spatial dimension already. By increasing the branching probability

p of the agent we can have a phase transition between the absorbing state and an active steady state with finite density of A -s. If the transition is continuous it is very likely that it belongs to a robust universality (DP) class. For a long time all examples of such absorbing phase transitions were found to belong to the DP class and a conjecture was advanced by [211]. This claims that in one component systems exhibiting continuous phase transitions to a single absorbing state (without extra symmetry, inhomogeneity or disorder) short ranged interactions can generate DP class transition only. This hypothesis has been confirmed by all examples up to now, moreover DP class exponents were discovered in some systems with multiple absorbing states. For example in systems with infinitely many frozen absorbing states [274, 275, 368] the static exponents were found to coincide with those of DP. Furthermore by models without any special symmetry of the absorbing states DP behavior was reported [276, 279, 281] too. So although the necessary conditions for the DP behavior seem to be confirmed the determination of sufficient conditions is an open problem. There are many introductory works available now to DP [9, 10, 11, 210] therefore I shall not go very deeply into the discussions of details of various representations.

In the reaction-diffusion language the DP is built up from the following processes



The mean-field equation for the coarse-grained particle density $\rho(t)$ is

$$\frac{d\rho}{dt} = (\sigma - \gamma)\rho - (\lambda + \sigma)\rho^2 \quad (83)$$

This has the stationary stable solution

$$\rho(\infty) = \begin{cases} \frac{\sigma - \gamma}{\lambda + \sigma} & \text{for : } \sigma > \gamma \\ 0 & \text{for : } \sigma \leq \gamma \end{cases} \quad (84)$$

exhibiting a continuous transition at $\sigma = \gamma$. A small variation of σ or γ near the critical point implies a linear change of ρ , therefore the order parameter exponent in the mean-field approximation is $\beta = 1$. Near the critical point the $O(\rho)$ term is the dominant one, hence the density approaches the stationary value exponentially. For $\sigma = \gamma$ the remaining $O(\rho^2)$ term causes power-law decay: $\rho \propto t^{-1}$ indicating $\alpha = 1$. To get information about other scaling exponents we have to take into account the diffusion term $D\nabla^2$ describing local density fluctuations. Using rescaling invariance two more independent exponents can be determined: $\nu_{\perp} = 1/2$ and $Z = 2$ if $d \geq 4$. Therefore the upper critical dimension of directed percolation is $d_c = 4$.

Below the critical dimension the RG analysis of the Langevin equation

$$\begin{aligned} \frac{\partial \rho(x, t)}{\partial t} &= D\nabla^2 \rho(x, t) + (\sigma - \gamma)\rho(x, t) - \\ &- (\lambda + \sigma)\rho^2(x, t) + \sqrt{\rho(x, t)}\eta(x, t) \end{aligned} \quad (85)$$

critical exponent	$d = 1$ [291]	$d = 2$ [292]	$d = 3$ [293]	$d = 4 - \epsilon$ [211, 294]
$\beta = \beta'$	0.276486(8)	0.584(4)	0.81(1)	$1 - \epsilon/6 - 0.01128 \epsilon^2$
ν_{\perp}	1.096854(4)	0.734(4)	0.581(5)	$1/2 + \epsilon/16 + 0.02110 \epsilon^2$
ν_{\parallel}	1.733847(6)	1.295(6)	1.105(5)	$1 + \epsilon/12 + 0.02238 \epsilon^2$
$Z = 2/z$	1.580745(10)	1.76(3)	1.90(1)	$2 - \epsilon/12 - 0.02921 \epsilon^2$
$\delta = \alpha$	0.159464(6)	0.451	0.73	$1 - \epsilon/4 - 0.01283 \epsilon^2$
η	0.313686(8)	0.230	0.12	$\epsilon/12 + 0.03751 \epsilon^2$
γ_p	2.277730(5)	1.60	1.25	$1 + \epsilon/6 + 0.06683 \epsilon^2$

TABLE XII: Estimates for the critical exponents of directed percolation.

is necessary [211]. Here $\eta(x, t)$ is the Gaussian noise field, defined by the correlations

$$\langle \eta(x, t) \rangle = 0 \quad (86)$$

$$\langle \eta(x, t) \eta(x', t') \rangle = \Gamma \delta^d(x - x') \delta(t - t') \quad (87)$$

The noise term is proportional $\sqrt{\rho(x, t)}$ ensuring that in the absorbing state ($\rho(x, t) = 0$) it vanishes. The square-root behavior stems from the definition of $\rho(x, t)$ as a coarse-grained density of active sites averaged over some mesoscopic box size. Note that DP universality occurs in many other processes like in odd offspring, branching and annihilating random walks (BARWo) (see Section IV A 3) or in models described by field theory with higher order terms like $\rho^3(x, t)$ or $\nabla^4 \rho(x, t)$, which are irrelevant under the RG transformation. This stochastic process can through standard techniques [282] be transformed into a Lagrangian formulation with the action

$$S = \int d^d x dt \left[\frac{D}{2} \psi^2 \phi + \psi (\partial_t \phi - \nabla^2 \phi - r \phi + u \phi^2) \right] \quad (88)$$

where ϕ is the density field and ψ is the response field (appearing in response functions) and the action is invariant under the following time-reversal symmetry

$$\phi(x, t) \rightarrow -\psi(x, -t) \quad , \quad \psi(x, t) \rightarrow -\phi(x, -t) \quad (89)$$

This symmetry yields [39, 285] the scaling relations

$$\beta = \beta' \quad (90)$$

$$4\delta + 2\eta = dz \quad (91)$$

This field theory was found to be equivalent [283] to the Reggeon field theory (RFT) [284], which is a model of scattering elementary particles at high energies and low-momentum transfers.

Perturbative $\epsilon = 4 - d$ renormalization group analysis [211, 294] up to two-loop order resulted in estimates for the critical exponents shown in the Table XII. The best results obtained by approximative techniques for DP like improved mean-field [286], coherent anomaly method [287], Monte Carlo simulations [285, 295, 296, 297], series expansions [291, 298], DMRG [308], and numerical integration of eq.85 [288] are also shown in Table XII.

The **local persistence** probability may be defined as the probability ($p_l(t)$) that a particular site never becomes active up to time t . Numerical simulations [289] for this in the 1+1 d Domany-Kinzel SCA (see Sect. IV A 2) found power-law with exponent

$$\theta_l = 1.50(1) \quad (92)$$

The **global persistence** probability defined here as the probability ($p_g(t)$) that the deviation of the global density from its mean value does not change its sign up to time t . The simulations of [289] in 1+1 dimensions claim $\theta_g \geq \theta_l$. This agrees with field theoretical $\epsilon = 4 - d$ expansions [290] that predict $\theta_g = 2$ for $d \geq 4$ and for $d < 4$:

$$\theta_g = 2 - \frac{5\epsilon}{24} + O(\epsilon^2). \quad (93)$$

The **crossover from isotropic to directed percolation** was investigated by perturbative RG [309] up to one loop order. They found that while for $d > 6$ the isotropic, for $d > 5$ the directed Gaussian fixed point is stable. For $d < 5$ the asymptotic behavior is governed by the DP fixed point. On the other hand in $d = 2$ exact calculations and simulations [310] found that the isotropic percolation is stable with respect to DP if we control the crossover by a spontaneous particle birth parameter. It is still an open question what happens for $2 < d < 5$. Crossovers to mean-field behavior generated by long-range interactions IV A 7 and to compact directed percolation IV C will be discussed later.

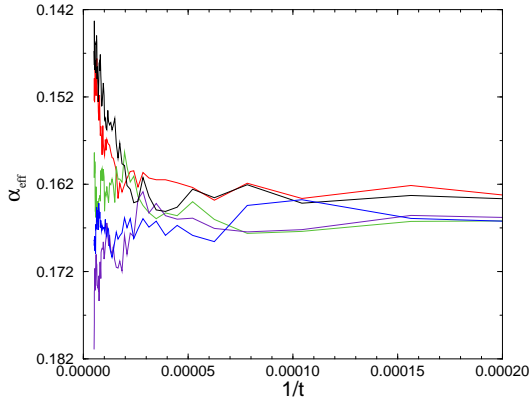


FIG. 4: Local slopes of the density decay in a bosonic BARW1 model (Sect. IV A 3). Different curves correspond to $\lambda = 0.12883, 0.12882, 0.12881, 0.1288, 0.12879$ (from bottom to top) [313].

It was conjectured [312] that in 1d “fermionic” (single site occupancy) and bosonic (multiple site occupancy) models may exhibit different critical behavior. An attempt for a fermionic field theoretical treatment of the DP in 1+1 d was shown in [270, 311]. This run into severe convergence problems and has not resulted in precise quantitative estimates for the critical exponents. Although the bosonic field theory is expected to describe

the fermionic case owing to the asymptotically low density at criticality it has never been proven rigorously. Since only bosonic field theory exists that gives rather inaccurate critical exponent estimates, in [313] simulations of a a BARW1 process (102) with unrestricted site occupancy were performed to investigate the density ($\rho(t)$) decay of a DP process from random initial state. Figure 4 shows the local slopes of density decay defined as

$$\alpha_{eff} = -\frac{d \log \rho(t)}{d \log t} \quad (94)$$

around the critical point for several annihilation rates (λ). The critical point is estimated at $\lambda_c = 0.12882(1)$ (corresponding to straight line) with the extrapolated decay exponent $\alpha = 0.165(5)$, which agrees well with fermionic model simulation and series expansion results 0.1595(1) [298].

Note that in site restricted models already the

$$A \xrightarrow{\gamma} \emptyset \quad A\emptyset \xrightarrow{D} \emptyset A \quad A \xrightarrow{\sigma} 2A \quad (95)$$

processes generate a DP class phase transition, while in the bosonic version the $2A \xrightarrow{\lambda} A$ process is also necessary to ensure an active steady state (without it the density blows up for $\sigma > \gamma$).

Models exhibiting DP transitions have been reviewed in great detail in [9] and in [11]. In the next subsections I recall only three important examples.

1. The Contact process

The contact process is one of the earliest and simplest lattice model for DP with **asynchronous** update introduced by Harris [299] to model epidemic spreading without immunization. Its dynamics is defined by nearest-neighbor processes that occur spontaneously due to specific rates (rather than probabilities). In numerical simulations models of this type are usually realized by random sequential updates. In one dimension this means that a pair of sites $\{s_i, s_{i+1}\}$ is chosen at random and an update is attempted according to specific transition rates $w(s_i, t+dt, s_{i+1}, t+dt | s_i, t, s_{i+1}, t)$. Each attempt to update a pair of sites increases the time t by $dt = 1/N$, where N is the total number of sites. One time step (sweep) therefore consists of N such attempts. The contact process is defined by the rates

$$w(A, I | A, A) = w(I, A | A, A) = \mu, \quad (96)$$

$$w(I, I | A, I) = w(I, I | I, A) = \lambda, \quad (97)$$

$$w(A, A | A, I) = w(A, A | I, A) = 1, \quad (98)$$

where $\lambda > 0$ and $\mu > 0$ are two parameters (all other rates are zero). Equation (96) describes the creation of inactive (I) spots within active (A) islands. Equations (97) and (98) describe the shrinkage and growth of active islands. In order to fix the time scale, we chose the

rate in Eq. (98) to be equal to one. The active phase is restricted to the region $\lambda < 1$ where active islands are likely to grow. In one dimension series expansions and numerical simulations determined the critical point and critical exponents precisely [297, 298, 300]. In two dimensions Dickman et al. determined the order parameter moments and the cumulant ratios [300].

2. DP-class stochastic cellular automata

There are many stochastic cellular automata (SCA) that exhibit DP transition [301] perhaps the first and simplest one is the (1+1)-dimensional Domany-Kinzel (DK) model [227]. In this model the state at a given time t is specified by binary variables $\{s_i\}$, which can have the values A (active) and I (inactive). At odd times odd-indexed, whereas at even times the rest of the sites are updated according to specific conditional probabilities. This defines a cellular automaton with **parallel** updates (discrete time evolution) acting on two independent triangular sub-lattices (Fig.5). The conditional probabili-

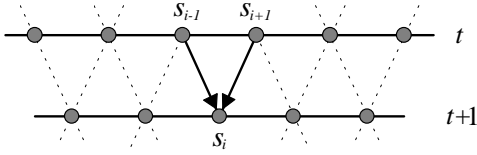


FIG. 5: Update in the Domany-Kinzel model [221].

ties in the Domany-Kinzel model $P(s_{i,t+1} | s_{i-1,t}, s_{i+1,t})$ are given by

$$P(I|I, I) = 1, \quad (99)$$

$$P(A|A, A) = p_2, \quad (100)$$

$$P(A|I, A) = P(A|A, I) = p_1, \quad (101)$$

and $P(I|s_{i-1}, s_{i+1}) + P(A|s_{i-1}, s_{i+1}) = 1$, where $0 \leq p_1 \leq 1$ and $0 \leq p_2 \leq 1$ are two parameters. Equation (99) ensures that the configuration \dots, I, I, I, \dots is the absorbing state. The process in Eq. (100) describes the creation of inactive spots within active islands with probability $1 - p_2$. The random walk of boundaries between active and inactive domains is realized by the processes in Eq. (101). A DP transitions can be observed only if $p_1 > \frac{1}{2}$, when active islands are biased to grow [302]. The phase diagram of the 1d DK model is shown in Fig. 6. It comprises an active and an inactive phase, separated by a phase transition line (solid line) belonging to DP class. The dashed lines corresponds to *directed bond percolation* ($p_2 = p(2 - p_1)$) and *directed site percolation* ($p_1 = p_2$) models. At the special symmetry endpoint ($p_1 = \frac{1}{2}, p_2 = 1$) compact domain growth occurs (CDP) and the transition becomes first order (see Section IV C). The transition on the $p_2 = 0$ axis corresponds to the transition of the stochastic version of Wolfram's rule-18

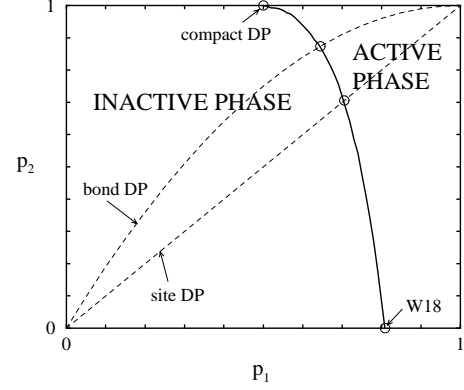


FIG. 6: Phase diagram of the 1d Domany-Kinzel SCA [221].

cellular automaton [302]. This range-1 SCA generates A at time t only when the right or left neighbor was A at $t - 1$:

$$\begin{array}{ccc} t-1: & AII & IIA \\ t: & A & A \end{array}$$

with probability p_1 [301]. The critical point was determined by precise simulations ($p_1^* = 0.80948(1)$) [303]. In the $t \rightarrow \infty$ limit the steady state is built up from II and IA blocks [305]. This finding permits us to map this model onto an even simpler one, the rule-6/16 SCA with new variables: $IA \rightarrow A$ and $II \rightarrow I$:

$$\begin{array}{cccc} t-1: & I & I & I & A & A & A & A \\ t: & I & A & A & A & I & I & I \end{array}$$

By solving GMF approximations and applying Padé approximations [304] or CAM method [287] very precise order parameter exponent estimates were found: $\beta = 0.2796(2)$.

The **DS phase structure** of the 1d DK model was explored by [34] and DP class transitions were found.

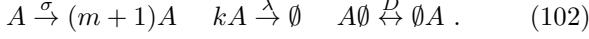
Another SCA example I mention is the family of **range-4 SCA** with an acceptance rule

$$s(t+1, j) = \begin{cases} X & \text{if } y \leq \sum_{j=4}^{j+4} s(t, j) \leq 6 \\ 0 & \text{otherwise} \end{cases},$$

where $X \in \{0, 1\}$ is a two valued random variable such that $\text{Prob}(X = 1) = p$ [53]. The $y = 3$ case was introduced and investigated by [306] in $d = 1, 2, 3$. The very first simulations in one dimension [306] suggested a counter-example to the DP conjecture. More precise spreading simulations of this model [307], GMF + CAM calculations and simulations of the $y < 6$ family in one and two dimensions have proven that this does not happen for any case [53]. The transitions are either belong to DP class or first order.

3. Branching and annihilating random walks with odd number of offspring

Branching and annihilating random walks (BARW) introduced by [213] can be regarded as generalizations of the DP process. They are defined by the following reaction-diffusion processes:



The $2A \rightarrow A$ and $2A \rightarrow \emptyset$ reactions dominating in the inactive phase are shown to be equivalent [359] (see Sect.IV C 1). Therefore the $k = 2$ and $m = 1$ (BARW1) model differs from the DP process (82) that spontaneous annihilation of particles is not allowed. The action of the BARW process was set up by [215]

$$S = \int d^d x dt [\psi(\partial_t - D\nabla^2)\phi - \lambda(1 - \psi^k)\phi^k + \sigma(1 - \psi^m)\psi\phi] \quad (103)$$

The bosonic RG analysis of BARW systems [215] proved that for $k = 2$ all the lower branching reactions with $m = 2, m = 4, \dots$ are generated via fluctuations involving combinations of branching and annihilation processes. As a consequence for **odd** m the $A \rightarrow \emptyset$ reaction appears (via $A \rightarrow 2A \rightarrow \emptyset$). Therefore after the first coarse graining step in the BARW1 (and in general in the odd m BARW (BARWo) cases) the action becomes the same as that of the DP process. The fluctuations are relevant for $d \leq 2$ and the universal behavior is DP type, with $d_c = 2$. This prediction was confirmed by simulations (see for example [314]).

For even m (BARWe), when the parity of the number of particles is conserved the spontaneous decay $A \rightarrow \emptyset$ is not generated, hence there is an absorbing state with a lonely wandering particle. This system exhibits a non-DP class critical transition, which will be discussed in Sect.IV D 2.

4. DP with spatial boundary conditions

For a review of critical behavior at surfaces of *equilibrium* models see Iglói *et al.* [315]). Cardy [316] suggested that surface critical phenomena may be described by introducing an additional *surface exponent* for the order parameter field which is generally independent of the other bulk exponents. In nonequilibrium statistical physics one can introduce spatial, temporal (see Sect.IV A 7) or mixed (see Sect.IV A 5) boundary conditions. In DP an absorbing wall may be introduced by cutting all bonds (**IBC**) crossing a given $(d-1)$ -dimensional hyperplane in space. In case of reflecting boundary condition (**RBC**) where the wall acts like a mirror so that the sites within the wall are always a mirror image of those next to the wall. A third type of boundary condition is the active boundary condition (**ABC**) where the sites within the wall are forced to be active.

The density at the wall is found to scale as

$$\rho_s^{stat} \sim (p - p_c)^{\beta_1} \quad (104)$$

with a surface critical exponent $\beta_1 > \beta$. Owing to the time reversal symmetry of DP (89) only one extra exponent is needed to describe surface effects, hence the cluster survival exponent is the same

$$\beta'_1 = \beta_1. \quad (105)$$

The mean lifetime of finite clusters at the wall is defined as

$$\langle t \rangle \sim |\Delta|^{-\tau_1} \quad (106)$$

where $\Delta_s = (p - p_c)$, and is related to β_1 by the scaling relation

$$\tau_1 = \nu_{||} - \beta_1 \quad (107)$$

The average size of finite clusters grown from seeds on the wall is

$$\langle s \rangle \sim |\Delta|^{-\gamma_1}, \quad (108)$$

Series expansions [317] and numerical simulations [318] in 1+1 dimensions indicate that the presence of the wall alters several exponents. However, the scaling properties of the correlation lengths (as given by $\nu_{||}$ and ν_{\perp}) are *not* altered.

The field theory for DP in a semi-infinite geometry was first analyzed by Janssen *et al.* [319]. They showed that the appropriate action for DP with a wall at $x_{\perp} = 0$ is given by $S = S_{\text{bulk}} + S_{\text{surface}}$, where

$$S_{\text{surface}} = \int d^{d-1}x \int dt \Delta_s \psi_s \phi_s, \quad (109)$$

with the definitions $\phi_s = \phi(\mathbf{x}_{||}, x_{\perp} = 0, t)$ and $\psi_s = \psi(\mathbf{x}_{||}, x_{\perp} = 0, t)$. The surface term S_{surface} corresponds to the most relevant interaction consistent with the symmetries of the problem and which also respects the absorbing state condition. The appropriate surface exponents were computed to first order in $\epsilon = 4 - d$ using renormalization group techniques:

$$\beta_1 = \frac{3}{2} - \frac{7\epsilon}{48} + O(\epsilon^2). \quad (110)$$

They also showed that the corresponding hyperscaling relation is

$$\nu_{||} + d\nu_{\perp} = \beta_1 + \beta + \gamma_1 \quad (111)$$

relating β_1 to

$$\gamma_1 = \frac{1}{2} + \frac{7\epsilon}{48} + O(\epsilon^2). \quad (112)$$

The schematic phase diagram for boundary DP is shown in Fig. 7, where Δ and Δ_s represent, respectively, the

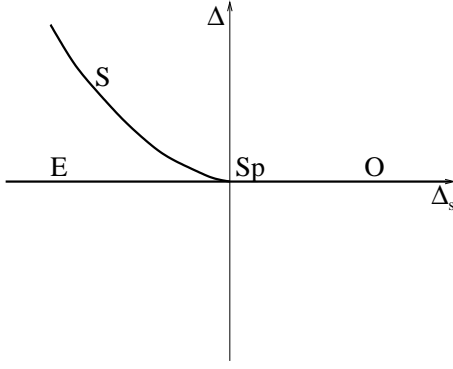


FIG. 7: Schematic mean field phase diagram for boundary DP [278]. The transitions are labeled by O=ordinary, E=extraordinary, S=surface, and Sp=special.

deviations of the bulk and surface from criticality. For $\Delta > 0$ and for Δ_s sufficiently negative the boundary orders even while the bulk is disordered, there is a *surface transition*. For $\Delta_s < 0$ and $\Delta \rightarrow 0$, the bulk orders in the presence of an already ordered boundary, there is an *extraordinary transition* of the boundary. Finally at $\Delta = \Delta_s = 0$, where all the critical lines meet, and where both the bulk and isolated surface are critical, we find a multi-critical point, i.e. the *special transition*.

For $\Delta_s > 0$ and $\Delta \rightarrow 0$ there is an *ordinary transition*, since the bulk orders in a situation in which the boundary, if isolated, would be disordered. At the ordinary transition, one finds just **one extra independent exponent** related to the boundary: this can be the surface density exponent $\beta_{1,\text{dens}}$. In 1d the IBC and RBC cases belong to the same universality class [277] that was identified as the ordinary transition. There are numerical data for the exponents of the extraordinary and special transitions (however see [319] for an RG analysis).

The best exponent estimates currently available were summarized in [278]. Some of them are shown in Table XIII. In $d = 1$ the best results are from series expansions [317, 320]; in all other cases are from Monte-Carlo data. [277, 318, 321, 322] The exponent τ_1 was conjectured to

	$d = 1$	$d = 2$	Mean Field
β_1	0.733 71(2)	1.07(5)	3/2
$\delta_1 = \alpha_1$	0.423 17(2)	0.82(4)	3/2
τ_1	1.000 14(2)	0.26(2)	0
γ_1	1.820 51(1)	1.05(2)	1/2

TABLE XIII: Critical exponents for DP in $d = 1$ and $d = 2$ for the ordinary transition at the boundary.

equal unity, [317] although this has now been challenged by the estimate $\tau_1 = 1.00014(2)$ [320].

It has been known for some time that the presence of an **edge** introduces new exponents, independent of those associated with the bulk or with a surface (see [316]).

For an investigation showing numerical estimates in 2d and mean-field values see [321]. Table IV A 4 summarizes results for the ordinary edge exponents. A closely related application is the study of spreading processes in narrow channels [323].

Angle (α)	$\pi/2$	$3\pi/4$	π	$5\pi/4$
β_2^O ($d = 2$)	1.6(1)	1.23(7)	1.07(5)	0.98(5)
β_2^O (MF)	2	5/3	3/2	7/5

TABLE XIV: Numerical estimates for the ordinary β_2^O exponents for edge DP together with the mean field values. Note that $\beta_2^O(\pi) = \beta_1^O$

5. DP with mixed (parabolic) boundary condition scaling

Kaiser and Turban [324] investigated the 1+1 d DP process confined in a parabola-shaped geometry. Assuming an absorbing boundary of the form $x = \pm Ct^\sigma$ they proposed a general scaling theory. It is based on the observation that the coefficient of the parabola (C) scales as $C \rightarrow \Lambda^{Z\sigma-1}C$ under rescaling

$$x \rightarrow \Lambda x, \quad t \rightarrow \Lambda^Z t, \quad \Delta \rightarrow \Lambda^{-1/\nu_\perp} \Delta, \quad \rho \rightarrow \Lambda^{-\beta/\nu_\perp} \rho, \quad (113)$$

where $\Delta = |p - p_c|$ and Z is the dynamical exponent of DP. By referring to conformal mapping of the parabola to straight lines and deriving it in the mean-field approximation they claimed that this boundary is a relevant perturbation for $\sigma > 1/Z$, irrelevant for $\sigma < 1/Z$ and marginal for $\sigma = 1/Z$ (see Fig. 8). The marginal case results in C dependent non-universal power-law decay, while for the relevant case stretched exponential functions have been obtained. The above authors have given support to these claims by numerical simulations.

6. Lévy flight anomalous diffusion in DP

The effect of Lévy flight anomalous diffusion was already mentioned in Sections III A 5 and III B 4 in case of equilibrium models. In non-equilibrium systems following the suggestion of Mollison [3] Grassberger [158] introduced a variation of the epidemic processes with infection probability distribution $P(R)$, which decays with the distance R as a power-law like

$$P(R) \propto \frac{1}{R^{d+\sigma}}. \quad (114)$$

This can model long-range epidemics mediated by flies, wind, ... etc. He claimed that the critical exponents should depend continuously on σ . This result was confirmed in 1d by estimating β based on CAM calculations in [159]. The study of anomalous diffusion was extended for GEP processes (see Sect. IV B) and for annihilating

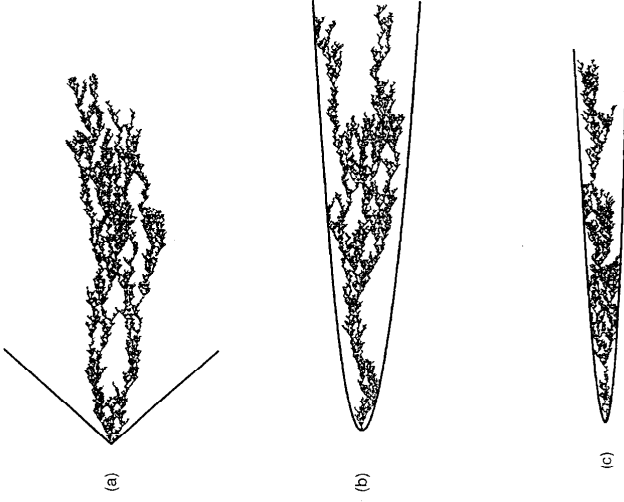


FIG. 8: The space-time evolution of the critical, 1+1 dimensional directed site percolation process confined by parabola [324]. (a) $\sigma < 1/Z$, (b) $\sigma = 1/Z$, (c) $\sigma > 1/Z$.

random walks (see Sect. IV C 4) too. The effective action of the Lévy flight DP model is

$$S[\psi, \phi] = \int d^d x dt \left[\psi(\partial_t - \tau - D_N \nabla^2 - D_A \nabla^\sigma) \phi + \frac{g}{2}(\psi \phi^2 - \psi^2 \phi) \right], \quad (115)$$

where D_N denotes the normal, D_A the anomalous diffusion constant and g is the interaction coupling constant. Field theoretical RG method up to first order in $\epsilon = 2\sigma - d$ expansion [160] gives:

$$\begin{aligned} \beta &= 1 - \frac{2\epsilon}{7\sigma} + O(\epsilon^2), \\ \nu_\perp &= \frac{1}{\sigma} + \frac{2\epsilon}{7\sigma^2} + O(\epsilon^2), \\ \nu_\parallel &= 1 + \frac{\epsilon}{7\sigma} + O(\epsilon^2), \\ Z = \frac{\nu_\parallel}{\nu_\perp} &= \sigma - \epsilon/7 + O(\epsilon^2). \end{aligned} \quad (116)$$

Moreover, it was shown that the hyperscaling relation

$$\eta + 2\delta = d/Z \quad (\delta = \beta/\nu_\parallel), \quad (117)$$

for the so-called critical initial slip exponent η and the relation

$$\nu_\parallel - \nu_\perp(\sigma - d) - 2\beta = 0. \quad (118)$$

hold exactly for arbitrary values of σ . Numerical simulations on 1+1 d bond percolation confirmed these results except in the neighborhood of $\sigma = 2$ [161] (see Fig.9).

7. Long-range correlated initial conditions in DP

It is well known that initial conditions influence the temporal evolution of nonequilibrium systems. The

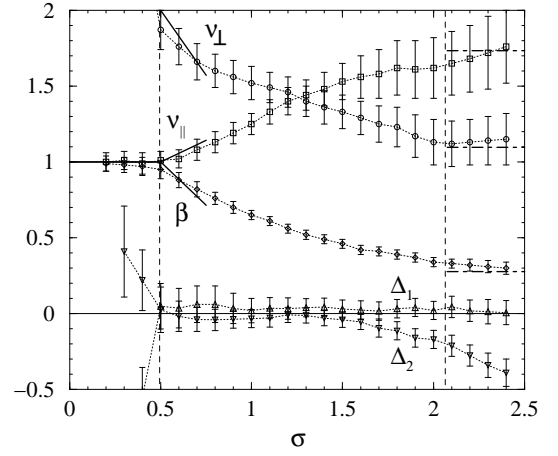


FIG. 9: Estimates for the exponent β and the derived exponents ν_\perp and ν_\parallel in comparison with the field-theoretic results (solid lines) and the DP exponents (dot-dashed lines) [161]. The quantities Δ_1 and Δ_2 represent deviations from the scaling relations (117) and (118), respectively.

“memory” of systems for the initial state usually depends on the dynamical rules. For example, stochastic processes with a finite temporal correlation length relax to their stationary state in an exponentially short time. An interesting situation emerges when a system undergoes a nonequilibrium phase transition in which the temporal correlation length diverges. This setup motivates the question whether it is possible construct initial states that affect the *entire* temporal evolution of such systems.

Monte-Carlo simulations of critical models with absorbing states usually employ two different types of initial conditions. On the one hand *uncorrelated random initial conditions* (Poisson distributions) are used to study the relaxation of an initial state with a finite particle density towards the absorbing state. In this case the particle density $\rho(t)$ decreases on the infinite lattice asymptotically as

$$\rho(t) \sim t^{-\beta/\nu_\parallel}. \quad (119)$$

On the other hand, in spreading simulations [285], each run starts with a *single particle* as a localized active seed from where a cluster originates (this is a long-range correlated state). Although many of these clusters survive for only a short time, the number of particles $n(t)$ averaged over many independent runs *increases* as

$$\langle n(t) \rangle \sim t^{+\eta}, \quad (120)$$

These two cases seem to represent extremal situations where the average particle number either decreases or increases.

A *crossover* between these two extremal cases takes place in a critical spreading process that starts from a random initial condition of very low density. Here the particles are initially separated by empty intervals of a

certain typical size, wherefore the average particle number first increases according to Eq. (120). Later, when the growing clusters begin to interact with each other, the system crosses over to the algebraic decay of Eq. (119) – a phenomenon which is referred to as the “critical initial slip” of nonequilibrium systems [56].

In [165, 379] it was investigated whether it is possible to interpolate *continuously* between the two extremal cases in cases of 1+1 dimensional DP and PC processes. It was shown that one can in fact generate certain initial states in a way that the particle density on the infinite lattice varies as

$$\rho(t) \sim t^\kappa \quad (121)$$

with a continuously adjustable exponent κ in the range

$$-\beta/\nu_\parallel \leq \kappa \leq +\eta. \quad (122)$$

To this end artificial initial configurations with algebraic long-range correlations of the form

$$C(r) = \langle s_i s_{i+r} \rangle \sim r^{-(d-\sigma)}, \quad (123)$$

were constructed, where $\langle \rangle$ denotes the average over many independent realizations, d the spatial dimension, and $s_i = 0, 1$ inactive and active sites. The exponent σ is a free parameter and can be varied continuously between 0 and 1. This initial condition can be taken into account by adding the term

$$S_{ic} = \mu \int d^d x \psi(x, 0) \phi_0(x) \quad (124)$$

to the action, where $\phi_0(x)$ represents the initial particle distribution. The long-range correlations limit $\sigma \rightarrow d$ corresponds to a constant particle density and thus we expect Eq. (119) to hold ($\phi_0(x) = \text{const.}$ is irrelevant under rescaling). On the other hand, the short-range limit $\sigma \rightarrow 0$ represents an initial state where active sites are separated by infinitely large intervals ($\phi_0(x) = \delta^d(x)$) so that the particle density should increase according to Eq. (120). In between we expect $\rho(t)$ to vary algebraically according to Eq. (121) with an exponent κ depending continuously on σ .

In case of the 1+1 d **Domany-Kinzel SCA** (see Sect. IV A 2) field-theoretical renormalization group calculation and simulations proved [165] the exact functional dependence

$$\kappa(\sigma) = \begin{cases} \eta & \text{for } \sigma < \sigma_c \\ \frac{1}{z}(d - \sigma - \beta/\nu_\perp) & \text{for } \sigma > \sigma_c \end{cases} \quad (125)$$

with the critical threshold $\sigma_c = \beta/\nu_\perp$.

8. Quench disordered DP systems

Perhaps the lack of experimental observation of the robust DP class lies in the fact that even weak disorder

changes the critical behavior of such models. Therefore this section provides a view onto interesting generalizations of DP processes that may be observable in physical systems.

First Noest showed [167] using Harris criterion [166] that **spatially quenched disorder** (frozen in space) changes the critical behavior of DP systems for $d < 4$. Janssen [168] studied the problem by field theory taking into account the disorder in the action by adding the term

$$S \rightarrow S + \gamma \int d^d x \left[\int dt \psi \phi \right]^2. \quad (126)$$

This additional term causes **marginal perturbation** and the stable fixed point is shifted to an unphysical region, leading to runaway solutions of the flow equations in the physical region of interest. This means that spatially quenched disorder changes the critical behavior of DP. This conclusion is supported by the simulation results of Moreira and Dickman [169] who reported logarithmic spreading behavior in two-dimensional contact process at criticality. In the sub-critical region they found Griffiths phase in which the time dependence is governed by non-universal power-laws, while in the active phase the relaxation of $P(t)$ is algebraic.

In 1+1 dimension Noest predicted [167] generic scale invariance. Webman et al. [170] reported glassy phase with non-universal exponents in a 1+1 d DP process with quenched disorder. Cafiero *et al.* [171] showed that DP with spatially quenched randomness in the large time limit can be mapped onto a non-Markovian spreading process with memory, in agreement with previous results. They showed that the time reversal symmetry of the DP process (89) is not broken therefore

$$\delta = \delta', \quad (127)$$

and derived a hyper-scaling law for the inactive phase

$$\eta = dz/2 \quad (128)$$

and for the absorbing phase

$$\eta + \delta = dz/2. \quad (129)$$

They confirmed these relations by simulations and found that the dynamical exponents change continuously as the function of the disorder probability. An RG study by Hooyberghs et al. [172] showed that in case of strong enough disorder the critical behavior is controlled by an infinite randomness fixed point (IRFP), the static exponents of which in 1d are

$$\beta = (3 - \sqrt{5})/2, \quad \nu_\perp = 2 \quad (130)$$

and $\xi^{1/2} \propto \ln \tau$. For disorder strengths outside the attractive region of the IRFP disorder dependent critical exponents are detected.

The **temporally quenched disorder** can be taken into the action by adding the term:

$$S \rightarrow S + \gamma \int dt \left[\int d^d x \psi \phi \right]^2. \quad (131)$$

This is a **relevant** perturbation for the DP processes. Jensen [173] investigated the 1+1 d directed bond percolation (see Sect. IV A 2) with temporal disorder via series expansions and Monte Carlo simulations. The temporal disorder was introduced by allowing time slices to become fully deterministic ($p_1 = p_2 = 1$), with probability α . He found α dependent, continuously changing critical point and critical exponent values between those of the the 1+1 d DP class and those of the deterministic percolation. This latter class is defined by the exponents:

$$\beta = 0, \quad \delta = 0, \quad \eta = 1, \quad Z = 1, \quad \nu_{||} = 2, \quad \nu_{\perp} = 2. \quad (132)$$

For small disorder parameter values violation of the Harris criterion is reported.

If **quenched disorder takes place in both space and time** the corresponding term to action is

$$S \rightarrow S + \gamma \int dt d^d x [\psi \phi]^2. \quad (133)$$

and becomes an **irrelevant** perturbation to the Reggeon field theory. This has the same properties as the intrinsic noise in the system and can be considered as being annealed.

B. Dynamical percolation (DyP) classes

If we allow memory in the unary DP spreading process (Sect.IV A) such that the infected sites may have a different re-infection probability (p) than the virgin ones (q) we obtain different percolation behavior [325]. The model in which the re-infection probability is zero is called the General Epidemic Model (GEP) [326]. In this case the epidemic stops in finite systems but an infinite epidemic is possible in the form of a solitary wave of activity. When starting from a single seed this leads to annular growth patterns. The transition between survival and extinction is a critical phenomenon called dynamical percolation [327]. Clusters generated at criticality are the ordinary percolation clusters of the lattice in question. Field theoretical treatment was given by [328, 329, 330, 332, 334]. The action of the model is

$$S = \int d^d x dt \frac{D}{2} \psi^2 \phi - \psi \left(\partial_t \phi - \nabla^2 \phi - r \phi + w \phi \int_0^t ds \phi(s) \right) \quad (134)$$

This is invariant under the non-local symmetry transformation

$$\phi(x, t) \leftrightarrow -\partial_t \psi(x, -t), \quad (135)$$

which results in the hyperscaling relation [39]:

$$\eta + 2\delta + 1 = \frac{dz}{2} \quad (136)$$

As in case of the DP, the relations $\beta = \beta'$ and $\delta = \alpha$ again hold. The upper critical dimension is $d_c = 6$. The dynamical critical exponents as well as spreading and avalanche exponents are summarized in [343]. The dynamical exponents are $Z = 1.1295$ for $d = 2$, $Z = 1.336$ for $d = 3$ and $Z = 2$ for $d = 6$. Dynamical percolation was observed in forest fire models [1, 344] and in some Lotka-Volterra type lattice prey-predator models [345] as well.

1. Isotropic percolation universality classes

The ordinary percolation [17, 18] is a geometrical phenomenon that describes the occurrence of infinitely large connected clusters by **completely random** displacement of some variables (sites, bonds, etc) (with probability p) on lattices (see Fig.10).

The dynamical percolation process is known to generate such percolating clusters (see Sect.IV B). At the transition point moments of the s cluster size distribution $n_s(p)$ show singular behavior. The ordinary percolation corresponds to the $q = 1$ limit of the Potts model. That means its generating functions can be expressed in terms of the free energy of the $q \rightarrow 1$ Potts model. In the

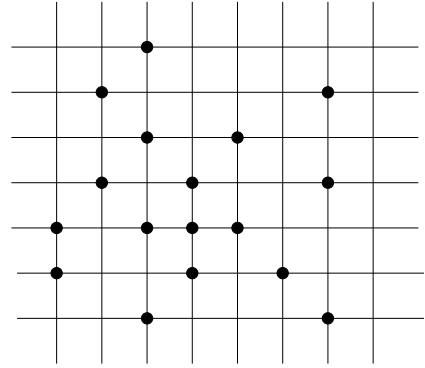


FIG. 10: Isotropic site percolation in $d = 2$ dimensions

low-temperature dilute Ising model the occupation probability (p) driven magnetization transition is an ordinary percolation transition as well. As a consequence the critical exponents of the magnetization can be related to the cluster-size exponents. For example the susceptibility obeys simple homogeneity form with $p - p_c$ replacing $T - T_c$

$$\chi \propto |p - p_c|^{-\gamma} \quad (137)$$

Table XV summarizes the known critical exponents of the ordinary percolation. The exponents are from the overview [156]. Field theoretical treatment [157] provided

an upper critical dimension $d_c = 6$. The $d = 1$ case is special : $p_c = 1$ and the order parameter jumps ($\beta = 0$). Furthermore here some exponents exhibit non-universal behavior by increasing the interaction length unless the we redefine the scaling variable (see [17]).

d	$\beta = \beta'$	γ_p	ν_\perp	σ	τ
1	0	1	1	1	2
2	5/36	43/18	4/3	36/91	187/91
3	0.418(1)	1.793(4)	0.8765(17)	0.452(1)	2.189(1)
4	0.64	1.44	0.68	0.48	2.31
5	0.84	1.18	0.57	0.49	2.41
6	1	1	1/2	1/2	3/2

TABLE XV: Critical exponents of the ordinary percolation

2. DyP with spatial boundary conditions

There are very few numerical results exists for surface critical exponents of the dynamical percolation. The GEP process in 3d was investigated numerically by Grassberger [346]. The surface and edge exponents (for angle $\pi/2$) were determined in case of IBC. Different measurements (density and cluster simulations) resulted in a single surface $\beta_1 = 0.848(6)$ and a single edge $\beta_e = 1.36(1)$ exponent.

3. Lévy flight anomalous diffusion in DyP

To model long-range epidemic spreading in a system with immunization the effect of Lévy flight diffusion (114) was investigated by Janssen et al [160]. The renormalization group analysis of the GEP with anomalous diffusion resulted in the following $\epsilon = 3\sigma - d$ expansion results for the critical initial slip exponent:

$$\eta = \frac{3\epsilon}{16\sigma} + O(\epsilon^2), \quad (138)$$

for the order parameter (density of removed (immune) individuals) exponent:

$$\beta = 1 - \frac{\epsilon}{4\sigma} + O(\epsilon^2), \quad (139)$$

for the spatial correlation exponent

$$\nu_\perp = \frac{1}{\sigma} + \frac{\epsilon}{4\sigma^2} + O(\epsilon^2), \quad (140)$$

and for the temporal correlation length exponent

$$\nu_\parallel = 1 + \frac{\epsilon}{16\sigma} + O(\epsilon^2). \quad (141)$$

C. Voter model (VM) classes

The voter model [2, 348] is defined by the following spin-flip dynamics. A site is selected randomly which takes the “opinion” (or spin) of one of its nearest neighbors (with probability p). This rule ensures that the model has two homogeneous absorbing states (all spin up or down) and is invariant under the Z_2 symmetry. General feature of these models is that dynamics takes place only at the boundaries. The action, which describes this behavior was proposed in [347, 359]

$$S = \int d^d x dt \left[\frac{D}{2} \phi(1 - \phi) \psi^2 - \psi(\partial_t \phi - \lambda \nabla^2 \phi) \right] \quad (142)$$

is invariant under the symmetry transformation:

$$\phi \leftrightarrow 1 - \phi, \quad \psi \leftrightarrow -\psi \quad . \quad (143)$$

This results in the “hyperscaling” relation[39]

$$\delta + \eta = dz/2 \quad (144)$$

that is valid for all first order transitions ($\beta = 0$) with $d \leq 2$, hence $d_c = 2$ is the upper critical dimension. It is also valid for all **compact growth processes** (where “compact” means that the density in surviving colonies remains finite as $t \rightarrow \infty$).

In **one dimension** at the upper terminal point of the DK SCA (Fig.6 $p_1 = \frac{1}{2}$, $p_2 = 1$) an extra Z_2 symmetry exists between 1-s and 0-s, hence the scaling behavior is not DP class like but corresponds to the fixed point of the inactive phase of PC class models (Sect. IV D). As a consequence *compact domains* of 0-s and 1-s grow such as the domain walls follow annihilating random walks (ARW) (see Sect.IV C 1) and belong to the 1d VM class. In 1d the compact directed percolation (CDP) is also equivalent to the $T = 0$ Glauber Ising model (see Sections II,III A). By applying non-zero temperature (corresponding to spin flips in domains) or symmetry breaking (like changing p_2 or adding an external magnetic field) a first order transition takes place ($\beta = 0$).

In **two (and higher) dimensions** the $p = 1$ situation corresponds to the $p_1 = 3/4$, $p_2 = 1$ point in the phase diagram of Z_2 symmetric models (see Fig.1). This model has a “duality” symmetry with coalescing random walks: going backward in time, the successive ancestors of a given spin follow the trail of a simple random walk; comparing the values of several spins shows that their associated random walks necessarily merge upon encounter [2]. This correspondence permits us to solve many aspects of the kinetics. In particular, the calculation of the density of interfaces $\rho_m(t)$ (i.e. the fraction of $+-$ nearest neighbour (n.n.) pairs) starting from random initial conditions of magnetization m , is ultimately given by the probability that a random walk initially at unit distance from the origin, has not yet reached it at time t . Therefore, owing to the recurrence properties of random walks, the VM shows coarsening for $d \leq 2$ (i.e. $\rho_m(t) \rightarrow 0$ when

$t \rightarrow \infty$). For the the ‘marginal’ $d = 2$ case one finds the slow logarithmic decay [349, 350]:

$$\rho_m(t) = (1 - m^2) \left[\frac{2\pi D}{\ln t} + \mathcal{O}\left(\frac{1}{\ln^2 t}\right) \right], \quad (145)$$

with D is being the diffusion constant of the underlying random walk ($D = 1/4$ for the standard case of n.n., square lattice walks, when each spin is updated on average once per unit of time).

Simulating general, Z_2 symmetric spin-flip rules in 2d Dornic et al. [102] conjectured that all critical Z_2 -symmetric rules without bulk noise form a co-dimension-1 ‘voter-like’ manifold separating order from disorder, characterized by the logarithmic decay of both ρ and m . The critical exponents for this class are summarized in Table XVI. Furthermore ref. [102] found that this Z_2

d	β	β'	γ	$\nu_{ }$	ν_{\perp}	Z	δ	η
1	0.0	1	2	2	1	2	1/2	0
2	0.0	1	1	1	1/2	2	1	0

TABLE XVI: Critical exponents of VM classes

symmetry is not a necessary condition, the VM behavior can also be observed in systems without bulk fluctuations, where the total magnetization is conserved. Field theoretical understanding of these results are still lacking.

1. The $2A \rightarrow \emptyset$ (ARW) and the $2A \rightarrow A$ models

As it was mentioned in Sect. IV C in one dimension the annihilating random walk and the voter model are equivalent. In higher dimensions this is not the case (see Sect. IV E). The simplest reaction-diffusion model – in which identical particles follow random walk and annihilate on contact of a pair – is adequately described by mean-field-type equations in $d_c > 2$ dimensions

$$\rho(t) \propto t^{-1}, \quad (146)$$

but in lower dimensions fluctuations become relevant. Omitting boundary and initial condition terms, the field theoretical action is

$$S = \int d^d x dt [\psi(\partial_t \phi - D \nabla^2 \phi) - \lambda(1 - \psi^2)\phi^2] \quad (147)$$

where, D denotes the diffusion coefficient and λ is the annihilation rate.

For $d = d_c = 2$ the leading order decay of the ARW was derived exactly by Lee using field theoretical RG method [356]:

$$\rho(t) = \frac{1}{8\pi D} \ln(t)/t + \mathcal{O}(1/t). \quad (148)$$

For $d = 1$ [357, 358] predicted that the particle density decays as

$$\rho(t) = A_2(Dt)^{-1/2}. \quad (149)$$

This scaling law was confirmed by ϵ expansion and the universal amplitude A_2 was found to be

$$\frac{1}{4\pi\epsilon} + \frac{2 \ln 8\pi - 5}{16\pi} + \mathcal{O}(\epsilon). \quad (150)$$

The universal scaling behavior of the ARW was shown to be equivalent to that of the $A + A \rightarrow A$ coagulation random walk process by Peliti [359]. The renormalization group approach provided universal decay amplitudes (different from those of the ARW) to all orders in epsilon expansion. It was also shown [227] that the motion of kinks in the compact version of directed percolation (CDP) [226] and the Glauber-Ising model [42] at the $T = 0$ transition point are also described exactly by (149). These reactions have also intimate relationship to the EW interface growth model (see Sect. VI B).

2. Compact DP (CDP) with spatial boundary conditions

By introducing a wall in CDP, the survival probability is altered and one obtains surface critical exponents just as for DP. With **IBC**, the cluster is free to approach and leave the wall, but not cross. For $d = 1$, this gives rise to $\beta'_1 = 2$.

On the other hand, for **ABC**, the cluster is stuck to the wall and therefore described by a single random walker for $d = 1$. By reflection in the wall, this may be viewed as *symmetric* compact DP which has the same β' as normal compact DP, giving $\beta'_1 = 1$ [228, 229].

3. CDP with parabolic boundary conditions

Cluster simulations in 1+1 d and MF approximations [363, 364] for CDP confined by repulsive parabolic boundary condition of the form $x = \pm Ct^\sigma$ resulted in C dependent δ and η exponents (see Fig.11) similarly to the DP case (see Sect. IV A 5) in case of marginal condition: $\sigma = 1/2$. In the mean-field approximations [363] similar results were obtained as for the DP [324]. Analytical results can be obtained only in limiting cases. For narrow systems (small C) one obtains the following asymptotic behavior for the connectedness function to the origin:

$$P(t, x) \sim t^{-\pi^2/8C^2} \cos\left(\frac{\pi x}{2C\sqrt{t}}\right). \quad (151)$$

Recently an analytical solution was derived for a related problem [364]. For a one-dimensional lattice random walk with an absorbing boundary at the origin and a movable partial reflector (with probability r) δ varies continuously between 1/2 and 1 as r varies between 0 and 1.

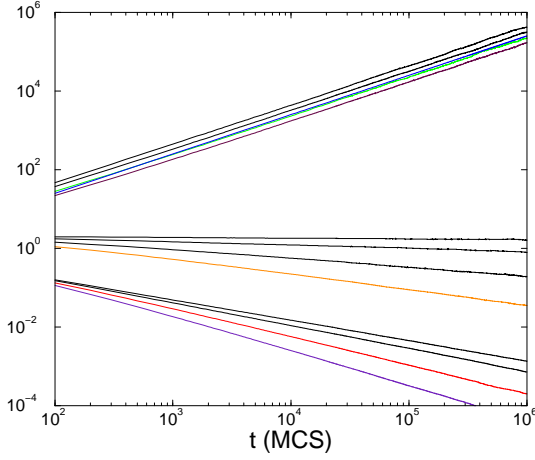


FIG. 11: Parabola boundary confinement cluster simulations for CDP [363]. Middle curves: number of active sites ($C = 2, 1.5, 1.2, 1$ top to bottom); Lower curves: survival probability ($C = 2, 1.5, 1.2, 1$ top to bottom); Upper curves: $R^2(t)$ ($C = 2, 1.5, 1.2, 1$ top to bottom).

4. Lévy flight anomalous diffusion in ARW-s

Particles performing simple random walks subject to the reactions $A + B \rightarrow \emptyset$ (Sect.IV C 1) and $A + A \rightarrow \emptyset$ (Sect.V A) in the presence of a quenched velocity field were investigated in [162]. The quenched velocity field enhances the diffusion in such a way that the effective action of the velocity field is reproduced if Lévy flights are substituted for the simple random walk motion. In the above mentioned reactions the particle density decay is algebraic with an exponent related to the step length distribution of the Lévy flights defined in Eq. (114). These results have been confirmed by several renormalization group calculations [163, 164].

The $A + A \rightarrow \emptyset$ process with anomalous diffusion was investigated by field theory [161]. The action of this model is

$$S[\bar{\psi}, \psi] = \int d^d x dt \left\{ \bar{\psi}(\partial_t - D_N \nabla^2 - D_A \nabla^\sigma) \psi + 2\lambda \bar{\psi} \psi^2 + \lambda \bar{\psi}^2 \psi^2 - n_0 \bar{\psi} \delta(t) \right\} \quad (152)$$

where n_0 is the initial (homogeneous) density at $t = 0$. The density decays for $\sigma < 2$ as :

$$n(t) \sim \begin{cases} t^{-d/\sigma} & \text{for } d < \sigma, \\ t^{-1} \ln t & \text{for } d = d_c = \sigma, \\ t^{-1} & \text{for } d > \sigma. \end{cases} \quad (153)$$

The simulation results of the corresponding 1+1 d lattice model [161] can be seen in Fig. 12. It was also shown in [161] that Lévy flight **annihilation and coagulation processes** ($A + A \rightarrow A$) are in the same universality class.

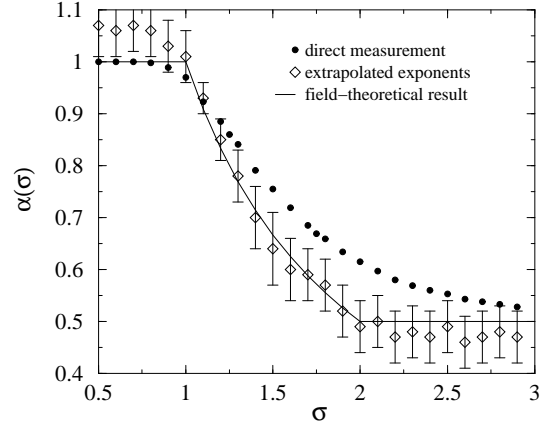


FIG. 12: The anomalous annihilation process: the graph from [161] shows direct estimates and extrapolations for the decay exponent α , as a function of σ . The solid line represents the exact result (neglecting log corrections at $\sigma = 1$).

D. Parity conserving (PC) classes

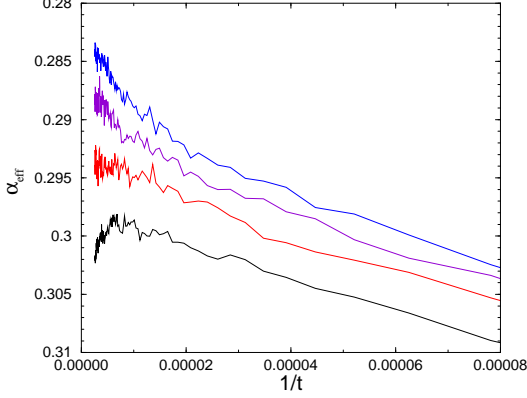
In an attempt to generalize DP and CDP like systems we arrive to new models, in which a conservation law is relevant. A new universality class appears among 1+1 dimensional, single component, reaction-diffusion models. Although it is usually named parity conserving class (PC) examples have proved that the parity conservation itself is not a sufficient condition for the PC class behavior. For example in [371] a 1d stochastic cellular automaton with a global parity conservation was shown to exhibit DP class transition. Binary spreading process (see Sect.V F) in one [372] and two dimensions [373] were also found to be insensitive to the presence of the parity conservation. Multi-component BARW2 models in 1d (see Sect.V K) generate different, robust classes again [215, 225, 375]. By this time it is known that the BARW2 dynamics in **single-component, single-absorbing** state systems (without inhomogeneities, long-range interactions and other symmetries) provides sufficient condition for the PC class [215]. In **single-component, multi-absorbing** state systems the Z_2 symmetry ensures necessary but not sufficient condition, the BARW2 dynamics (Sect.IV D 2) of domain walls is also a necessary condition. Some studies have shown [218, 376, 377] that an external field that destroys the Z_2 symmetry of absorbing states (but preserves the the BARW2 dynamics) yields a DP instead of a PC class transition in the system. Some other names for this class are also used, like directed Ising (DI) class, or BARW class.

1. Grassberger's A and B model

The first models in which non-DP class transition were observed were 1d stochastic cellular automata defined by Grassberger [216]. The **“B” model** defined by the fol-

d	β	β'	γ	δ	Z	$\nu_{ }$	η
1	0.92(3)	0.92(3)	0.00(5)	0.285(2)	1.75	3.25(10)	0.000(1)
2	1	0	1	0	2	1	-1/2

TABLE XVII: Critical exponents of BARWe.

FIG. 13: Local slopes (94) of the density decay in a bosonic BARW2 model. Different curves correspond to $\sigma = 0.466, 0.468, 0.469, 0.47$ (from bottom to top) [313].

theory exists, which gives rather inaccurate critical exponent estimates in [313] bosonic simulations were performed to investigate the density decay of BARW2 from random initial state. Figure 13 shows the local slopes of density decay (α_{eff} (94)) around the critical point for several branching rates (σ). The critical point is estimated at $\sigma_c = 0.04685(5)$, with the corresponding decay exponent $\alpha = 0.290(3)$. This value agrees with that of the PC class.

If there is no explicit diffusion of particles besides the $AA \rightarrow \emptyset$, $A \rightarrow 3A$ processes (called DBAP by Sudbury [381]) an implicit diffusion can still be generated. By spatially asymmetric branching: $A\emptyset\emptyset \rightarrow AAA$ and $\emptyset\emptyset A \rightarrow AAA$ a diffusion may go on by two lattice steps: $A\emptyset\emptyset \rightarrow AAA \rightarrow \emptyset\emptyset A$. As a consequence the decay process slows down, a single particle can not join a domain, hence domain sizes exhibit a parity conservation. This results in additional new sectors (besides the existing two BARW2 sectors) that depend on the initial conditions. For example in case of random initial distribution $\delta \sim 0.13(1)$ was measured by simulations [382]. Similar sector decomposition has been observed in diffusion of k -mer models (see for example M. Barma and co-workers [383]).

3. The NEKIM model

Nonequilibrium Ising models, in which the steady state is generated by kinetic processes in connection with heat baths at different temperatures have widely been investigated [91, 390, 391, 392]. The research of them have

shown that phase transitions are possible even in 1d under nonequilibrium conditions (for a review see Rácz Z. in [81]). In short ranged interaction models any non-zero temperature spin-flip dynamics cause disordered steady state. Menyhárd proposed a class of general nonequilibrium kinetic Ising models (NEKIM) with combined spin flip dynamics at $T = 0$ and Kawasaki spin exchange dynamics at $T = \infty$ in which, for a range of parameters of the model, a PC-type transition takes place [217].

A general form [42] of the Glauber spin-flip transition rate in one-dimension for spin $s_i = \pm 1$ sitting at site i is :

$$W_i = \frac{\Gamma}{2}(1 + \tilde{\delta}s_{i-1}s_{i+1}) \left(1 - \frac{\tilde{\gamma}}{2}s_i(s_{i-1} + s_{i+1})\right). \quad (158)$$

Here $\tilde{\gamma} = \tanh(2J/kT)$, J denotes the coupling constant in the ferromagnetic Ising Hamiltonian, Γ and $\tilde{\delta}$ are further parameters, which can in general, also depend on temperature. The Glauber model is a special case corresponding to $\tilde{\delta} = 0$, $\Gamma = 1$. There are three independent rates:

$$\begin{aligned} w_{same} &= \frac{\Gamma}{2}(1 + \tilde{\delta})(1 - \tilde{\gamma}) \\ w_{oppo} &= \frac{\Gamma}{2}(1 + \tilde{\delta})(1 + \tilde{\gamma}) \\ w_{indif} &= \frac{\Gamma}{2}(1 - \tilde{\delta}), \end{aligned} \quad (159)$$

where the suffices *same* etc. indicate the three possible neighborhoods of a given spin ($\uparrow\uparrow\uparrow, \downarrow\downarrow\downarrow$ and $\uparrow\uparrow\downarrow$, respectively). In the NEKIM model $T = 0$ is taken, thus $\tilde{\gamma} = 1$, $w_{same} = 0$ and $\Gamma, \tilde{\delta}$ are the control parameters to be varied.

The Kawasaki spin-exchange rate of neighboring spins is:

$$w_{ii+1}(s_i, s_{i+1}) = \frac{p_{ex}}{2}(1 - s_i s_{i+1}) \left[1 - \frac{\tilde{\gamma}}{2}(s_{i-1}s_i + s_{i+1}s_{i+2})\right]. \quad (160)$$

At $T = \infty$ ($\tilde{\gamma} = 0$) the above exchange is simply an unconditional nearest neighbor exchange:

$$w_{ii+1} = \frac{1}{2}p_{ex}[1 - s_i s_{i+1}] \quad (161)$$

where p_{ex} is the probability of spin exchange.

The transition probabilities in eqs.(158) and (161) are responsible for the basic elementary processes of kinks (K). Kinks separating two ferromagnetically ordered domains can carry out random walks with probability

$$p_{rw} \propto 2w_{indif} = \Gamma(1 - \tilde{\delta}), \quad (162)$$

while two kinks getting into neighboring positions will annihilate with probability

$$p_{an} \propto w_{oppo} = \Gamma(1 + \tilde{\delta}) \quad (163)$$

(w_{same} is responsible for creation of kink pairs inside of ordered domains at $T \neq 0$). In case of the spin exchanges, which act only at domain boundaries, the process of main importance here is that a kink can produce two offspring at the next time step with probability

$$p_{K \rightarrow 3K} \propto p_{ex}. \quad (164)$$

The abovementioned three processes compete, and it depends on the values of the parameters Γ , δ and p_{ex} what the result of this competition will be. It is important to realize that the process $K \rightarrow 3K$ can develop into propagating offspring production only if $p_{rw} > p_{an}$, i.e. the new kinks are able to travel on the average some lattice points away from their place of birth and can thus avoid immediate annihilation. It is seen from the above definitions that $\tilde{\delta} < 0$ is necessary for this to happen. In the opposite case the only effect of the $K \rightarrow 3K$ process on the usual Ising kinetics is to soften domain walls. In the NEKIM model investigations the normalization condition $p_{rw} + p_{an} + p_{k \rightarrow 3k} = 1$ was set.

The phase diagram determined by simulations and GMF calculations [52, 379] is shown in Fig. 14. The

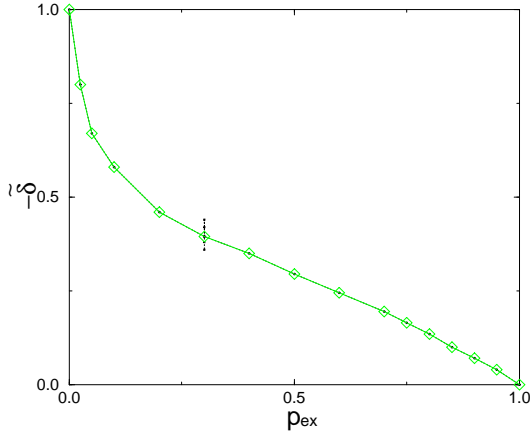


FIG. 14: Phase diagram of the two-parameter model. The transversal dotted line indicates the critical point that was investigated in more detail [379].

line of phase transitions separates two kinds of steady states reachable by the system for large times: in the Ising phase, supposing that an even number of kinks are present in the initial states, the system orders in one of the possible ferromagnetic states of all spins up or all spins down, while the active phase is disordered from the point of view of the underlying spins. The cause of disorder is the steadily growing number of kinks with time. While the low-level, $N = 1, 2$ GMF solutions for the SCA version of NEKIM exhibit first order transitions, for $N > 2$ this becomes continuous. GMF approximations (up to $N = 6$) with CAM extrapolation found $\beta \simeq 1$ [52]. Recent high precision Monte Carlo simulations [379] resulted in critical exponents $\beta = 0.95(2)$ (see Fig. 15) and

$\delta = 0.280(5)$ at the dotted line of the phase diagram.

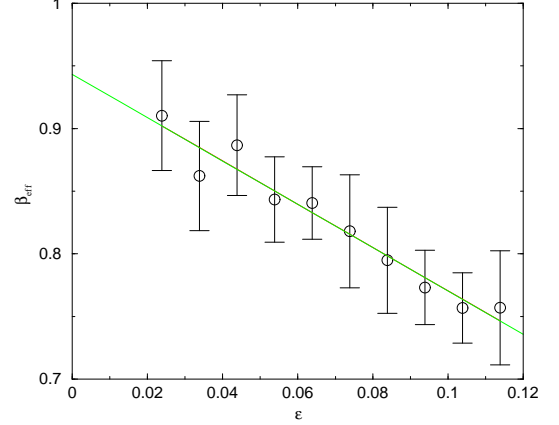


FIG. 15: $\beta_{eff} = \frac{d \log \rho_\infty}{d \log \epsilon}$ of kinks (circles) near the critical point ($\epsilon = |\tilde{\delta} - \tilde{\delta}'|$) and linear extrapolation (dashed line) to the asymptotic value ($\beta = 0.95(2)$). Simulations were performed on a 1d NEKIM ring of size $L = 24000$ [379].

Mussawisade et al. [380] have shown that an exact duality mapping exist in the phase diagram of the NEKIM:

$$\begin{aligned} p'_{an} &= p_{an}, \\ p'_{rw} &= p_{an} + 2p_{ex}, \\ 2p'_{ex} &= p_{rw} - p_{an}. \end{aligned} \quad (165)$$

The regions mapped onto each other have the same physical properties. In particular, the line $p_{ex} = 0$ maps onto the line $p_{rw} = p_{an}$ and the fast-diffusion limit to the limit $p_{ex} \rightarrow \infty$. There is a self-dual line at

$$\tilde{\delta} = \frac{-2p_{ex}}{1 - p_{ex}}. \quad (166)$$

By various static and dynamical simulations spin and kink density critical exponents have been determined in [279] and as the consequence of the generalized hyper-scaling law for the structure factor

$$S(0, t) = L[< M^2 > - < M >^2] \propto t^x, \quad (167)$$

and kink density

$$n(t) = \frac{1}{L} < \sum_i \frac{1}{2} (1 - s_i s_{i+1}) > \propto t^{-y} \quad (168)$$

the exponent relation

$$2y = x \quad (169)$$

is established. Spins-clusters at the PC point grow by compact domains as in the Glauber point albeit with different exponents [43]. The spin-cluster critical exponents in magnetic field are summarized in Table (II). The global persistence (θ_g) and time autocorrelation exponents (λ) were determined both at the Glauber and at the

	β_s	γ_s	$\nu_{\perp,s}$	Z	θ_g	λ_s
Glauber-Ising	0	1/2	1/2	2	1/4	1
PC	.00(1)	.444(2)	.444(2)	1.75(1)	.67(1)	1.50(2)

TABLE XVIII: Simulation data for static and dynamic critical spin exponents for NEKIM.

PC critical points [29] and are shown in Table (XVIII). While at the Glauber point the scaling relation (17) is satisfied by these exponents it is not the case at PC criticality, therefore the magnetization is non-Markovian process here.

By applying an external magnetic field h that breaks the Z_2 symmetry the transition type of the model changes to DP type (see Table XIX). [279]

h	0.0	0.01	0.05	0.08	0.1	DP
β	1.0	0.281	0.270	0.258	0.285	0.2767(4)
γ		0.674	0.428	0.622	0.551	0.5438(13)

TABLE XIX: CAM estimates for the kink density and its fluctuation exponents.

A generalization is the probabilistic cellular automaton version of NEKIM, which consists in keeping the spin-flip rates given in eqs.(159) and prescribing *synchronous updating*. In this case the $K \rightarrow 3K$ branching is generated without the need of additional, explicit spin-exchange process and for certain values of parameter-pairs (Γ, δ) with $\tilde{\delta} < 0$ PC-type transition takes place. The phase boundary of NEKIM-CA in the $(\Gamma, -\tilde{\delta})$ plane is similar to that in Fig. 14 except for the highest value of $\Gamma = 1$, $\tilde{\delta}_c = 0$ cannot be reached, the limiting value is $\tilde{\delta}_c = -.065$.

An other possible variant of NEKIM was introduced in [379] in which the Kawasaki rate eq.(160) is considered at some finite temperature, instead of $T = \infty$, but keeping $T = 0$ in the Glauber-part of the rule. By lowering the temperature the spin exchange process acts against the kink production and a PC class transition occurs. In this case the active phase part of the phase diagram shrinks. For more details see ([280]).

The **DS transition** of this model coincides with the critical point and the scaling behavior of spin and kink damages is the same as that of the corresponding NEKIM variables [281].

4. The generalized Domany-Kinzel model (GDK)

A generalization of the Domany-Kinzel stochastic cellular automaton [227] (see Section IV A 2) was introduced by Hinrichsen (GDK) [221]. This model has $n + 1$ states per site: one active state Ac and n different inactive

states I_1, I_2, \dots, I_n . The conditional updating probabilities are given by $(k, l = 1, \dots, n; k \neq l)$

$$P(I_k | I_k, I_k) = 1, \quad (170)$$

$$P(Ac | Ac, Ac) = 1 - n P(I_k | Ac, Ac) = q, \quad (171)$$

$$P(Ac | I_k, Ac) = P(Ac | Ac, I_k) = p_k, \quad (172)$$

$$P(I_k | I_k, Ac) = P(I_k | Ac, I_k) = 1 - p_k,$$

$$P(Ac | I_k, I_l) = 1, \quad (173)$$

and the symmetric case $p_1, \dots, p_n = p$ was explored. Equations (170)–(172) are straightforward generalizations of Eqs. (99)–(101). The only different process is the creation of active sites between two inactive domains of different colors in Eq. (173). For simplicity the probability of this process was chosen to be equal to one.

For $n = 1$ the model defined above reduces to the original Domany-Kinzel model. For $n = 2$ it has two Z_2 symmetrical absorbing states. The phase diagram of this model is very similar to that of the DK model (Fig. 6) except the transition line is PC type. If we call the regions separating inactive domains I_1 and I_2 as domain walls (denoted by K), they follow BARW2 process

$$K \rightarrow 3K \quad 2K \rightarrow \emptyset \quad K\emptyset \leftrightarrow \emptyset K \quad (174)$$

but for $1 > q > 0$ the size of active regions, hence the domain walls stays finite. Therefore a the observation of the BARW2 process is not so obvious and can be done on coarse grained level only (except at the end-point at $q = 0$, where active sites really look like kinks of the NEKIM model). Series expansions for the transition point and for the order parameter critical exponent resulted in $\beta = 1.00(5)$ [222] that is slightly higher than the most precise simulation results [379] but agrees with the GMF+CAM estimates [52]. Similarly to the NEKIM model the application of external symmetry breaking field changes the PC class transition into a DP class one [221]. The other symmetrical endpoint ($q = 1, p = \frac{1}{2}$) in the phase diagram again shows different scaling behavior (here three types of compact domains grow in competition, the boundaries perform annihilating random walks with exclusion (see. Section VB).

Models with $n > 3$ symmetric absorbing states in 1d do not show phase transitions (they are always active). In terms of domain walls as particles they are related to $N > 1$ component N-BARW2 processes, which exhibit phase transition for zero branching rate only (see Sect.V K) [215, 225].

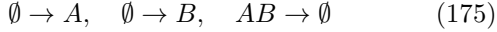
GDK type models – exhibiting n symmetric absorbing states – can be generalized to higher dimensions. In two dimensions Hinrichsen's spreading simulations for the $n = 2$ case yielded mean-field like behavior with $\delta = 1, \eta = 0$ and $z = 1$ leading to the conjecture that $1 < d_c < 2$. A similar model exhibiting Potts-like Z_n symmetric absorbing states in $d = 2$ yielded similar spreading exponents but a first order transition ($\beta = \alpha = 0$) for $n = 2$ [104]. In three dimensions the same model seems to exhibit mean-field like transition

with $\beta = 1$. The verification of these findings would require further research.

5. PC class surface catalytic models

In this subsection I discuss some one-dimensional, surface catalytic-type reaction-diffusion models exhibiting PC class transition. Strictly speaking they are multi-component models, but I show that the symmetries among species enables us to interpret the domain-wall dynamics as a simple BARW2 process.

The two-species monomer-monomer (MM) model was first introduced by [105]. Two monomers, called A and B , adsorb at the vacant sites of a one-dimensional lattice with probabilities p and q , respectively, where $p + q = 1$. The adsorption of a monomer at a vacant site is affected by monomers present on neighboring sites. If either neighboring site is occupied by the same species as that trying to adsorb, the adsorption probability is reduced by a factor $r < 1$, mimicking the effect of a nearest-neighbor repulsive interaction. Unlike monomers on adjacent sites react immediately and leave the lattice, leading to a process limited by adsorption only. The basic reactions are



The phase diagram, displayed in Fig. 16 with p plotted *vs.* r , shows a reactive steady state containing vacancies bordered by two equivalent saturated phases (labeled A and B). The transitions from the reactive phase to ei-

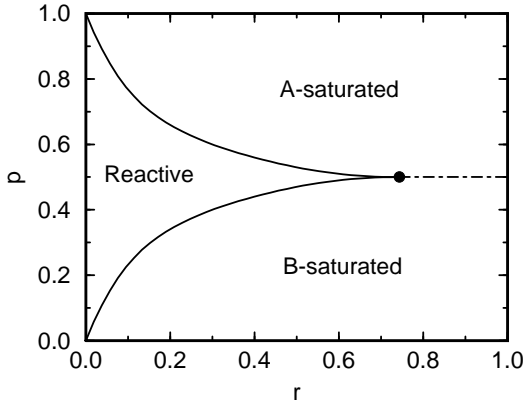


FIG. 16: Phase diagram of the MM from [107].

ther of the saturated phases are continuous, while the transition between the saturated phases is first-order discontinuous. The two saturated phases meet the reactive phase at a *bi-critical* point at a critical value of $r = r_c$. In the case of $r = 1$, the reactive region no longer exists and the only transition is a first-order discontinuous line between the saturated phases. Considering the density of vacancies between unlike species as the order parameter (that can also be called a species “ C ”) the model is the so called “three species monomer-monomer model”.

Simulations and cluster mean-field approximations were applied to investigate the phase transitions of these models [106, 107, 108, 220]. As Fig.17 shows if we call the extended objects filled with vacancies between different species as domain-walls (C) we can observe $C \rightarrow 3C$ and $2C \rightarrow \emptyset$ BARW2 processes in terms of them. These

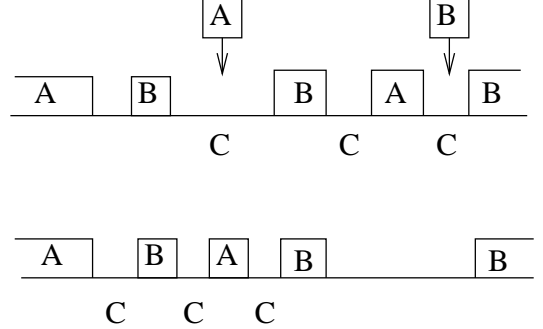


FIG. 17: Domain-wall dynamics in the interacting monomer-monomer model. Left part: branching; right part: annihilation

C parity conserving processes arise as the combination of the elementary reaction steps (175). The reactions always take place at domain boundaries, hence the Z_2 symmetric A and B saturated phases are absorbing.

The interacting monomer-dimer model (IMD) [219] is a generalization of the simple monomer-dimer model [4], in which particles of the same species have nearest-neighbor repulsive interactions. The IMD is parameterized by specifying that a monomer (A) can adsorb at a nearest-neighbor site of an already-adsorbed monomer (restricted vacancy) at a rate $r_A k_A$ with $0 \leq r_A \leq 1$, where k_A is an adsorption rate of a monomer at a free vacant site with no adjacent monomer-occupied sites. Similarly, a dimer (B_2) can adsorb at a pair of restricted vacancies (B in nearest-neighbor sites) at a rate $r_B k_B$ with $0 \leq r_B \leq 1$, where k_B is an adsorption rate of a dimer at a pair of free vacancies. There are no nearest-neighbor restrictions in adsorbing particles of different species and the $AB \rightarrow \emptyset$ desorption reaction happens with probability 1. The case $r_A = r_B = 1$ corresponds to the ordinary noninteracting monomer-dimer model which exhibits a first-order phase transition between two saturated phases in one dimension. In the other limiting case $r_A = r_B = 0$, there exists no fully saturated phase of monomers or dimers. However, this does not mean that this model no longer has any absorbing states. In fact, there are two equivalent (Z_2 symmetric) absorbing states in this model. These states comprise of only the monomers at the odd- or even-numbered lattice sites. A pair of adjacent vacancies is required for a dimer to adsorb, so a state with alternating sites occupied by monomers can be identified with an absorbing state. The PC class phase transition of the $r_A = r_B = 0$ infinite repulsive case has been investigated in [109, 110, 219, 276, 377]. As one can see the basic reactions are similar to those of the MM model (eq. (175)) but the order parameter here is

the density of dimers (K) that may appear between ordered domains of alternating sequences: '0A0..A0A.' and 'A0A..0A0', where monomers are on even or odd sites only. The recognition of an underlying BARW2 process (174) is not so easy in this case, still considering regions between odd and even filled ordered domains one can identify domain wall random-walk, annihilation and branching processes through the reactions with dimers as one can see on the examples below. The introduction of Z_2 symmetry-breaking field, that makes the system prefer one absorbing state to the other was shown to change that transition type from PC to DP [276].

t	A 0 A 0 A 0 A 0 A 0 0 A 0 A 0 A	K
t+1	A 0 A 0 A 0 A 0 A B B A 0 A 0 A	K
t+2	A 0 A 0 A 0 A 0 0 0 B A 0 A 0 A	K K K

t	A 0 A 0 A 0 A 0 A 0 0 0 A 0 A 0	K K
t+1	A 0 A 0 A 0 A 0 A 0 A 0 A 0 A 0	

6. NEKIM with long-range correlated initial conditions

In case of the NEKIM model (see Sect. IV D 3) simulations [280, 379] found that the density of kinks $\rho_k(t)$ changes as

$$\rho_k(t) \propto t^{\kappa(\sigma)} \quad (176)$$

by starting the system with long-range correlated kink distributions of the form (123). The $\kappa(\sigma)$ changes linearly between the two extremes $\beta/\nu_{||} = \pm 0.285$ shown in Fig. 18. This behavior is similar to that of the DP

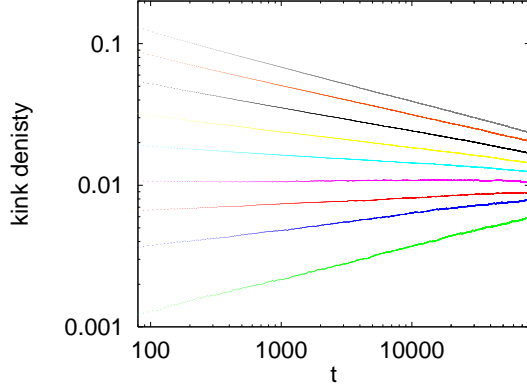


FIG. 18: $\log(\rho_k(t))$ versus $\log(t)$ in NEKIM simulations for $\sigma = 0, 0.1, 0.2, \dots, 1$ initial conditions (from bottom to top curves) [379].

model case (Sect. IV A 7), but here one can observe a symmetry:

$$\sigma \leftrightarrow 1 - \sigma, \quad \kappa \leftrightarrow -\kappa \quad (177)$$

which is related to the duality symmetry of the NEKIM model (165).

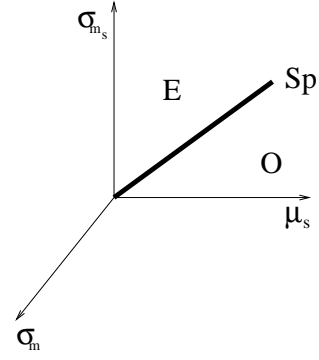


FIG. 19: Schematic mean field boundary phase diagram for BARW from [278]. See text for an explanation of the labeling.

7. GDK with spatial boundary conditions

The surface critical behavior of the GDK model belonging to the PC class (Sect. IV D 4) has been explored by [277, 278, 322]. The basic idea is that on the surface one may include not only the usual BARW2 reactions (174) but potentially also a parity symmetry breaking $A \rightarrow \emptyset$ reaction. Depending on whether or not the $A \rightarrow \emptyset$ reaction is actually present, we may then expect different boundary universality classes. Since the time reversal symmetry (89) is broken for BARW2 processes two independent exponents ($\beta_{1,\text{seed}}, \beta_{1,\text{dens}}$) characterize the surface critical behavior.

The surface phase diagram for the mean field theory of BARW (valid for $d > d_c = 2$) is shown in Fig. 19. Here σ_m, σ_{m_s} are the rates for the branching processes $A \rightarrow (m+1)A$ in the bulk and at the surface, respectively, and μ_s is the rate for the surface spontaneous annihilation reaction $A \rightarrow \emptyset$. Otherwise, the labeling is the same as that for the DP phase diagram (see Figure 7). The $\mu_s > 0$ corresponds to the parity symmetry breaking RBC.

For $\mu_s = 0$ (IBC) parity conserving case the surface action is of the form

$$S_s = \int d^{d-1}x_{||} \int_0^\tau dt \sum_{l=1}^{m/2} \sigma_{2l_s} (1 - \psi_s^{2l} \psi_s \phi_s), \quad (178)$$

where $\psi_s = \psi(\mathbf{x}_{||}, x_\perp = 0, t)$ and $\phi_s = \phi(\mathbf{x}_{||}, x_\perp = 0, t)$. In $d = 1$ the boundary and bulk transitions inaccessible to controlled perturbative expansions, but scaling analysis shows that surface branching is *irrelevant* leading to the Sp* and Sp special transitions. For the $\mu_s > 0$ (RBC) parity symmetry breaking case the surface action is

$$S_2 = \int d^{d-1}x_{||} \int_0^\tau dt \left[\sum_{l=1}^m \sigma_{l_s} (1 - \psi_s^l) \psi_s \phi_s + \mu_s (\psi_s - 1) \phi_s \right]. \quad (179)$$

and the RG procedure shows that the stable fixed point corresponds to the ordinary transition. Therefore in 1d

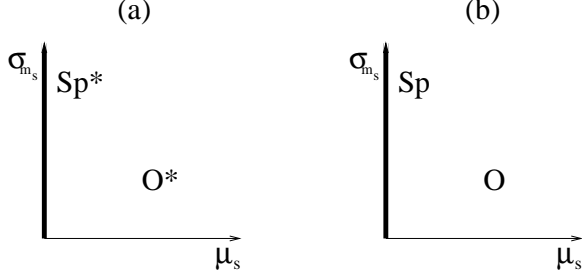


FIG. 20: Schematic surface phase diagrams for BARW in $d = 1$ for (a) $\sigma_m < \sigma_{m,\text{critical}}$, and (b) $\sigma_m = \sigma_{m,\text{critical}}$ [278]. See text for an explanation of the labeling.

the phase diagram looks very differently from the mean-field case (Fig. 20). One can differentiate two cases corresponding to (a) the annihilation fixed point of the bulk and (b) the PC critical point of the bulk. As one can see in both cases the ordinary transition (O, O^*) corresponds to $\mu_s > 0$, RBC and the special transitions (Sp, Sp^*) to $\mu_s = 0$, IBC. The ABC condition obviously behaves as if there existed a surface reaction equivalent to $\emptyset \rightarrow A$, and thus it belongs to the normal transition universality class. By scaling considerations the following scaling relations can be derived:

$$\tau_1 = \nu_{||} - \beta_{1,\text{dens}} \quad , \quad (180)$$

$$\nu_{||} + d\nu_{\perp} = \beta_{1,\text{seed}} + \beta_{\text{dens}} + \gamma_1. \quad (181)$$

In [322] Howard et al. showed that on the self-dual line of the 1d BARWe model (see Sect. IV D 3 and [380]) the scaling relations between exponents of ordinary and special transitions

$$\beta_{1,\text{seed}}^O = \beta_{1,\text{dens}}^{\text{Sp}} \quad (182)$$

and

$$\beta_{1,\text{seed}}^{\text{Sp}} = \beta_{1,\text{dens}}^O. \quad (183)$$

hold. Relying on universality they claim that they should be valid elsewhere close to the transition line. Numerical simulations support this hypothesis as shown in Table XX.

	$d = 1$ (IBC)	$d = 1$ (RBC)	$d = 2$ (O)	$d = 2$ (Sp)
$\beta_{1,\text{seed}}$	2.06(2)	1.37(2)	0	0
$\beta_{1,\text{dens}}$	1.34(2)	2.04(2)	3/2	1
τ_1	1.16(4)	1.85(4)	1	1
γ_1	2.08(4)	2.77(4)	1/2	1/2

TABLE XX: Critical boundary exponents of the PC class in $d = 1, 2$ for ordinary and special cases.

E. Branching with $kA \rightarrow \emptyset$ annihilation

In Sect. IV C 1 the $2A \rightarrow \emptyset$ annihilating random walk (ARW) has already been introduced. By adding branching processes to it we defined the BARWo and BARWe models exhibiting continuous phase transitions (see Sects. IV A 3 and IV D 2). Now we generalize this construction to m -branching and $kA \rightarrow \emptyset$ annihilation type of models (BkARW) formulating it by the field theoretical action:

$$S = \int d^d x dt [\psi(\partial_t - D\nabla^2)\phi - \lambda(1 - \psi^k)\phi^k + \sigma(1 - \psi^m)\psi\phi] \quad (184)$$

These systems for $k > 2$ exhibit an upper critical dimension: $d_c = 2/(k - 1)$ [215, 356] with the mean-field exponents

$$\alpha = \beta = 1/(k - 1), \quad Z = 2, \quad \nu_{\perp} = 1/2 \quad (185)$$

At d_c (which falls below physical dimensions for $k > 3$) the decay has logarithmic corrections:

$$\rho(t) = A_k(\ln(t)/t)^{1/(k-1)} \quad (186)$$

So for the $AAA \rightarrow \emptyset$ process in one dimension this gives the decay behavior [356]:

$$\rho(t) = \left(\frac{1}{4\pi\sqrt{3}D}\right)^{\frac{1}{2}}(\ln(t)/t)^{\frac{1}{2}} + O(t^{\frac{1}{2}}) \quad (187)$$

which is the dominant behavior of the 1d bosonic PCPD model at the transition point (see Sect. V F). Note that for $k = 3, m = 1, 2$ the field theory of [215] predicts DP class transitions in $d = 1$ owing to the BARWo terms generated by the renormalization.

F. General $nA \rightarrow (n + k)A$, $mA \rightarrow (m - l)A$ processes

For a long time branching and annihilating type of RD models with only single parent have been investigated, although there was and early forgotten numerical result by Grassberger [246] claiming a non-DP type of continuous phase transition in a model where particle production can occur by the reaction of two parents. Later it turned out than in such binary production lattice models, where solitary particles follow random walk (hence they behave like a coupled system) different universal behavior emerges indeed (see Sect. V F). In this subsection I shall discuss the mean-field classes in models

$$nA \xrightarrow{\sigma} (n + k)A, \quad mA \xrightarrow{\lambda} (m - l)A, \quad (188)$$

with $n > 1, m > 1, k > 0, l > 0$ and $m - l \geq 0$. In low dimensions the site restricted and bosonic versions of these models exhibit different behavior. The field theory of the $n = m = l = 2$, bosonic model was investigated in [247] and concluded non-DP type of criticality with

$d_c = 2$ (see Sect. VF). For other cases no rigorous field theoretical treatment exist. Numerical simulations in one and two dimensions for various $n = 3$ and $n = 4$ models resulted in somewhat contradictory results [352, 353, 354]. There is a disagreement in the value of the upper critical dimension, but in any case d_c seems to be very low ($d_c = 1-2$) hence the number of non-mean-field classes in such models is limited. On contrary there is a series of mean-field classes **depending on n and m** .

1. The $n = m$ symmetric case

In such models there is a continuous phase transition at finite production probability: $\sigma_c = \frac{l}{k+l}$ characterized by the order parameter exponents [352, 354]:

$$\beta^{MF} = 1, \quad \alpha_{MF} = 1/n. \quad (189)$$

These classes generalize the mean-field class of the DP (Sect.IV A) and binary production models (Sect.VF). For referencing it in Table XXXIII of the Summary I call it as: PARWs (symmetric production and m-annihilating random walk class).

2. The $n > m$ symmetric case

In this case the mean-field solution provides a first order transition (see [354]), hence it does not imply anything with respect to possible classes for models below the critical dimension ($d < d_c$). Note however, that by higher order cluster mean-field approximations, when the diffusion plays a role the transition may turn into a continuous one (see for example [51, 52, 53]).

3. The $n < m$ case

In this case the critical point is at zero production probability $\sigma_c = 0$, where the density decays as $\alpha^{MF} = 1/(m-1)$ as in case of the $n = 1$ branching and $m = l$ annihilating models (BkARW classes see Sect. IV E), but the steady state exponent is different: $\beta^{MF} = 1/(m-n)$, defining an other series of mean-field classes (PARWa) [354]. Again cluster mean-field approximations may predict the appearance of other $\sigma > 0$ transitions with different critical behavior.

V. UNIVERSALITY CLASSES OF MULTI-COMPONENT SYSTEMS

First I recall some well known results (see refs. in [355]) for multi-component reaction-diffusion systems without particle creation. From the viewpoint of phase transitions these describe the behavior in the inactive phase or in case of some N-BARW models right at the critical

point. Then I show the effect of particle exclusions in 1d. Later universal behavior of more complex, coupled multi-component systems are discussed. This field is quite new and some of the results are still under debate.

A. The $A + B \rightarrow \emptyset$ classes

The simplest two-component reaction-diffusion model involves two types of particles undergoing diffusive random walks and reacting upon contact to form an inert particle. The action of this model is:

$$S = \int d^d x dt [\psi_A(\partial_t - D_A \nabla^2) \phi_A + \psi_B(\partial_t - D_B \nabla^2) \phi_B - \lambda(1 - \psi_A \psi_B) \phi_A \phi_B] - \rho(0)(\psi_A(0) + \psi_B(0)) \quad (190)$$

where D_A and D_B denotes the diffusion constants of species A and B . In $d < d_c = 4$ dimensions and for homogeneous, initially equal density of A and B particles (ρ_0) the density decays asymptotically as [360, 361]

$$\rho_A(t) = \rho_B(t) \propto C \sqrt{\Delta} t^{-d/4}, \quad (191)$$

where $\Delta = \rho(0) - C' \rho^{d/2}(0) + \dots$, C is a universal C' is a non-universal constant. This slow decay behavior is due to the fact that in the course of the reaction, local fluctuations in the initial distribution of reactants lead to the formation of clusters of like particles that do not react and they will be asymptotically segregated for $d < 4$. The asymptotically dominant process is the diffusive decay of the fluctuations of the initial conditions. Since this is a short ranged process the system has a long-time memory – appearing in the amplitude dependence – for the initial density $\rho(0)$. For $d \leq 2$ controlled RG calculation is not possible, but the result (191) gives the leading order term in $\epsilon = 2 - d$ expansion. For $D_A \neq D_B$ case a RG study [361] found new amplitude but the same exponents.

The **persistence** behavior in 1d with homogeneous, equal initial density of particles ($\rho_0 = \rho_A(0) + \rho_B(0)$) was studied by [362]. The probability $p(t)$, that an annihilation process has not occurred at a given site (“type I persistence”) has the asymptotic form

$$p(t) \sim \text{const.} + t^{-\theta_l}. \quad (192)$$

For a density of particles $\rho \gg 1$, θ_l is identical to that governing the persistence properties of the one-dimensional diffusion equation, where $\theta_l \approx 0.1207$. In the case of an initially low density, $\rho_0 \ll 1$, $\theta_l \approx 1/4$ was found asymptotically. The probability that a site remains unvisited by any random walker (“type II persistence”) decays in a stretched exponential way

$$p(t) \sim \exp(-\text{const.} \times \rho_0^{1/2} t^{1/4}) \quad (193)$$

provided $\rho_0 \ll 1$.

B. $AA \rightarrow \emptyset, BB \rightarrow \emptyset$ with hard-core repulsion

At the symmetric point of the GDK model (see Sect. IV D 4) compact domains of $I1$ and $I2$ grow separated by $A = Ac - I1$ and $B = Ac - I2$ kinks that cannot penetrate each other. In particle language this system is a reaction-diffusion model of two types $A + A \rightarrow \emptyset, B + B \rightarrow \emptyset$ with exclusion $AB \not\leftrightarrow BA$ and special **pairwise initial conditions** (because the domains are bounded by kinks of the same type):

$$\dots A \dots A \dots B \dots B \dots B \dots B \dots A \dots A \dots$$

In the case of homogeneous, pairwise initial conditions simulations [363] showed a density decay of kinks $\rho \propto t^{-\alpha}$ characterized by a power-law with an exponent somewhat larger than $\alpha = 0.5$. The $\alpha = 1/2$ would have been expected in case of two copies of ARW systems which do not exclude each other. Furthermore the deviation of α from $1/2$ showed an initial density dependence. Ref. [363] provided a possible explanation based on permutation symmetry between types, according to which hard-core interactions cause **marginal perturbation** resulting in non-universal scaling. The situation is similar to that of the compact directed percolation that is confined by parabolic boundary conditions (see Sect. IV C 3) if we assume that AB and BA pairs exert parabolic space-time confinement on coarsening domains. Non-universal scaling can also be observed at surface critical phenomena. Similarly here AB, BA pairs produce 'multi-surfaces' in the bulk. However simulations and independent interval approximations in a similar model predict logarithmic corrections to the single component decay with the form $\rho \sim t^{-1/2}/\ln(t)$ [366]. Note that both kind of behavior may occur in case of marginal perturbations. Cluster simulations [363] also showed initial density ($\rho_{I1}(0)$) dependent survival probability of $I2$ -s in the sea of $I1$ -s:

$$P_{I2}(t) \propto t^{-\delta(\rho_{I1}(0))}. \quad (194)$$

(see Fig.21 with the local slopes defined as $\delta_{eff} = -\frac{d \log P(t)}{d \log t}$)

However this reaction-diffusion model with homogeneous, **random initial distribution** of A -s and B -s exhibits a much slower density decay. An exact duality mapping [365] helps to understand the coarsening behavior. Consider the leftmost particle, which may be either A or B , and arbitrarily relabel it as a particle of species X . For the second particle, we relabel it as Y if it is the same species as the initial particle; otherwise we relabel the second particle as X . We continue to relabel each subsequent particle according to this prescription until all particles are relabeled from $\{A, B\}$ to $\{X, Y\}$. For example, the string

$$AABABBBBA \dots$$

translates to

$$XYYYYXY \dots$$

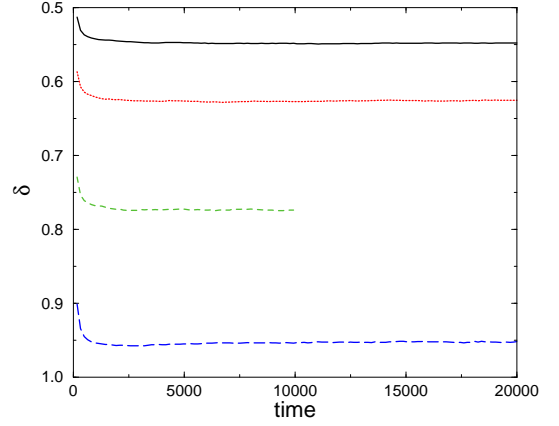
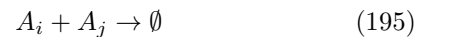


FIG. 21: Local slopes of the $I2$ cluster survival probability in the GDK model at point “A”. The initial state contains uniformly distributed $I1$ -s with initial densities: $\rho_0(I1) = 0.1$ (solid line), 0.25 (dotted line), 0.5 (dashed line), 0.75 (long-dashed line) [363].

The diffusion of the original A and B particles at equal rates translates into diffusion of the X and Y particles. Furthermore, the parallel single-species reactions, $A + A \rightarrow \emptyset$ and $B + B \rightarrow \emptyset$, translate directly to two-species annihilation $X + Y \rightarrow \emptyset$ (see Sect. V A) in the dual system. The interesting point is that in the $X + Y \rightarrow \emptyset$ model blockades do not exist, because XY pairs annihilate, and there is no blockade between XX and YY pairs. Therefore the density decay should be proportional to $t^{-1/4}$. Simulations confirmed this for the $A + A \rightarrow \emptyset, B + B \rightarrow \emptyset$ [223] model, nevertheless corrections to scaling were also observed. The pairwise initial condition transforms in the dual system to domains of $\dots XYXY \dots$ separated by YY and XX pairs, which do not allow X and Y particles to escape each other.

C. Multi-species $A_i + A_j \rightarrow \emptyset$ classes

By generalizing the diffusion-limited reactions $AB \rightarrow \emptyset$ (Sect. V A) for $q > 2$ species



in $d \geq 2$ dimensions the asymptotic density decay for such mutual annihilation processes with equal rates and initial densities is the same as for single-species pair annihilation $AA \rightarrow \emptyset$.

In $d = 1$, however, particles of different types can not pass each other and a segregation occurs for all $q < \infty$. The total density decays according to a q dependent power law, $\rho \propto t^{-\alpha(q)}$ with

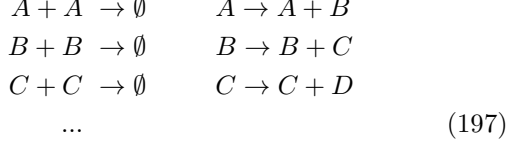
$$\alpha = (q - 1)/2q \quad (196)$$

exactly [367]. These findings were also supported through Monte Carlo simulations. Special initial condi-

tions such as ...*ABCDABCD*... prevent the segregation and lead to decay of the $2A \rightarrow \emptyset$ model (Sect.IV C 1).

D. Unidirectionally coupled ARW classes

An unidirectionally coupled ARW (Sect.IV C 1) system



was introduced and analyzed with RG and simulations by Goldschmidt et al.[407]. This kind of coupling was chosen because $A \rightarrow B$ would constitute a spontaneous death process of A particles leading to exponential density decay. On the other hand quadratic coupling of the form $A + A \rightarrow B + B$ leads to asymptotically decoupled systems [247]. The mean-field theory is described by the rate equation for the density $\rho_i(x, t)$ at level i :

$$\frac{\partial \rho_i(x, t)}{\partial t} = D \nabla^2 \rho_i(x, t) - 2\lambda_i \rho_i(x, t)^2 + \sigma_{i,i-1} \rho_{i-1}(x, t), \quad (198)$$

which relates the long time behavior of level i to level $i - 1$:

$$n_i(t) \propto n_{i-1}^{1/2}. \quad (199)$$

By inserting into this the exact solution for ARW (Sect.IV C 1) one gets:

$$\rho_i(t) \sim \begin{cases} t^{-d/2^i} & \text{for } d < 2, \\ (t^{-1} \ln t)^{1/2^{i-1}} & \text{for } d = d_c = 2, \\ t^{-1/2^{i-1}} & \text{for } d > 2, \end{cases} \quad (200)$$

The action of a two-component system with fields a, \hat{a}, b, \hat{b} for equal annihilation rates (λ) takes the form

$$\begin{aligned} S &= \int d^d x \int dt \left[\hat{a}(\partial_t - D \nabla^2) a - \lambda(1 - \hat{a}^2) a^2 + \right. \\ &\quad \left. + \hat{b}(\partial_t - D \nabla^2) b - \lambda(1 - \hat{b}^2) b^2 + \sigma(1 - \hat{b}) \hat{a} a \right] \end{aligned} \quad (201)$$

The RG solution is plagued by IR-divergent diagrams similarly to UCDP (see Sect.VIH) that can be interpreted as eventual *non-universal* crossover to the decoupled regime. Simulation results – exhibiting finite particle numbers and coupling strengths – really show the breakdown of scaling (200), but the asymptotic behavior could not be determined. Therefore the results (200) are valid for an intermediate time region.

E. DP coupled to frozen field classes

One of the first generalizations of absorbing phase transition models were such systems, which exhibit many

absorbing states, hence the conditions of DP hypothesis [211] (Sect. IV) are not satisfied. Several variants of models with infinitely many absorbing states containing frozen particle configurations have been introduced. The common behavior of these models that non-diffusive (slave) particles are coupled to a DP-like (order parameter) process. In case of homogeneous, uncorrelated initial conditions DP class exponents were found, on the other hand in cluster simulations – that involve correlated initial state of the order parameter particles – initial density dependent scaling exponents (η and δ) arise. These cluster exponents take the DP class values only if the initial density of the slave particles agrees with the “natural density” that occurs in the steady state. The first such models introduced by Jensen and Dickman [368] were the so called pair contact process (PCP) (see Sect. V E 1) and dimer the reaction model. These systems seem to be single component ones by defining rules for the pairs, but the isolated, frozen particles behave as a second component. In the threshold transfer process (TTP) [275] (Sect.V E 2) the two components defined as: the ‘2’-s following DP process and the ‘1’-s which decay or reappear as: $\emptyset \xrightarrow{r} 1 \xrightarrow{1-r} \emptyset$.

For the PCP model defined by the simple processes (207) a set of coupled Langevin equations were set up [331, 332] for the fields $n_1(\mathbf{x}, t)$ and $n_2(\mathbf{x}, t)$ (order parameter):

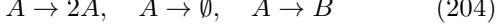
$$\begin{aligned} \frac{\partial n_2}{\partial t} &= [r_2 + D_2 \nabla^2 - u_2 n_2 - w_2 n_1] n_2 + \sqrt{n_2} \eta_2 \\ \frac{\partial n_1}{\partial t} &= [r_1 + D_1 \nabla^2 - u_1 n_2 - w_1 n_1] + \sqrt{n_2} \eta_1 \end{aligned} \quad (202)$$

where D_i, r_i, u_i , and w_i are constants and $\eta_1(\mathbf{x}, t)$ and $\eta_2(\mathbf{x}, t)$ are Gaussian white noises. Owing to the multiple absorbing states and the lack of the time reversal symmetry (89) a generalized hyperscaling law (156) has been derived by Mendes et al. [275]. As discussed in [332] this set of equations can be simplified by dropping the D_1, u_1 , and noise terms in the n_1 equation, and then solving that equation for n_1 in terms of n_2 . Substituting in the n_2 equation, one obtains

$$\begin{aligned} \frac{\partial n_2(\mathbf{x}, t)}{\partial t} &= D_2 \nabla^2 n_2(\mathbf{x}, t) + m_2 n_2(\mathbf{x}, t) - u_2 n_2^2(\mathbf{x}, t) + \\ &\quad + w_2 (r_1/w_1 - n_1(\mathbf{x}, 0)) n_2(\mathbf{x}, t) e^{-w_1 \int_0^t n_2(\mathbf{x}, s) ds} \\ &\quad + \sqrt{n_2(\mathbf{x}, t)} \eta_2(\mathbf{x}, t), \end{aligned} \quad (203)$$

where $n_1(\mathbf{x}, 0)$ is the initial condition of the n_1 field, and $m_2 = r_2 - w_2 r_1/w_1$. The “natural density” [368], n_1^{nat} , then corresponds to the uniform density, $n_1(t = 0) = r_1/w_1$, for which the coefficient of the exponential term vanishes, and we get back the Langevin equation of the RFT (85). This derivation provides a simple explanation for the numerical observation of DP exponents in case of natural initial conditions. However it does not take into account the long-time memory and the fluctuations

of passive particles (with power-law time and p dependences [335]). Therefore, some of the terms omitted in this derivation (as for instance the term proportional to n_2^2 in the equation for n_1) cannot be safely eliminated [336] and this simplified theory does not generate critical fluctuations for its background field. To overcome these problems a more rigorous field theoretical analysis involving path integral representation of a two-component variant of this class (with 'A' activity and 'B' slave):



has been done [337] and provided some evidence that the homogeneous state critical properties of the activity field are DP like irrespectively of the criticality of the slave field. For this model Muñoz et al. [337] could also prove the numerical result [335] that the slave field decays as

$$\rho_B(t) - \rho_B^{nat} \propto t^{-\alpha_{DP}}. \quad (205)$$

However this treatment has still not provided theoretical proof for the initial density dependent spreading exponents observed in simulations [275, 335, 368] and by the numerical integration of the Langevin equation [338]. Furthermore the situation is much more complicated when approaching criticality from the **inactive phase**. In particular, the scaling behavior of n_A in this case seems to be unrelated to n_B (this is similar to the diffusive slave field case [373] Sect. VF 4). In this case it is more difficult to analyze the field theory and dynamical percolation type of terms are generated that can be observed in 2d by simulations and by mean-field analysis [331, 332, 333]. Very recently it was claimed, based on the field theoretical analysis of the GEP model (Sect.IV B) – that exhibits similar long-time memory terms – that the cluster variables should follow stretched exponential decay behavior [334].

In **two dimensions** the critical point of spreading (p_s) moves (as the function of initial conditions) and do not necessarily coincide with the bulk critical point (p_c). The spreading behavior depends on the coefficient of the exponential, non-Markovian term of (203). For positive coefficient the p_s falls in the inactive phase of the bulk and the spreading follows **dynamical percolation** (see Sect. IV B). For negative coefficient the p_s falls in the active phase of the bulk and spreading exponents are **non-universal** (like in 1d) but satisfy the hyper-scaling (156).

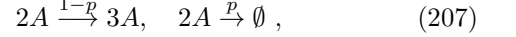
Simulations and GMF analysis [336, 337] in the **inactive phase** in 1d showed, that the steady state density of slave particles approaches the natural value by a power-law

$$|\rho_1^{nat} - \rho_1| \propto |p - p_c|^{\beta_1}, \quad (206)$$

with $\beta_1 \sim 0.9$ for PCPD and $\beta_1 = 1$ for TTP models. This difference might be the consequence that in TTP models the slave field fluctuates and relaxes to r quickly, while in the PCP case it is frozen. Due to this fact one might expect initial condition dependence here again.

1. The pair contact process model

Up to now I discussed spreading processes with unary particle production. Now I introduce a family of systems with **binary** particle production (i.e for a new particle production two particles are needed to collide). The PCP model is defined on the lattice by the following processes:



such that reactions take place at nearest-neighbor (NN) sites and we allow single particle occupancy at most. The order parameter is the density of NN pairs ρ_2 . The PCP exhibits an active phase for $p < p_c$; for $p \geq p_c$ the system eventually falls into an absorbing configuration devoid of NN pairs, (but that contains a density ρ_1 of isolated particles). The best estimate for the critical parameter **in one dimension** is $p_c = 0.077090(5)$ [339]. Static and dynamic exponents corresponding to initially uncorrelated homogeneous state agree well with those of 1+1 d DP (XII). Spreading exponents that involve averaging over all runs, hence involving the survival probability are non-universal (see Fig. 22) [335]. The anomalous criti-

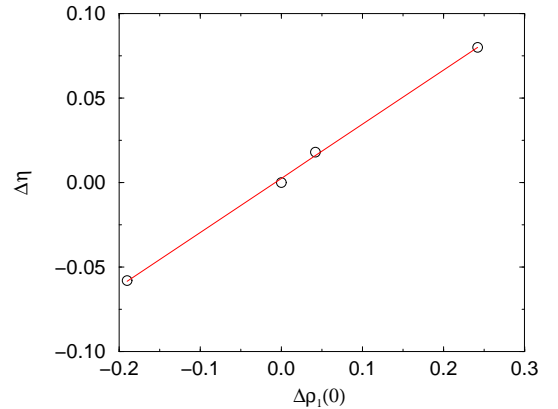


FIG. 22: Initial concentration dependence of the exponent η for PCP model [335]. Linear regression gives a slope $0.320(7)$ between $\eta - \eta_{DP}$ and $\rho_1(0) - \rho_1^{nat}$

cal spreading of PCP can be traced to a long memory in the dynamics of the order parameter ρ_2 , arising from a coupling to an auxiliary field (the local particle density ρ), that remains frozen in regions where $\rho_2 = 0$. In [335] a slight variation of the spreading critical point (as the function of $\rho_1(0)$) was observed (similarly to the 2d case), but more detailed simulations [340] suggest that this can be explained by strong corrections to scaling. Simulations provided numerical evidence that the ρ_1 exhibits anomalous scaling as eq.(206) to $\rho_1^{nat} = 0.242(1)$ with a DP exponent [335] for $p < p_c$ and with $\beta_1 = 0.9(1)$ for $p > p_c$ [336].

The **DS transition** point and the DS exponents of this model coincide with the critical point and the critical exponents of the PCP [335].

The effect of an **external particle source** that creates isolated particles, hence do not couple to the order parameter was investigated by simulations and by GMF+CAM approximations [341]. While the critical point p_c shows a singular dependence on the source intensity, the critical exponents appear to be unaffected by the presence of the source, except possibly for a small change in β .

The properties of the **two dimensional PCP** in case of homogeneous, uncorrelated initial conditions was investigated by simulations [342]. In this case all six NN of a pair was considered for reactions (207). The critical point is located at $p_c = 0.2005(2)$. By determining α , β/ν_\perp and Z exponents and order parameter moment ratios by simulations, the universal behavior of the 2+1 dimensional DP class (XII) was confirmed. The spreading exponents are expected to behave as described in Sect. V E.

2. The threshold transfer process (TTP)

In the 1d TTP model [275], each site may be vacant, single or doubly (active) occupied, and this can be described by a 3-state variable $\sigma_i = 0, 1, 2$. In each time step, a site is chosen at random. In the absence of active sites, the dynamics is indeed trivial: if $\sigma_i(t) = 0$ (or 1), then $\sigma_i(t+1) = 1(0)$ with probability p (or $1-p$). The system relaxes exponentially to a steady state where a fraction p of sites have $\sigma_i = 1$ and the others are vacant. If $\sigma_i(t) = 2$ (active), then $\sigma_i(t+1) = 0$, $\sigma_{i-1}(t+1) = \sigma_{i-1}(t) + 1$, $\sigma_{i+1}(t+1) = \sigma_{i+1}(t) + 1$ if $\sigma_{i+1}(t)$ and $\sigma_{i-1}(t)$ both < 2 and $\sigma_i(t+1) = 1$ if only one of the nearest neighbors of site i ($j = i-1$ or $i+1$) has $\sigma_j(t) < 2$, in which case $\sigma_j(t+1) = \sigma_j(t) + 1$. As can be easily seen, the number of active sites either decreases or remains the same in all processes other than $(1, 2, 1) \rightarrow (2, 0, 2)$; the frequency of these processes depends on the concentration of '1'-s, which is controlled by the parameter p . Any configuration consisting of only '0'-s or '1'-s is absorbing in what concerns the active sites. The absorbing states in the model are fluctuating - in the respective sector of phase space, ergodicity is not broken. It was shown in [335] that the dynamics of '1'-s is strongly affected by the presence of active sites. At the critical point, the concentration of '1'-s relaxes to its steady state value (equal to p_c) by a power-law (205), with 1+1 dimensional DP exponent. The steady state value of ρ_1 was also shown to exhibit anomalous scaling as (206), with $\rho_1^{nat} = p_c = 0.6894(3)$ [275]. In the supercritical region this exponent is DP like [335] (see Fig.23), while in the passive phase $\beta_1 = 1$ [336]. The order-parameter (ρ_2) exponents belong DP class (XII) except for δ and η that are non-universal. They depend on $\rho_1(0)$ linearly and satisfy the hyperscaling law (156).

The **DS transition** and DS exponents of this model co-

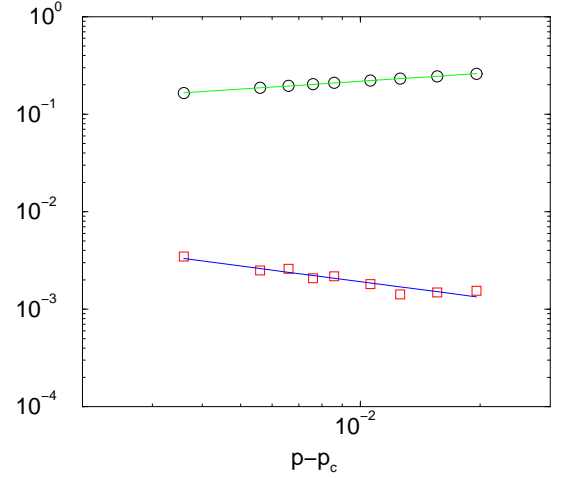
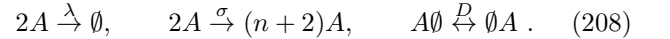


FIG. 23: Log-log plot of $\rho_1(r) - \rho_1(r_c)$ (\circ) and respective fluctuation (square) v.s. $p - p_c$ above the critical point of the TTP model. Least-square regression results in $\beta = 0.27(2)$ and $\gamma = 0.53(6)$ [335]

incide with the critical point and critical exponent values of the TTP model [335].

F. DP with coupled diffusive field classes

The next question one can pose following Section V E is whether a diffusive field coupled to a DP process is relevant. Prominent representatives of such models are binary particle production systems with explicit diffusion of solitary particles. The critical behavior of such systems are still under investigations. The annihilation-fission (AF) process is defined as



The corresponding action for bosonic particles was derived from master equation by Howard and Täuber [247]

$$S = \int d^d x dt [\psi(\partial_t - D\nabla^2)\phi - \lambda(1 - \psi^2)\phi^2 + \sigma(1 - \psi^n)\psi^2\phi^2]. \quad (209)$$

Usually bosonic field theories describe well the critical behavior of “fermionic” systems (i.e. with maximum one particle per site occupation). This is due to the fact that at absorbing phase transitions the occupation number vanishes. In this case however the active phase of bosonic and fermionic models differ significantly: in the bosonic model the particle density diverges, while in the fermionic model there is a steady state with finite density. As a consequence the bosonic field theory cannot describe the active phase and the critical behavior of the fermionic particle system.

As one can see this theory lacks interaction terms linear in the field variable ϕ (massless) in contrast with the DP

action (88). Although the field theory of **bosonic AF** has turned out to be non-renormalizable Howard and Täuber [247] concluded that critical behavior cannot be in DP class. In fact the upper critical behavior is $d_c = 2$ that is different from that of DP and PC classes [373]. In the Langevin formulation

$$\frac{\partial \rho(x, t)}{\partial t} = D \nabla^2 \rho(x, t) + (n\sigma - 2\lambda)\rho^2(x, t) + \rho(x, t)\eta(x, t) \quad (210)$$

the noise is complex:

$$\begin{aligned} \langle \eta(x, t) \rangle &= 0 \\ \langle \eta(x, t)\eta(x', t') \rangle &= [n(n+3)\sigma - 2\lambda]\delta^d(x-x')(t-t'), \end{aligned} \quad (211)$$

that is again a new feature (it is real in case of DP and purely imaginary in case of CDP and PC classes).

Eq.(210) without noise gives the **MF behavior of the bosonic model**: for $n\sigma > 2\lambda$ the density diverges, while for $n\sigma < 2\lambda$ it decays with a power-law with $\alpha_b^{MF} = 1$. The MF description in the **inactive phase** of the bosonic model was found to be valid for the 2d fermionic AF system too [373]. Here the pair density decays as $\rho_2(t) \propto t^{-2}$ [373] in agreement with the MF approximation. Contrary to this for $\lambda \leq \lambda_c$ ρ and ρ_2 seem to be related by a logarithmic ratio $\rho(T)/\rho_2(t) \propto \ln(t)$. This behavior could not be described by the mean-field approximations.

The field theory suggests that the critical behavior of the **1d bosonic model** in the inactive phase is dominated by the $3A \rightarrow \emptyset$ process, that has an upper critical dimension $d_c = 1$. Therefore in one dimension the particle density decays with a power-law exponent: $\alpha = 1/2$ with logarithmic corrections (see Sect. IV E). This behavior has been confirmed by simulations in case of the 1d annihilation-fission model [313].

The field theoretical description of the **fermionic AF** process run into even more serious difficulties [374] than that of the bosonic model and predicted an upper critical dimension $d_c = 1$ that contradicts simulation results [373]. For the fermionic AF system **mean-field** approximations [249, 373] give a continuous transition with exponents

$$\beta = 1, \quad \beta' = 0, \quad Z = 2, \quad \nu_{||} = 2, \quad \alpha = 1/2, \quad \eta = 0. \quad (212)$$

These MF exponents are distinct from those of other well known classes (DP, PC, VM ...). They were confirmed in a 2d fermionic AF model, with logarithmic corrections, indicating $d_c = 2$ [373]. An explanation for the new type of critical behavior based on symmetry arguments are still missing but numerical simulations suggest [248, 252] that the behavior of this system can be described (at least for strong diffusion) by coupled sub-systems: single particles performing annihilating random walk coupled to pairs (B) following DP process: $B \rightarrow 2B$, $B \rightarrow \emptyset$. The model has two non-symmetric absorbing states: one is completely empty, in the other a single particle walks randomly. Owing to this fluctuating absorbing state this model does not oppose the conditions of the DP hypothesis. It was conjectured by Henkel and Hinrichsen

[253] that this kind of phase transition appears in models where (i) solitary particles diffuse, (ii) particle creation requires two particles and (iii) particle removal requires at least two particles to meet. The exploration of other conditions that affect these classes are still under investigation.

1. The PCPD model

A PCPD like model was introduced in an early work by Grassberger [246]. His preliminary simulations in 1d showed non-DP type transition, but the model has been forgotten for a long time. The PCPD model introduced by Carlon et al. [249] is controlled by two parameters, namely the probability of pair annihilation p and the probability of particle diffusion D . The dynamical rules are

$$\begin{aligned} AA\emptyset, \emptyset AA &\rightarrow AAA && \text{with rate } (1-p)(1-D)/2 \\ AA &\rightarrow \emptyset\emptyset && \text{with rate } p(1-D) \\ A\emptyset &\leftrightarrow \emptyset A && \text{with rate } D. \end{aligned} \quad (213)$$

The *mean-field* approximation gives a continuous transition at $p = 1/3$. For $p \leq p_c(D)$ the particle and pair densities exhibit singular behavior:

$$\rho(\infty) \propto (p_c - p)^\beta \quad \rho_2(\infty) \propto (p_c - p)^{\beta_2} \quad (214)$$

while at $p = p_c(D)$ they decay as:

$$\rho(t) \propto t^{-\alpha}, \quad \rho_2(t) \propto t^{-\alpha_2}, \quad (215)$$

with the exponents:

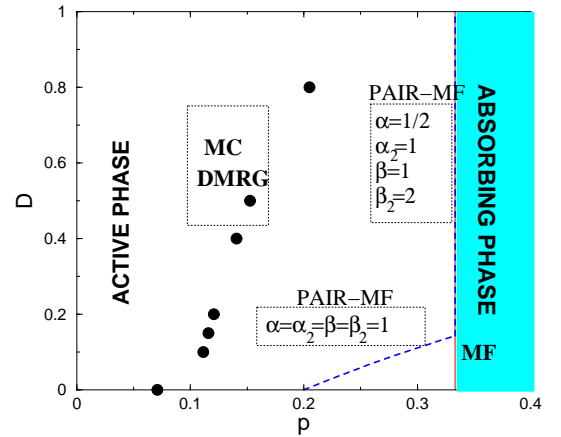


FIG. 24: Schematic phase diagram of the 1d PCPD model. Circles correspond to simulation and DMRG results, solid line to mean-field, dashed line to pair-approximation.

$$\alpha = 1/2, \quad \alpha_2 = 1, \quad \beta = 1, \quad \beta_2 = 2. \quad (216)$$

According to *pair mean-field* approximations the phase diagram can be separated into two regions (see Fig.24).

While for $D > 1/7$ the pair approximation gives the same $p_c(D)$ and exponents as the simple MF, for $D < 1/7$ -s the transition line breaks and the exponents are different

$$\alpha = 1, \quad \alpha_2 = 1, \quad \beta = 1, \quad \beta_2 = 1. \quad (217)$$

In the entire inactive phase the decay is characterized by the exponents:

$$\alpha = 1, \quad \alpha_2 = 2. \quad (218)$$

The DMRG [249] method and simulations of the 1d PCPD model [250] resulted in agreeing $p_c(D)$ values but for the critical exponents no clear picture was found. They could not clarify if the two distinct universality suggested by the pair mean-field approximations was really observable in the 1d PCPD model. It is still a debated topic whether one new class, two new classes or continuously changing exponents occur in 1d. Since the model has two absorbing states (besides the vacuum state there is another one with a single wandering particle) and some exponents were found to be close to those of the PC class ($Z = 1.6 - 1.87$, $\beta/\nu_\perp = 0.47 - 0.51$) Carlon et al. suspected that the transition (at least for low- D values) is PC type [249]. However the lack of Z_2 symmetry, parity conservation and further numerical data [248, 250] exclude this possibility. Note, that the MF exponents are also different from those of the PC class. Simulations and CAM calculations for the one dimensional $n = 1$ AF model [248, 255] corroborated the two new universality class prospect (see Fig.25 and Table XXI). The

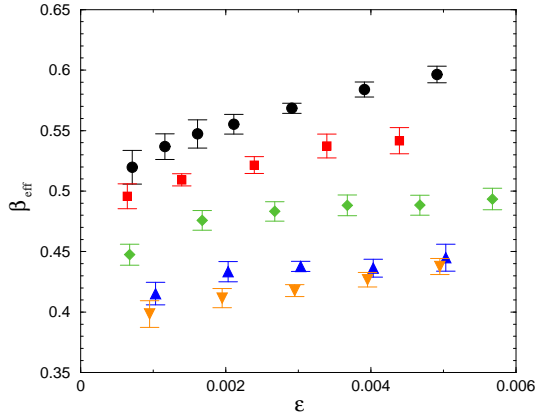


FIG. 25: Effective β exponents for different diffusion rates. The circles correspond to $D = 0.05$, the squares to $D = 0.1$ the diamonds to $D = 0.2$, the up-triangles to $D = 0.5$ and the down-triangles to $D = 0.7$.

order parameter exponent (β) seems to be very far from both of the DP and PC class values [248, 255]. The two distinct class behavior may be explained on the basis of competing diffusion strengths of particles and pairs (i.e. for large D -s the explicit diffusion of lonely particles is stronger). Similar behavior was observed in case of 1d models with coupled (conserved) diffusive field (see Sect.

D	0.05	0.1	0.2	0.5	0.7
p_c	0.10439(1)	0.10688(1)	0.11218(1)	0.13353(1)	0.15745(1)
β	0.39(1)	0.40(1)	0.43(3)	0.49(1)	0.50(1)
α	0.245(5)	0.245(5)	0.21(1)	0.21(1)	0.21(1)

TABLE XXI: Summary of results for the $n = 1$ AF model in 1d[255]. The critical parameter p_c of the random-sequential model is shown here.

VH). However a full agreement has not been achieved in the literature with respect the precise values of the critical exponents. The low- D α is supported by Park et al. [256] who considered the case with coagulation and annihilation rates three times the diffusion rate. On the other hand the high- D α of Table XXI coincides with that of [353], who claim a single value for $0 < D < 1$. By assuming logarithmic corrections it was shown [255] that a single universality class can be supported indeed with exponents

$$\alpha = 0.21(1), \quad \beta = 0.40(1), \\ Z = 1.75(15), \quad \beta/\nu_\perp = 0.38(1), \quad (219)$$

however there is no strong evidence for such corrections. Although the upper critical dimension is expected to be at $d_c = 2$ [373] one may not exclude the possibility of a second critical dimension ($d'_c = 1$) or topological effects in 1d that may cause logarithmic corrections to scaling. The spreading exponent η seems to change continuously by varying D . Whether this is true asymptotically or the effect of some huge correction to scaling is still not clear. The simulations of [248] confirmed that it is irrelevant whether the particles production is spatially symmetric: $A\emptyset A \rightarrow AAA$ or spatially asymmetric: $AA\emptyset \rightarrow AAA$, $\emptyset AA \rightarrow AAA$. Recent simulations and higher level GMF approximations suggest [255, 373] that the peculiarities of the pair approximation are not real; for $N > 2$ cluster approximations the low- D region scaling disappears. Recently two studies [257, 258] reported non-universality in the dynamical behavior of the PCPD. While the former one by Dickman and Menezes explored different sectors (a reactive and a diffusive one) in the time evolution and gave nontrivial exponent estimates, the latter one by Hinrichsen provided a hypothesis that the ultimate long time behavior should be characterized by DP behavior.

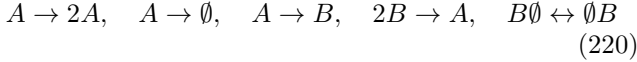
2. The annihilation-coagulation model

If we replace the annihilation process $2A \rightarrow \emptyset$ by coagulation $2A \rightarrow A$ in (208) we get the annihilation-coagulation model. GMF approximations and simulations of this model resulted in similar phase diagram than that of the PCPD model albeit without any sign of two distinct regions. In agreement with this CAM approximations and simulations for the 1d model found the same kind of continuous transition independently from D , with

exponents in agreement with those of the PCPD in the low- D region [251, 256]. Again the spatial symmetry of particle production was found to be irrelevant. An exact solution was found by Henkel and Hinrichsen [253] for the special case in 1d, when the diffusion rate is equal to the coagulation rate, corresponding to the inactive phase according to which the particle decay is like of ARW: $\rho \propto t^{-1/2}$.

3. Cyclically coupled spreading with pair annihilation

A cyclically coupled two-component reaction-diffusion system was introduced by Hinrichsen [252]



which mimics the PCPD model (Sect. VF 1) by mapping pairs to A -s and single particles to B -s. This model is a coupled DP+ARW system. Its $1 + 1d$ critical space-time evolution pattern looks very similar to that of the PCPD model. The appearance of the evolution in space-time seems to be a particular feature of this class. It is built up from compact domains with a cloud of lonely particles wandering and interacting with them. Furthermore this model also has two non-symmetric absorbing states: a completely empty one and another with a single wandering B . By fixing the annihilation and diffusion rates of B -s ($r = D = 1$) the model exhibits continuous phase transition by varying the production rate of A -s and the $A \rightarrow B$ transmutation rate. The simulations in 1d showed that $\rho_A \propto \rho_B$ for large times and resulted in the following critical exponent estimates

$$\alpha = 0.21(2), \quad \beta = 0.38(6), \quad \beta' = 0.27(3), \\ Z = 1.75(5), \quad \nu_{||} = 1.8(1), \quad (221)$$

satisfying the generalized hyperscaling relation (156). These exponents are similar to those of PCPD model in the high diffusion region (see Table XXI) that is reasonable since $D = 1$ is fixed here.

4. The parity conserving AF model

Recently Park et al. [254] investigated a parity conserving representative ($n = 2$) of the 1d AF model (208). By performing simulations for low- D -s they found critical exponents that are in the range of values determined for the corresponding PCPD class. They claim that the conservation law does not affect the critical behavior and that the binary nature of the offspring production is sufficient condition for this class (see however Sect. VF 3, where there is no such condition).

The two dimensional version of the parity conserving AF model was investigated by GMF and simulation techniques [373]. While the $N = 1, 2$ GMF approximations showed similar behavior as in case of the PCPD

model (Sect. VF 1) (including the two class prediction for $N = 2$) the $N = 3, 4$ approximations do not show D dependence of the critical behavior: $\beta = 1, \beta_2 = 2$ was obtained for $D > 0$. For $D = 0$ GMF approximations give $\beta = \beta_2 = 1$ in agreement with DP mean-field type of behavior (see Table XXII). Large scale simulations of

D	$N = 2$			$N = 3$			$N = 4$		
	p_c	β	β_2	p_c	β	β_2	p_c	β	β_2
0.75	0.5	1	2	0.4597	1	2	0.4146	1	2
0.5	0.5	1	2	0.4	1	2	0.3456	1	2
0.25	0.5	1	2	0.3333	1	2	0.2973	1	2
0.1	0.4074	1	1	0.2975	1	2	0.2771	1	2
0.01	0.3401	1	1	0.2782	1	2	0.2759	1	2
0.00	0.3333	1	1	0.1464	1	1	0.1711	1	1

TABLE XXII: Summary of $N = 2, 3, 4$ approximation results of the $n = 2$ AF process

the particle density confirmed the mean-field scaling behavior (212) with logarithmic corrections. This result can be interpreted as a numerical evidence supporting that the upper critical dimension in this model is: $d_c = 2$. The pair density decays in a similar way but with an additional logarithmic factor to the order parameter. This kind of strongly coupled behavior at and above criticality was observed in case of the PCP model too (see Sect. VE 1). At the $D = 0$ endpoint of the transition line $2+1$ d class DP criticality (see Sect. IV A) was found for ρ_2 and for $\rho - \rho(p_c)$. In the inactive phase for $\rho(t)$ we can observe the two-dimensional ARW class scaling behavior (see Sect. IV C 1), while the pair density decays as $\rho_2 \propto t^{-2}$. Again like in $d = 1$ the parity conservation seems to be irrelevant.

G. BARWe with coupled non-diffusive field class

A parity conserving version of the 1d PCP model (Sect. VE 1) was introduced by Marques and Mendes [259], in which pairs follow a BARW2 process, while lonely particles are frozen. This model has infinitely many absorbing states. Simulations showed that while the critical behavior of pairs in case of homogeneous, random initial distribution belongs to the PC class (Sect. IVD 2), the spreading exponents satisfy hyperscaling (156) and change continuously by varying the initial particle density. These results are similar to those found in the PCP model. Again long-memory effects are responsible for the non-universal behavior in case of seed-like initial conditions. The slowly decaying memory was confirmed by studying a one-dimensional, interacting monomer-monomer model [260] by simulations.

H. DP with diffusive conserved slave field classes

One can deduce from the BARW1 spreading process (Sect. IV A 3) a two-component, reaction-diffusion model (DCF) [261, 262] that exhibits total particle density conservation as follows:

$$A + B \xrightarrow{k} 2B, \quad B \xrightarrow{1/\tau} A. \quad (222)$$

By varying the initial particle density ($\rho = \rho_A(0) + \rho_B(0)$) continuous phase transition occurs. General field theoretical investigation was done by Wijland et al. [262] (for the equal diffusion case: $D_A = D_B$ by Kree et al. [261]). The mean-field exponents that are valid above $d_c = 4$ are shown in Table XXIII. The rescaled action of this model is

$$\begin{aligned} S[\varphi, \bar{\varphi}, \psi, \bar{\psi}] = \int d^d x dt & \left[\bar{\varphi}(\partial_t - \Delta)\varphi + \bar{\psi}(\partial_t + \lambda(\sigma - \Delta))\psi \right. \\ & + \mu\bar{\varphi}\Delta\psi + g\psi\bar{\psi}(\psi - \bar{\psi}) + u\psi\bar{\psi}(\varphi + \bar{\varphi}) \\ & + v_1(\psi\bar{\psi})^2 + v_2\psi\bar{\psi}(\psi\bar{\varphi} - \bar{\psi}\varphi) + v_3\varphi\bar{\varphi}\psi\bar{\psi} \\ & \left. - \rho_B(0)\delta(t)\bar{\psi} \right] \end{aligned} \quad (223)$$

where ψ and ϕ are auxiliary fields, defined such that their average values coincide with the average density of B particles and the total density of particles respectively. The coupling constants are related to the original parameters of the master equation by

$$\begin{aligned} \mu &= 1 - D_B/D_A & g &= k\sqrt{\rho}/D_A & \lambda\sigma &= k(\rho_c^{\text{mf}} - \rho)/D_A \\ v_1 &= v_2 = -v_3 = k/D_A & u &= -k\sqrt{\rho}/D_A & \lambda &= D_B/D_A \\ \rho_B(0) &= \rho_B(0)/\sqrt{\rho} \end{aligned} \quad (224)$$

If one omits from the action Eq. (223) the initial time term proportional to $\rho_B(0)$, then the remainder is, for $\mu = 0$ (i. e. $D_A = D_B$), invariant under the time reversal symmetry

$$\begin{aligned} \psi(x, t) &\rightarrow -\bar{\psi}(x, -t) \\ \bar{\psi}(x, t) &\rightarrow -\psi(x, -t) \\ \varphi(x, t) &\rightarrow \bar{\varphi}(x, -t) \\ \bar{\varphi}(x, t) &\rightarrow \varphi(x, -t) \end{aligned} \quad (225)$$

Its epsilon expansion solution [261] and simulation results [263, 264] are summarized in Table XXIII. Interestingly RG predicts $Z = 2$ in all orders of perturbation theory.

d	β	Z	ν_\perp
1	0.44(1)	2	2.1(1)
$4 - \epsilon$	$1 - \epsilon/32$	2	$\frac{1}{2} + \epsilon/8$

TABLE XXIII: Summary of results for DCF classes for $D_A = D_B$

The breaking of this symmetry for $\mu \neq 0$, that is, when the diffusion constants D_A and D_B are different

causes different critical behavior for this system. For $D_A < D_B$ RG [262] predicts new classes with $Z = 2$, $\beta = 1$, $\nu_\perp = 2/d$, but simulations in 1d [264] show different behavior (see Table XXIV). For non-poissonian initial particle density distributions the critical initial slip exponent η varies continuously with the width of the distribution of the conserved density. The $D_A = 0$ extreme

d	β	Z	ν_\perp
1	0.33(2)		2
$4 - \epsilon$	1	2	$2/d$

TABLE XXIV: Summary of results for DCF classes for $D_A < D_B$

case is discussed in Section VI.

For $D_A > D_B$ no stable fixed point solution was found by RG hence [262] conjectured first order transition for which signatures were found in 2d by simulations [265]. However ϵ expansion may break down in case of the occurrence of another critical dimension $d'_c < d_c = 4$ for which simulations in 1d [264] provided numerical support (see Table XXV).

I. DP with frozen conserved slave field classes

If the conserved field coupled to BARW1 process eq. (222) is non-diffusive non-DP universality class (NDCF) behavior is reported [230, 232]. The corresponding action can be derived from (223) in the $D_A = 0$ limit:

$$\begin{aligned} S = \int d^d x dt & \left[\bar{\varphi}(\partial_t + r - D\nabla^2)\varphi + \bar{\psi}(\partial_t - \lambda\nabla^2)\psi \right. \\ & + g\psi\bar{\psi}(\psi - \bar{\psi}) + u\psi\bar{\psi}(\varphi + \bar{\varphi}) + v_1(\psi\bar{\psi})^2 \\ & \left. + v_2\psi\bar{\psi}(\psi\bar{\varphi} - \bar{\psi}\varphi) + v_3\varphi\bar{\varphi}\psi\bar{\psi} \right] \end{aligned} \quad (226)$$

By neglecting irrelevant terms (226) is invariant under the shift transformation

$$\psi \rightarrow \psi + \Delta, \quad r \rightarrow r - v_2\Delta \quad (227)$$

where Δ is any constant. The field theoretical analysis of this action has run into difficulties [232]. The main examples for the NDCF classes are the conserved threshold transfer process (CTTR) and the conserved reaction-diffusion model [230, 232]. Furthermore the models described by the NDCF classes embrace a large group

d	β	Z	ν_\perp
1	0.67(1)		2
$4 - \epsilon$	0		

TABLE XXV: Summary of results for DCF classes for $D_A > D_B$

of stochastic sandpile models [233] in particular fixed-energy Manna models [234, 235, 236]. The upper critical dimension $d_c = 4$ was confirmed by simulations [242].

It was also shown [237] that these classes describe the depinning transition of **quenched Edwards-Wilkinson** (see Sect. VIC) or linear interface models (LIM) [176, 240] owing to the fact that quenched disorder can be mapped onto long-range temporal correlations in the activity field [241]. However this mapping could not be done on the level of Langevin equations of the representatives of NDCF and LIM models and in 1d this equivalence may break down [237, 238, 239]. The critical exponents determined by simulations [230, 232, 243, 244] and GMF+CAM method in 1d [245] are summarized in Table XXVI. Similarly to the PCP these models exhibit infinitely many absorbing states, therefore non-universal spreading exponents are expected (in Table XXVI the exponent η corresponding to natural initial conditions is shown).

d	α	β	γ	Z	$\nu_{ }$	σ	η
1	0.16(4)	0.41(1)		1.5(1)	2.5		
2	0.49(1)	0.64(1)	1.59(3)	1.55(4)	1.29(8)	2.22(3)	0.29(5)
3	0.76(2)	0.84(2)	1.23(4)	1.80(5)	1.10(8)	2.0(4)	0.16(5)
4	1	1	1	2	1	2	0

TABLE XXVI: Summary of results for NDCF classes

J. Coupled N-component DP classes

In [351, 387] Janssen introduced and analyzed by field theoretical RG method (up to two loop order) the quadratically coupled, N-species generalization of the DP process of the form:

$$\begin{aligned}
 A_\alpha &\leftrightarrow 2A_\alpha \\
 A_\alpha &\rightarrow \emptyset \\
 A_\alpha + A_\beta &\rightarrow kA_\alpha + lA_\beta,
 \end{aligned} \tag{228}$$

where k, l may take the values (0,1). He has shown that the multi-critical behavior is always described by the Reggeon field theory (DP class), but this is unstable and leads to unidirectionally coupled DP systems (see Fig.26).

He has also shown that by this model the linearly, unidirectionally coupled DP (UCDP) (see Sect.VIH) case can be described. The universality class behavior of UCDP is discussed in Sect.VIH.

In **one dimension**, if BARWo type of processes are coupled (which alone exhibit DP class transition (see Sect. IV A 3) **hard-core interactions** can modify the phase transition universality (see Sect. VL1).

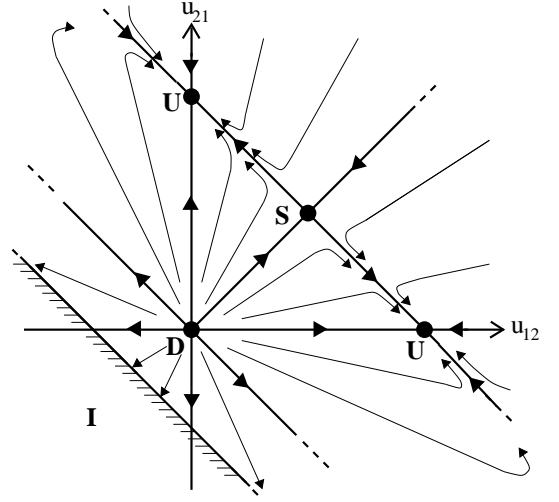


FIG. 26: Flow of the interspecies couplings in the two-component, DP model under renormalization. D means decoupled, S symmetric, U unidirectional fixed points [351].

K. Coupled N-component BARW2 classes

Bosonic, N component BARW systems with two off-springs (N-BARW2), of the form

$$A_\alpha \rightarrow 3A_\alpha \tag{229}$$

$$A_\alpha \rightarrow A_\alpha + 2A_\beta \tag{230}$$

$$2A_\alpha \rightarrow \emptyset \tag{231}$$

were introduced and investigated by Cardy and Täuber [215] via field theoretical RG method. These models exhibit parity conservation of each species and permutation symmetry on N types (generalization for $O(N)$ symmetry is violated by the annihilation term). The $A \rightarrow 3A$ processes turn out to be irrelevant, because like pairs annihilate immediately. Models with (230) branching terms exhibit continuous phase transitions at **zero branching rate**. The universality class is expected to be independent from N and coincides with that of the $N \rightarrow \infty$ (N-BARW2) model that could be solved exactly. The critical dimension is $d_c = 2$ and for $d \leq 2$ the exponents are

$$\beta = 1, \quad Z = 2, \quad \alpha = d/2, \quad \nu_{||} = 2/d, \quad \nu_\perp = 1/d, \tag{232}$$

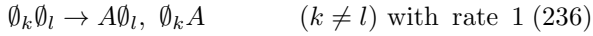
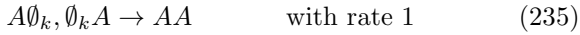
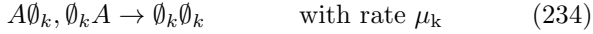
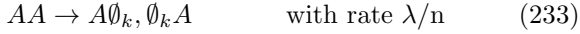
while at $d = d_c = 2$ logarithmic correction to the density decay is expected. Simulations on a $d = 2$ (fermionic) lattice model confirmed these results [223].

In one dimension it turns out that **hard-core interactions** can be relevant and different universal behavior emerges for fermionic models (see Sect. VL). The bosonic description of fermionic models in one dimension works (at least for static exponents) in case of *pairwise initial conditions* (see Sect. VB) when different types of particles do not make up blockades for each other. Such situation happens when these particles are gener-

ated as domain walls of $N+1$ component systems exhibiting S_{N+1} symmetric absorbing states (see Sects. V K 1, V K 2).

1. Generalized contact processes with $n > 2$ absorbing states in 1d

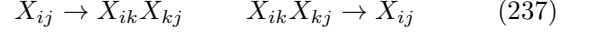
The generalized contact process was introduced by Hinrichsen [221] with the main purpose to show an example for PC class universality class transition in case of Z_2 symmetric absorbing states. The more general case with $n > 2$ permutation symmetric absorbing states was investigated using DMRG method by Hooyberghs et al. [225]. In the one dimensional model, where each lattice site can be occupied by at most one particle (A) or can be in any of n inactive states ($\emptyset_1, \emptyset_2 \dots \emptyset_n$) the reactions are:



The original contact process (Sect. IV A 1), corresponds to the $n = 1$ case, in which the reaction (236) is obviously absent. The reaction (236) in the case $n \geq 2$ ensures that configurations as $(\emptyset_i \emptyset_i \dots \emptyset_i \emptyset_i \emptyset_j \emptyset_j \dots \emptyset_j \emptyset_j)$, with $i \neq j$ are not absorbing. Such configurations do evolve in time until the different domains coarsen and one of the n absorbing states $(\emptyset_1 \emptyset_1 \dots \emptyset_1)$, $(\emptyset_2 \emptyset_2 \dots \emptyset_2)$, $\dots (\emptyset_n \emptyset_n \dots \emptyset_n)$ is reached. For generalized contact processes with $n = 2$, simulations [221] and a DMRG study [225] proved that the transition falls in the PC class if $\mu_1 = \mu_2$, while if the symmetry between the two absorbing states was broken ($\mu_1 \neq \mu_2$) a DP transition was recovered.

The DMRG study for $n = 3$ and $n = 4$ showed that, the model is in the active phase in the whole parameter space and the critical point is shifted to the limit of infinite reaction rates. In this limit the dynamics of the model can be mapped onto the zero temperature n -state Potts model (see also the simulation results of Lipowski and Droz [104]). It was conjectured by [225] the model is in the same N-BARW2 universality class for all $n \geq 3$. By calling a domain wall between \emptyset_i and \emptyset_j as X_{ij} one can follow the dynamics of such variables. In the limit $\lambda \rightarrow \infty$, X_{ij} coincides with the particle A and in the limit $\mu \rightarrow \infty$ X_{ij} coincides with the bond variable $\emptyset_i \emptyset_j$. For finite values of these parameters one still can apply this reasoning at a coarse-grained level. In this case X_{ij} is not a sharp domain wall, but an object with a fluctuating thickness. For $n = 2$ it was shown in Section IV D 4 that such domain wall variables follow BARW2 dynamics (174). For $n > 2$ one can show that besides the N-BARW2 reactions (229),(230) (involving two types of

particles maximum) reaction types involving three different domains ($i \neq j$, $i \neq k$ and $j \neq k$):



occur with increasing importance as $n \rightarrow \infty$. These reactions break the parity conservation of the N-BARW2 process, therefore the numerical findings in [225] for $n = 3, 4$ indicate that they are probably **irrelevant** or the conditions for N-BARW2 universal behavior could be relaxed. Owing to the fact that the X_{ij} variables are domain walls they appear in pairwise manner, hence **hard-core exclusion** effects are ineffective for the critical behavior in 1d. To see the effect of pairwise initial conditions for dynamical exponents see Section V B.

For $n = 3$ upon breaking the global S_3 symmetry to a lower one, one gets a transition either in the directed percolation (Sect. IV A), or in the parity conserving class (Sect. IV D), depending on the choice of parameters [225]. Simulations indicate [394] that for this model local symmetry breaking may also generate PC class transition).

2. The NEKIMA model

By breaking the symmetry of the spin updates in the NEKIM model [393] (Sect. IV D 3) phase transitions with non-PC class behavior emerge. The following changes to the Glauber spin-slip rates (159) with $\Gamma = 1$, $\tilde{\delta} = 0$ were introduced:

$$w(-;++) = 0, \quad (238)$$

$$w(+;+-) = w(+;-+) = p_+ < 1/2, \quad (239)$$

while the spin-exchange part remains the same. In the terminology of domain walls as particles the following reaction-diffusion picture arises. Owing to the symmetry breaking there are two kinds of domain walls $-+ \equiv A$ and $+- \equiv B$, which can only occur alternately ($\dots B..A..B..A..B..A\dots$) owing to the spin background. Upon meeting $AB \rightarrow \emptyset$ happens, while in the opposite sequence, BA , the two domain-walls are repulsive due to (238). The spin exchange leads to $A \leftrightarrow ABA$ and $B \leftrightarrow BAB$ type of kink reactions, which together with the diffusion of A -s and B -s leads to a kind of two-component, coupled branching and annihilating random walk. There are two control parameters in this model: p_{ex} that regulates the kink production-annihilation and p_+ that is responsible for the local symmetry breaking (239). By varying these the phase diagram shown in Fig. 27 occurs. Simulations show that for $p_{ex} \rightarrow 0$, $p_+ < 0.5$ an absorbing phase emerges with N-BARW2 class exponents (owing to the pairwise order of kinks hard-core effects cannot play a role), while the transition on the $p_{ex} > 0$ line belongs to the 1+1 d DP class. Since the $AB \rightarrow \emptyset$ reaction breaks the parity conservation of species (but preserves the global parity conservation) the necessary conditions for N-BARW2 class can be eased. On the other hand the occurrence of the DP transition

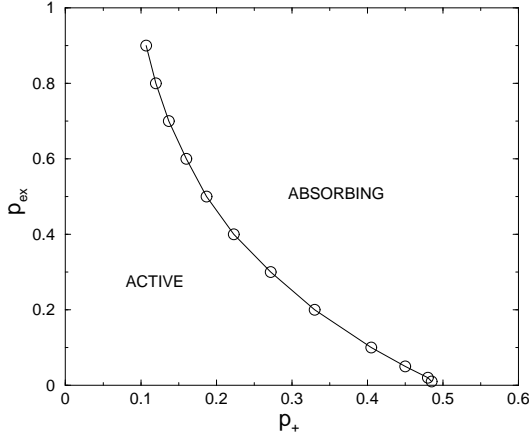


FIG. 27: Phase diagram of the NEKIMA model for $\tilde{\delta} = 0$, $\Gamma = 1$ [393].

introduces a zero branching rate condition for N-BARW2 universal behavior. This study and the results for the generalized contact process (Sect.V K 1) emphasize that the conditions for the N-BARW2 class should be further investigated.

L. Hard-core 2-BARW2 classes in 1d

The effect of particle exclusion (i.e. $AB \not\leftrightarrow BA$) in 2-BARW2 models (Sect.V K) was investigated in [223, 266]. For $d = 2$ the bosonic field theoretical predictions [215] were confirmed [223] (mean-field class transition with logarithmic corrections). In one dimension however two types of phase transitions were identified at zero branching rate ($\sigma = 0$) depending on the arrangement of offspring relative to the parent in process (230). Namely if the parent separates the two offsprings (2-BARW2s):



the steady state density is higher than in the case when they are created on the same site (2-BARW2a):



at a given branching rate, because in the former case they are unable to annihilate each other. This results in different order parameter exponents for the symmetric (2-BARW2s) and for the asymmetric (2-BARW2a) cases

$$\beta_s = 1/2, \quad \beta_a = 2. \quad (242)$$

This result is in contrast with a widespread belief that the bosonic field theory (where $AB \leftrightarrow BA$ is allowed) can describe these systems (because in that case the critical behavior is different (Sect. 232)). This observation led Kwon et al. [266] to the conjecture that in one-dimensional, reaction-diffusion systems a series of new universality classes should appear if particle exclusion is

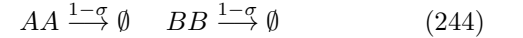
present. Note however, that since the transition is at $\sigma = 0$ in both cases the on-critical exponents do not depend on how particles are created and they can be identified with those described in Sect.(V B). In [223] a set of critical exponents satisfying scaling relations have been determined for this two new classes shown in Table XXVII.

exponent	N-BARW2	N-BARW2s	N-BARW2a
$\nu_{ }$	2	2.0(1) 0.915(2)	8.0(4) 3.66(2)
Z	2	4.0(2) 1.82(2)*	4.0(2) 1.82(2)*
α	1/2	0.25(1) 0.55(1)*	0.25(1) 0.55(1)*
β	1	0.50(1) 1.00(1)	2.0(1) 1.00(1)

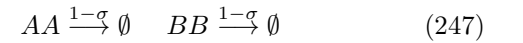
TABLE XXVII: Summary of critical exponents in one dimension for N-BARW2 like models. The N-BARW2 data are quoted from [215]. Data divided by "|" correspond to random vs. pairwise initial condition cases [225, 363, 393]. Exponents denoted by * exhibit slight initial density dependence.

1. Hard-core 2-BARWo models in 1d

Hard-core interactions in the two-component, one-offspring production model (2-BARW1) were investigated in [267]. Without interaction between different species one would expect DP class transition. By introducing the $AB \not\leftrightarrow BA$ blocking to the two-component model:



a DP class transition at $\sigma = 0.81107$ was located. Note that the effect exerted by different species on each other is irrelevant now unlike for the case of coupled ARW (Sect.V B). On the other hand if we couple the two subsystems by production:



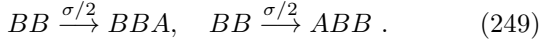
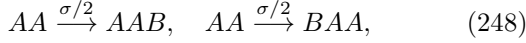
a continuous phase transition emerges at $\sigma = 0$ rate – therefore the on-critical exponents are the same as those described in Sect. (V B) – and the order parameter exponent was found to be $\beta = 1/2$. Therefore this transition belongs to the same class as the 2-BARW2s model (see Sect.V L). The parity conservation law, which is relevant in case of one component BARW systems (PC versus DP class) turns out to be irrelevant here. This finding reduces the expectations suggested by [266] for a whole new series of universality classes in 1d systems with exclusions. In fact the blockades introduced by exclusions generate robust classes. In [267] a hypothesis

was set up that **in coupled branching and annihilating random walk systems of N-types of excluding particles for continuous transitions at $\sigma = 0$ two universality classes exist, those of 2-BARW2s and 2-BARW2a models**, depending on whether the reactants can immediately annihilate (i.e. when similar particles are not separated by other type(s) of particle(s)) or not. Recent investigations in similar models [268, 370] are in agreement with this hypothesis.

2. Coupled binary spreading processes

Two-component versions of the PCPD model (Sect. VF1) with particle exclusion in 1d were introduced and investigated by simulations in [224] with the aim to test if the hypothesis for N-BARW systems set up in [267] (Sect.VL1) can be applied for such models. The following models with the same diffusion and annihilation terms ($AA \rightarrow \emptyset$, $BB \rightarrow \emptyset$) as in (Sect.VB) and different production processes were investigated.

1) Production and annihilation random walk model (2-PARW):

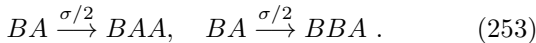
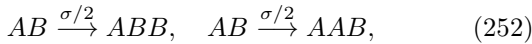


2) Symmetric production and annihilation random walk model (2-PARWS):



These two models exhibit active steady states for $\sigma > 0$ with a continuous phase transition at $\sigma_c = 0$. Therefore the exponents at the critical point are those of the 2-component ARW model with exclusion (Sect. VB). Together with the exponent $\beta = 2$ result for both cases this indicates that they belong to the N-BARW2a class. This also means that the hypothesis set up for N-BARW systems [267] (Sect.VL1) can be extended.

3) Asymmetric production and annihilation random walk model (2-PARWA):



This model does not have an active steady state. The AA and BB pairs annihilate themselves on contact, while if an A and B particle meet an $AB \rightarrow ABB \rightarrow A$ process eliminates blockades and the densities decay with the $\rho \propto t^{-1/2}$ law for $\sigma > 0$. For $\sigma = 0$ the blockades persist, and in case of random initial state $\rho \propto t^{-1/4}$ decay (see Sect. VB) can be observed here.

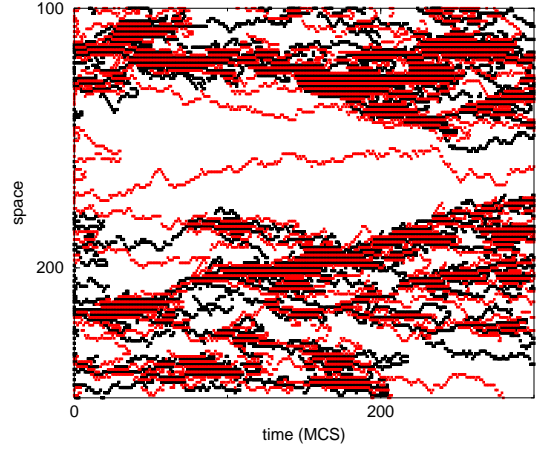
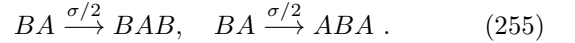
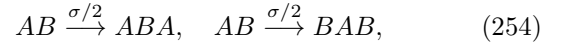


FIG. 28: Space-time evolution of the 2-PARWAS model at the critical point [224]. Black dots correspond to A particles, others to B -s.

4) Asymmetric production and annihilation random walk model with spatially symmetric creation (2-PARWAS):



In this case AB blockades proliferate by production events. As a consequence of this an active steady state appears for $\sigma > 0.3253(1)$ with a continuous phase transition. The space-time evolution from random initial state shows (Fig.28) that compact domains of alternating $...ABAB...$ sequences separated by lonely wandering particles are formed. This pattern is very similar to what was seen in case of one-component binary spreading processes [252]: compact domains within a cloud of lonely random walkers, except that now domains are built up from alternating sequences only. This means that the $...AAAA...$ and $...BBBB...$ domains decay by this annihilation rate and the particle blocking is responsible for the formation of compact clusters. In the language of coupled DP + ARW model [252] the pairs following DP process are the AB pairs now, which cannot decay spontaneously but through an annihilation process: $AB + BA \rightarrow \emptyset$. They interact with two types of particles executing annihilating random walk with exclusion. The simulations resulted in the critical exponent estimates: $\beta = 0.37(2)$, $\alpha = 0.19(1)$ and $Z = 1.81(2)$ which agree fairly well with those of the PCPD model in the high diffusion rate region [248].

VI. INTERFACE GROWTH CLASSES

Interface growth classes are strongly related to the basic universality classes discussed so far and can be observed in experiments more easily. For example one of the few experimental realizations of the robust DP class (IV A) is related to a depinning transition in inhomogeneous media.

geneous porous media [174] (see Sect.VIF). The interface models can either be defined by continuum equations or by lattice models of solid-on-solid (SOS) or restricted solid-on-solid (RSOS) types. In the latter case the height variables h_i of adjacent sites are restricted

$$|h_i - h_{i+1}| \leq 1. \quad (256)$$

The morphology of a growing interface is usually characterized by its width

$$W(L, t) = \left[\frac{1}{L} \sum_i h_i^2(t) - \left(\frac{1}{L} \sum_i h_i(t) \right)^2 \right]^{1/2}. \quad (257)$$

In the absence of any characteristic length, growth processes are expected to show power-law behavior of the correlation functions in space and height and the *Family-Vicsek* scaling [175] form:

$$W(L, t) = t^{\tilde{\alpha}/Z} f(L/\xi_{||}(t)), \quad (258)$$

describes the surface, with the scaling function $f(u)$

$$f(u) \sim \begin{cases} u^{\tilde{\alpha}} & \text{if } u \ll 1 \\ \text{const.} & \text{if } u \gg 1 \end{cases}. \quad (259)$$

Here $\tilde{\alpha}$ is the roughness exponent and characterizes the stationary regime in which correlation length $\xi_{||}(t)$ has reached a value larger than the system size L . The ratio $\tilde{\beta} = \tilde{\alpha}/Z$ is called as the growth exponent and characterizes the short time behavior of the surface. Similarly to equilibrium critical phenomena, these exponents do not depend on the microscopic details of the system under investigation. Using these exponents it is possible to divide growth processes into universality classes [176, 177]. The (258) scaling form of W^2 is invariant under Λ the rescaling

$$x \rightarrow \Lambda x, \quad t \rightarrow \Lambda^Z t, \quad h(x, t) \rightarrow \Lambda^{-\tilde{\alpha}} h(x, t) \quad (260)$$

Recently **anomalous roughening** has been observed in many growth models and experiments. In these cases the measurable $\tilde{\alpha}_{loc}$ roughness exponent is different from $\tilde{\alpha}$ and may satisfy different scaling law [89, 177, 179, 180, 181, 182, 183, 185, 186, 187, 188, 189].

Surfaces in $d + 1$ dimensional systems can be **mapped** onto a time step of a d dimensional particle reaction-diffusion or spin models. For example the 1d Kawasaki spin model corresponding to the $K \leftrightarrow 3K$ process with random walk of kinks the mapping onto the 1d surface is shown in Fig. 29.

This means that to a unique $\{s_j\}$ spin configuration at time t corresponds a spatial profile $\{h_i(t)\}$ by accumulating the spin values

$$h_i(t) = \sum_{j=1}^i s_j \quad (261)$$

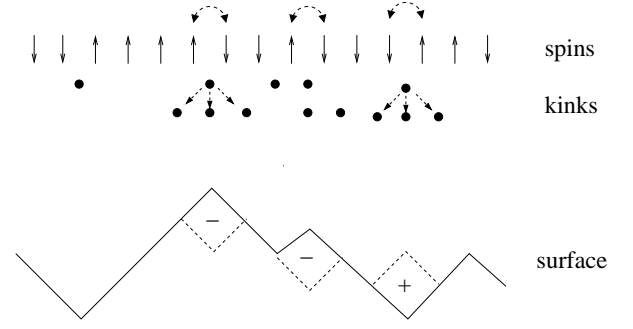


FIG. 29: Mapping between spins, kinks and surfaces

In 1d the surface can also be considered as a random walker with fluctuation

$$\Delta x \propto t^{1/Z_w} \quad (262)$$

hence the roughness exponent is related to the dynamical exponent Z_w as

$$\tilde{\alpha} = 1/Z_w. \quad (263)$$

The $\tilde{\alpha} = 1/2$ corresponds to uncorrelated (or finite correlation length) random walks. If $\tilde{\alpha} > 1/2$ the surface exhibits correlations, while if $\tilde{\alpha} < 1/2$ the displacements in the profile are anti-correlated. Since the surfaces may exhibit drifts the fluctuations around the mean is measured defining the local roughness (Hurst) exponent. Using this surface mapping Sales et al. [190] have characterized the different classes of Wolfram's 1d cellular automata [302].

One can show that by coarse graining the 1d Kawasaki dynamics

$$w_i = \frac{1}{4\tau} [1 - \sigma_i \sigma_{i+1} + \lambda(\sigma_{i+1} - \sigma_i)] \quad (264)$$

a mapping can be done onto the KPZ equation (274), and the surface dynamics for $\lambda \neq 0$ (corresponding to anisotropic case) is in the KPZ class (Sect.VID) while for $\lambda = 0$ it is in the Edward Wilkinson class (Sect. VIB).

While these classes are related to simple random walk with $Z_w = 1/\tilde{\alpha} = 2$ the question arises what surfaces are related to other kind of random walks (example Levy-flights or correlated random walks etc ...). Recently it was shown that globally constrained random walks (i.e. when a walker needs to visit each site an even number of times) can be mapped onto surfaces with dimer-type of dynamics [192] with $Z_w = 3 = 1/\tilde{\alpha}$.

By studying correspondence between lattice models with absorbing states and models of pinned interfaces in random media Dickman and Muñoz [191] established the scaling relation

$$\tilde{\beta} = 1 - \beta/\nu_{||} \quad (265)$$

that was confirmed numerically for $d = 1, 2, 3, 4$ contact processes (Sect. IV A 1). The local roughness exponent was found to be smaller than the global value indicating anomalous surface growth in DP class models.

In interface models different types of transitions may take place. **Roughening transitions** may occur between smooth phase characterized by finite width W (in an infinite system) and rough phase when the width and diverges in an infinite system (but saturates in finite ones) by varying some control parameters (ϵ). Near the transition point the spatial ($\xi_{||}$) and growth direction correlations (ξ_{\perp}) diverge as

$$\xi_{||} \propto \epsilon^{\nu_{||}} \quad (266)$$

$$\xi_{\perp} \propto \epsilon^{\nu_{\perp}} \quad (267)$$

(note that in RD systems $\xi_{||}$ denote temporal correlation length). In the smooth phase the heights $h_i(t)$ are correlated below ξ_{\perp} . While in equilibrium models roughening transitions exist in $d > 1$ dimensions only in nonequilibrium models this may occur in $d = 1$ as well.

An other surface transition is the **depinning transition**, when as the consequence of changing some control parameter (usually an external force F) the surface starts propagating with speed v and evolves in a rough state. Close to the transition v is expected to scale as

$$v \propto (F - F_c)^{\tilde{\theta}} \quad (268)$$

with the $\tilde{\theta}$ velocity exponent and the correlation exponents diverge. Known depinning transitions (in random media) are related to absorbing phase transitions with conserved quantities (see Sects. VIC, VIE).

In the rough phase a so-called **faceting phase transition** may also take place when up-down symmetrical facets appear. In this case the surface scaling behavior changes (see Section VII).

A. The random deposition class

The random deposition is the simplest surface growth process that involves uncorrelated adsorption of particles on top of each other. Therefore columns grow independently, linearly without bounds. The roughness exponent $\tilde{\alpha}$ (and correspondingly Z) is not defined here. The width of the surface grows as $W \propto t^{1/2}$ hence $\tilde{\beta} = 1/2$ in all dimensions. An example for such behavior is shown in a dimer growth model in Sect. VII 1.

B. Edwards-Wilkinson (EW) classes

If we postulate the following translation and reflection symmetries

$$\mathbf{x} \rightarrow \mathbf{x} + \Delta\mathbf{x} \quad t \rightarrow t + \Delta t \quad h \rightarrow h + \Delta h \quad \mathbf{x} \rightarrow -\mathbf{x} \quad h \rightarrow -h \quad (269)$$

we are led to the Edwards-Wilkinson (EW) equation [193]

$$\partial_t h(\mathbf{x}, t) = v + \sigma \nabla^2 h(\mathbf{x}, t) + \zeta(\mathbf{x}, t), \quad (270)$$

which is the simplest stochastic differential equation that describes a surface growth with these symmetries. Here v denotes the mean growth velocity, σ the surface tension and ζ the zero-average Gaussian noise field with variance

$$\langle \zeta(\mathbf{x}, t) \zeta(\mathbf{x}', t') \rangle = 2D \delta^{d-1}(\mathbf{x} - \mathbf{x}') (t - t') \quad (271)$$

This equation is linear and exactly solvable. The critical exponents of EW classes are

$$\tilde{\beta} = \left(\frac{1}{2} - \frac{d}{4}\right), \quad Z = 2 \quad (272)$$

C. Quenched EW classes

In random media linear interface growth is described by the so called quenched Edwards-Wilkinson equation

$$\partial_t h(\mathbf{x}, t) = \sigma \nabla^2 h(\mathbf{x}, t) + F + \eta(\mathbf{x}, h(\mathbf{x}, t)), \quad (273)$$

where F is a constant, external driving term and $\eta(\mathbf{x}, h(\mathbf{x}, t))$ is the quenched noise. The corresponding linear interface models (LIM) exhibit a depinning transition at F_c . The universal behavior of these models were investigated in [194, 195, 196] and it was shown to be equivalent with NDCF classes (Sect. VI). Analytical studies [196] predict $\tilde{\alpha} = (4 - d)/3$ and $Z = 2 - (2/9)(4 - d)$.

D. Kardar-Parisi-Zhang (KPZ) classes

If we drop the $h \rightarrow -h$ symmetry from (269) we can add a term to the (270) equation that is the most relevant term in renormalization sense breaking the up-down symmetry:

$$\partial_t h(\mathbf{x}, t) = v + \sigma \nabla^2 h(\mathbf{x}, t) + \lambda (\nabla h(\mathbf{x}, t))^2 + \zeta(\mathbf{x}, t) \quad (274)$$

that is the Kardar-Parisi-Zhang (KPZ) equation [197]. Here again v denotes the mean growth velocity, σ the surface tension and ζ the zero-average Gaussian noise field with variance

$$\langle \zeta(\mathbf{x}, t) \zeta(\mathbf{x}', t') \rangle = 2D \delta^{d-1}(\mathbf{x} - \mathbf{x}') (t - t') \quad (275)$$

This is non-linear, but exhibits a tilting symmetry as the result of the Galilean invariance of (274):

$$h \rightarrow h' + \epsilon \mathbf{x}, \quad \mathbf{x} \rightarrow \mathbf{x}' - \lambda \epsilon t, \quad t \rightarrow t' \quad (276)$$

where ϵ is an infinitesimal angle. As a consequence the scaling relation

$$\tilde{\alpha} + Z = 2 \quad (277)$$

holds in any dimensions. In one dimension the critical exponents are known exactly whereas for $d > 1$ dimensions numerical estimates exist [176] (see Table XXVIII). The

d	$\tilde{\alpha}$	$\tilde{\beta}$	Z
1	1/2	1/3	3/2
2	0.38	0.24	1.58
3	0.30	0.18	1.66

TABLE XXVIII: Scaling exponents of KPZ from [176]

upper critical dimension of this model is debated. Mode coupling theories and various phenomenological field theoretical schemes [198, 199] settle to $d_c = 4$. Contrary to analytical approaches numerical solution of the KPZ equation [200], simulations [201, 202], and the results of real-space renormalization group calculations [203] provide no evidence for a finite d_c . Furthermore, the only numerical study [204] of the mode-coupling equations gives no indication for the existence of a finite d_c either. Recently simulations of the restricted solid-on-solid growth models were used to build the width distributions of $d = 2 - 5$ dimensional KPZ interfaces. The universal scaling function associated with the steady-state width distribution was found to change smoothly as d is increased, thus strongly suggesting that $d = 4$ is not an upper critical dimension for the KPZ equation. The dimensional trends observed in the scaling functions indicate that the upper critical dimension is at infinity [205].

1. Multiplicative noise systems

Grinstein et al. [395] introduced and studied systems via the Langevin equation

$$\partial_t n(x, t) = D \nabla^2 n(x, t) - r n(x, t) - u n(x, t)^2 + n(x, t) \eta(x, t), \quad (278)$$

exhibiting real multiplicative noise (MN) :

$$\langle \eta(x, t) \rangle = 0, \quad \langle \eta(x, t) \eta(x', t') \rangle = 2\nu \delta^d(x - x') \delta(t - t'), \quad (279)$$

that is proportional to the field (n). Since for DP class the noise is square root proportional to the field; for ARW and PC systems the noise is imaginary one may expect distinct universal behavior for such systems. Howard and Täuber [247] on the other hand argued on field theoretical basis that such 'naive' Langevin equations fail to accurately describe systems controlled by particle pair reaction processes, where the noise is in fact 'imaginary' and one should derive a proper Langevin equation by starting from master equation of particles. Therefore they investigated the simplest RD

systems where both real and imaginary noise is present and compete:

- (a) $2A \rightarrow \emptyset$, $2A \rightarrow 2B$, $2B \rightarrow 2A$, and $2B \rightarrow \emptyset$
- (b) $2A \rightarrow \emptyset$ and $2A \rightarrow (n+2)A$ (see Sect. VF)

by setting up the action first – derived from the master equation of particles. In neither case were they able to recover the MN critical behavior reported in [395]. Therefore they suspected that there might not be real RD system possessing the MN behavior.

On the other hand [395] have established connection of MN systems via the Cole-Hopf transformation: $n(x, t) = e^{h(x, t)}$ to the KPZ theory. They have shown in 1d that the phase diagram and the critical exponents Z , ν_\perp and β of the two systems agree within numerical accuracy. They have found diverging susceptibility (with continuously changing exponent as the function of r) for the entire range of r .

E. Quenched KPZ classes

In random media nonlinear interface growth is described by the so called **quenched KPZ equation** [176],

$$\partial_t h(\mathbf{x}, t) = \sigma \nabla^2 h(\mathbf{x}, t) + \lambda (\nabla h(\mathbf{x}, t))^2 + F + \eta(\mathbf{x}, h(\mathbf{x}, t)) \quad (280)$$

where F is a constant, external driving term and $\eta(\mathbf{x}, h(\mathbf{x}, t))$ is the quenched noise (do not fluctuate in time). Its universal behavior was investigated in [206, 207] and predicted $\tilde{\alpha} \simeq 0.63$ in one dimension, $\tilde{\alpha} \simeq 0.48$ in two dimensions and $\tilde{\alpha} \simeq 0.38$ in three dimensions. It was shown numerically that in 1d this class is described by 1+1 d directed percolation depinning [208]. In higher dimensions however it is related to percolating directed surfaces [209].

F. Other continuum growth classes

For continuum growth models exhibiting the symmetries

$$\mathbf{x} \rightarrow \mathbf{x} + \Delta \mathbf{x} \quad t \rightarrow t + \Delta t \quad h \rightarrow h + \Delta h \quad \mathbf{x} \rightarrow -\mathbf{x} \quad (281)$$

the possible general Langevin equations with relevant terms were classified as follows [176].

- The deterministic part describes conservative or nonconservative process (i.e. the integral over the entire system is zero or not). Conservative terms are $\nabla^2 h$, $\nabla^4 h$ and $\nabla^2 (\nabla h)^2$. The only relevant nonconservative terms is the $(\nabla h)^2$.
- The system is linear or not.
- The noise term is conservative (i.e. the result of some surface diffusion) with correlator

$$\langle \zeta_d(\mathbf{x}, t) \zeta_d(\mathbf{x}', t') \rangle = (-2D_d \nabla^2 + D'_d \nabla^4) \delta(\mathbf{x} - \mathbf{x}') \delta(t - t') \quad (282)$$

or nonconservative like in eq.(271) (as the result of adsorption, desorption mechanisms).

Analyzing the surface growth properties of such systems besides the EW and KPZ classes five other universality classes were identified (see Table XXIX).

Langevin equation	$\tilde{\alpha}$	$\tilde{\beta}$	Z
$\partial_t h = -K\nabla^4 h + \zeta$	$\frac{4-d}{2}$	$\frac{4-d}{8}$	4
$\partial_t h = \nu\nabla^2 h + \zeta_d$	$\frac{-d}{2}$	$\frac{-d}{4}$	2
$\partial_t h = -K\nabla^4 h + \zeta_d$	$\frac{2-d}{2}$	$\frac{2-d}{8}$	4
$\partial_t h = -K\nabla^4 h + \lambda_1 \nabla^2 (\nabla h)^2 + \zeta$	$\frac{4-d}{3}$	$\frac{4-d}{8+d}$	$\frac{8+d}{3}$
$\partial_t h = -K\nabla^4 h + \lambda_1 \nabla^2 (\nabla h)^2 + \zeta_d$	$d \leq 1$		
	$\frac{2-d}{3}$	$\frac{2-d}{10+d}$	$\frac{10+d}{3}$
	$d > 1$		
	$\frac{2-d}{2}$	$\frac{2-d}{8}$	4

TABLE XXIX: Summary of continuum growth classes discussed in this section following ref. [176].

G. Classes of mass adsorption-desorption, aggregation and chipping models

Based on the interest in self-organized critical systems in which different physical quantities exhibit power law distributions in the steady state over a wide region of the parameter space [396] a family of lattice models, in which masses diffuse, aggregate on contact, and also chip off a single unit mass was introduced by Majumdar et al. [397, 398]. Self-organized criticality has been studied in a variety of model systems ranging from sandpiles to earthquakes. A particularly simple lattice model due to Takayasu, with mass diffusion, aggregation upon contact and adsorption of unit masses from outside at a constant rate, exhibits self-organized criticality[399]: the steady-state mass distribution has a nontrivial power law decay for large masses in all dimensions [399]. These mass adsorption-desorption models in one dimension are defined as follows. A site i is chosen randomly and then one of the following events can occur:

1. Adsorption: With rate q , a single particle is adsorbed at site i ; thus $m_i \rightarrow m_i + 1$.
2. Desorption: With rate p , a single particle is desorbed from site i ; thus $m_i \rightarrow m_i - 1$ provided $m_i \geq 1$.
3. Diffusion and Aggregation: With rate 1, the mass m_i at site i moves to a nearest neighbor site [either $(i-1)$ or $(i+1)$] chosen at random. If it moves to a site which already has some particles, then the total mass just adds up; thus $m_i \rightarrow 0$ and $m_{i\pm 1} \rightarrow m_{i\pm 1} + m_i$.

4. Chipping: With rate w a bit of mass at the site “chips” off, e. provided $m_i \geq 1$ a single particle leaves site i

While the Takayasu model ($p = 0, w = 0$) does not have a phase transition in the steady state, by introducing a nonzero desorption rate p induces a critical line $p_c(q)$ in the $p-q$ plane. For fixed q , if one increases p from 0, one finds that for all $p < p_c(q)$, the steady state mass distribution has the same large m behavior as in the Takayasu case, i.e.,

$$P(m) \propto m^{-\tau} \quad (283)$$

where the exponent τ is the Takayasu exponent and is independent of q . For $p = p_c(q)$, we find the steady state mass distribution still decays algebraically for large m , but with a new critical exponent τ_c which is bigger than the Takayasu exponent τ_t . For $p > p_c(q)$, we find that

$$P(m) \sim \exp(-m/m^*) \quad (284)$$

for large m where m^* is a characteristic mass that diverges if one approaches $p_c(q)$ from the $p > p_c(q)$ side. The critical exponent τ_c is the same everywhere on the critical line $p_c(q)$. This phase transition occurs in all spatial dimensions including $d = 1$. The τ exponent was determined for the mean-field and one dimensional cases ([399, 400])

$$\tau_t^{MF} = 3/2, \quad \tau_c^{MF} = 5/2, \quad \tau_t^{1d} = 4/3, \quad \tau_c^{1d} = 1.833, \quad (285)$$

although the location of d_c is not known.

This model can also be mapped onto an interface dynamics, if we interpret the configuration of masses as an interface profile regarding m_i as a local height variable. The phase transition of the model can be qualitatively interpreted as a nonequilibrium *wetting transition* of the interface. The corresponding surface growth exponents are [400]

$$\tilde{\beta}^{MF} = 1/6, \quad Z = 2, \quad \tilde{\beta}^{1d} = 0.358, \quad Z = 2. \quad (286)$$

In the $p = q = 0$ conserved model (CM) a nonequilibrium phase transition occurs by varying the chipping rate or the average mass per site ρ . There is a critical line $\rho_c(w)$ in the $\rho-w$ plane that separates two types of asymptotic behaviors of $P(m)$. For fixed w , as ρ is varied across the critical value $\rho_c(w)$, the large m behavior of $P(m)$ was found to be,

$$P(m) \sim \begin{cases} e^{-m/m^*} & \rho < \rho_c(w), \\ m^{-\tau} & \rho = \rho_c(w), \\ m^{-\tau} + \text{infinite aggregate} & \rho > \rho_c(w). \end{cases} \quad (287)$$

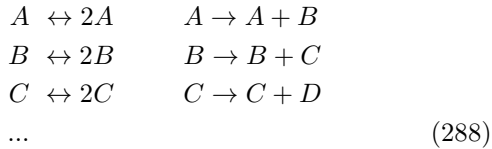
As one increases ρ beyond ρ_c , this asymptotic algebraic part of the critical distribution remains unchanged but in addition an infinite aggregate forms. This means that all the additional mass $(\rho - \rho_c)V$ (where V is the volume of the system) condenses onto a single site and does

not disturb the background critical distribution. This is analogous, in spirit, to the condensation of a macroscopic number of bosons onto the single $k = 0$ mode in an ideal Bose gas as the temperature goes below a certain critical value. Rajesh and Majumdar [401] proved analytically that the mean field phase boundary, $\rho_c(w) = \sqrt{w+1} - 1$, is *exact* and independent of the spatial dimension d . They also provided unambiguous numerical evidence that the exponent $\tau = 5/2$ is also independent of d . The corresponding growth exponents are: $Z = 2$, $\tilde{\alpha} = 2/3$ [398]. Even though the single site distribution $P(m)$ may be given exactly by the mean field solution, that does not prove that mean field theory or product measure is the exact stationary state in all dimensions.

The left-right asymmetric version of the CM model was also studied in [398]. This has a qualitatively similar phase transition in the steady state as the CM model but exhibits a different class phase transition owing to the mass current in this system. Simulations in one dimension predict: $Z = 1.67$, $\tilde{\alpha} = 0.67$.

H. Unidirectionally coupled DP classes

As it was mentioned in Section V J in case of coupled, multi-species DP processes field theoretical RG analysis [387] predicts DP criticality with an unstable, symmetrical fixed point, such that sub-systems with unidirectionally coupled DP behavior emerge. This was shown to be valid for linearly coupled N-component, contact processes too. Unidirectionally coupled DP systems of the form (UCDP)



were investigated by Täuber et al. [402, 403] with the motivation that such models can describe interface growth models, where adsorption-desorption are allowed at terraces and edges (see Sect. VI H 1). The simplest set of Langevin equations for such systems was set up by Alon et al. [404]:

$$\begin{aligned} \partial_t \phi_k(\mathbf{x}, t) &= \sigma \phi_k(\mathbf{x}, t) - \lambda \phi_k^2(\mathbf{x}, t) + D \nabla^2 \phi_k(\mathbf{x}, t) + \\ &+ \mu \phi_{k-1}(\mathbf{x}, t) + \zeta_k(\mathbf{x}, t), \end{aligned} \quad (289)$$

where ζ_k are independent multiplicative noise fields for level k with correlations

$$\begin{aligned} \langle \zeta_k(\mathbf{x}, t) \rangle &= 0, \\ \langle \zeta_k(\mathbf{x}, t) \zeta_l(\mathbf{x}', t') \rangle &= 2\Gamma \phi_k(\mathbf{x}, t) \delta_{k,l} \delta^d(\mathbf{x} - \mathbf{x}') \delta(t - t'), \end{aligned} \quad (290)$$

for $k > 0$, while for the lowest level ($k = 0$) $\phi_{-1} \equiv 0$ is fixed. The parameter σ controls the offspring production, μ is the coupling and λ is the coagulation rate. As one can see the $k = 0$ equation is just the Langevin equation

of RFT (85). The **mean-field** solution of these equations that is valid above $d_c = 4$ results in critical exponents for the level k :

$$\beta_{MF}^{(k)} = 2^{-k}. \quad (291)$$

and $\nu_{\perp}^{MF} = 1/2$ and $\nu_{\parallel}^{MF} = 1$ independently of k . For $d < d_c$ field theoretical RG analysis of the action for $k < K$ levels

$$\begin{aligned} S = \sum_{k=0}^{K-1} \int d^d x dt &\left\{ \psi_k \left(\tau \partial_t - D \nabla^2 - \sigma \right) \phi_k \right. \\ &\left. - \mu \psi_k \phi_{k-1} + \frac{\Gamma}{2} \psi_k \left(\phi_k - \psi_k \right) \phi_k \right\}, \end{aligned} \quad (292)$$

was performed in [402, 403]. The RG treatment run into several difficulties. Infrared-divergent diagrams were encountered [407] and the coupling constant μ was shown to be a relevant quantity (that means it diverges under RG transformations). Goldschmidt et al. [403] argued that this is the reason why scaling seems to break down in simulations for large times (in lattice realization μ is limited). The exponents of the one-loop calculations for the first few levels, corresponding to the interactive fixed line as well as results of lattice simulations are shown in Table XXX. These scaling exponents can be observed

	$d = 1$	$d = 2$	$d = 3$	$d = 4 - \epsilon$
β_1	0.280(5)	0.57(2)	0.80(4)	$1 - \epsilon/6 + O(\epsilon^2)$
β_2	0.132(15)	0.32(3)	0.40(3)	$1/2 - \epsilon/8 + O(\epsilon^2)$
β_3	0.045(10)	0.15(3)	0.17(2)	$1/4 - O(\epsilon)$
δ_1	0.157(4)	0.46(2)	0.73(5)	$1 - \epsilon/4 + O(\epsilon^2)$
δ_2	0.075(10)	0.26(3)	0.35(5)	$1/2 - \epsilon/6 + O(\epsilon^2)$
δ_3	0.03(1)	0.13(3)	0.15(3)	$1/4 - O(\epsilon)$
η_1	0.312(6)	0.20(2)	0.10(3)	$\epsilon/12 + O(\epsilon^2)$
η_2	0.39(2)	0.39(3)	0.43(5)	$1/2 + O(\epsilon^2)$
η_3	0.47(2)	0.56(4)	0.75(10)	$3/4 - O(\epsilon)$
$2/Z_1$	1.26(1)	1.10(2)	1.03(2)	$1 + \epsilon/24 + O(\epsilon^2)$
$2/Z_2$	1.25(3)	1.12(3)	1.04(2)	
$2/Z_3$	1.23(3)	1.10(3)	1.03(2)	
$\nu_{\perp,1}$	1.12(4)	0.70(4)	0.57(4)	$1/2 + \epsilon/16 + O(\epsilon^2)$
$\nu_{\perp,2}$	1.11(15)	0.69(15)	0.59(8)	
$\nu_{\perp,3}$	0.95(25)	0.65(15)	0.62(9)	
$\nu_{\parallel,1}$	1.78(6)	1.24(6)	1.10(8)	$1 + \epsilon/12 + O(\epsilon^2)$
$\nu_{\parallel,2}$	1.76(25)	1.23(17)	1.14(15)	
$\nu_{\parallel,3}$	1.50(40)	1.15(30)	1.21(15)	

TABLE XXX: Critical exponents of UCDP [403].

for intermediate times but it is not clear if in the asymptotically long time they drift to the decoupled values or not.

1. Monomer adsorption-desorption at terraces models

Alon et al. defined SOS and RSOS models [404, 405] that can be mapped onto UCDP (Sect.VIH). In this models adsorption and desorption processes may take place at terraces and edges. For each update a site i is chosen at random and an atom is adsorbed

$$h_i \rightarrow h_i + 1 \text{ with probability } q \quad (293)$$

or desorbed at the edge of a plateau

$$\begin{aligned} h_i &\rightarrow \min(h_i, h_{i+1}) \text{ with probability } (1-q)/2, \\ h_i &\rightarrow \min(h_i, h_{i-1}) \text{ with probability } (1-q)/2. \end{aligned} \quad (294)$$

Identifying empty sites at a given layer as A particles, the adsorption process can be interpreted as the decay of A particles ($A \rightarrow \emptyset$), while the desorption process corresponds to A particle production ($A \rightarrow 2A$). These processes generate reactions on subsequent layers, hence they are coupled. The simulations in 1d have shown that this coupling is relevant in the upward direction only hence the model is equivalent to the UCDP process. Defining the order parameters on the k -th layer as

$$n_k = \frac{1}{N} \sum_i \sum_{j=0}^k \delta_{h_i, j}, \quad (295)$$

where h_i is the height at site i , they are expected to scale as

$$n_k \sim (q_c - q)^{\beta^{(k)}}. \quad k = 1, 2, 3, \dots \quad (296)$$

By varying the growth rate (q) these models exhibit a roughening transition at $q_c = 0.189$ (for RSOS) and at $q_c = 0.233(1)$ (for SOS) from a non-moving, smooth phase to a moving, rough phase in one spatial dimension. The β^k (and other exponents) take those of the 1d UCDP class (see Table XXX).

The scaling behavior of the interface width is characterized by many different length scales. At criticality it increases as

$$W^2(t) \propto \tau \ln t \quad (297)$$

with $\tau \simeq 0.102(3)$ for RSOS [406].

2. Polynuclear growth models

Polynuclear growth models (PNG) are realizations of unidirectionally coupled DP processes (Sect.VIH). In these models depinning transition takes place [408, 409, 410]. The PNG model investigated by Kertész and Wolf [408] is defined by the following **parallel** update dynamic rules. In the first half time step atoms ‘nucleate’ stochastically at the surface by

$$h_i(t+1/2) = \begin{cases} h_i(t) + 1 & \text{with prob. } p, \\ h_i(t) & \text{with prob. } 1-p. \end{cases} \quad (298)$$

In the second half time step the islands grow deterministically in lateral direction by one step.

$$h_i(t+1) = \max_{j \in \langle i \rangle} [h_i(t+1/2), h_j(t+1/2)], \quad (299)$$

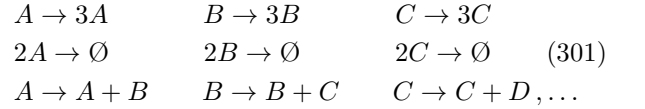
where j runs over the nearest neighbors of site i . For p large enough, the interface is smooth and propagates with velocity 1. Below a critical threshold, the density of active sites at the maximal height $h_i(t) = t$ vanishes, and the growth velocity is smaller than 1. Identifying the sites with $h_i = t$ as A particles, those with $h_i \geq t-1$ as B particles etc., the dynamical processes resemble the rules of coupled DP. The corresponding order parameters are defined by

$$\rho_k = \frac{1}{N} \sum_i \sum_{h=0}^{k-1} \delta_{h_i, t-h}. \quad (300)$$

Thus PNG models may be interpreted as realizations of coupled DP processes in a *co-moving* frame.

I. Unidirectionally coupled PC classes

Similarly to the UCDP case (see Sect.VIH) surface growth processes stimulated the introduction of unidirectionally coupled BARW2 (Sect.IV D 2) models [382, 411]:



generalizing the concept of UCDP. The mean field approximation of the reaction scheme (301) looks as

$$\begin{aligned} \partial_t n_A &= \sigma n_A - \lambda n_A^2, \\ \partial_t n_B &= \sigma n_B - \lambda n_B^2 + \mu n_A, \\ \partial_t n_C &= \sigma n_C - \lambda n_C^2 + \mu n_B, \dots \end{aligned} \quad (302)$$

where n_A, n_B, n_C correspond to the densities n_0, n_1, n_2 in the growth models. σ and λ are the rates for offspring production and pair annihilation respectively. The coefficient μ is an effective coupling constant between different particle species. Since these equations are coupled in only one direction, they can be solved by iteration. Obviously, the mean-field critical point is $\sigma_c = 0$. For small values of σ the stationary particle densities in the active state are given by

$$n_A = \frac{\sigma}{\lambda}, \quad n_B \simeq \frac{\mu}{\lambda} \left(\frac{\sigma}{\mu} \right)^{1/2}, \quad n_C \simeq \frac{\mu}{\lambda} \left(\frac{\sigma}{\mu} \right)^{1/4}, \quad (303)$$

corresponding to the mean field critical exponents

$$\beta_A^{MF} = 1, \quad \beta_B^{MF} = 1/2, \quad \beta_C^{MF} = 1/4, \dots \quad (304)$$

These exponents should be valid for $d > d_c = 2$. Solving the asymptotic temporal behavior one finds $\nu_{||} = 1$, implying that $\delta_k^{MF} = 2^{-k}$.

The effective action of unidirectionally coupled BARW2's should be given by

$$S[\psi_0, \psi_1, \psi_2, \dots, \bar{\psi}_0, \bar{\psi}_1, \bar{\psi}_2, \dots] = \int d^d x dt \sum_{k=0}^{\infty} \left\{ \bar{\psi}_k (\partial_t - D \nabla^2) \psi_k - \lambda (1 - \bar{\psi}_k^2) \psi_k^2 + \sigma (1 - \bar{\psi}_k^2) \bar{\psi}_k \psi_k + \mu (1 - \bar{\psi}_k) \bar{\psi}_{k-1} \psi_{k-1} \right\} \quad (305)$$

where $\psi_{-1} = \bar{\psi}_{-1} \equiv 0$. Here the fields ψ_k and $\bar{\psi}_k$ represent the configurations of the system at level k . Since even the RG analysis of the one component BARW2 model suffered serious problems [215] the solution of the theory of (305) seems to be hopeless. Furthermore one expects similar IR diagram problems and diverging coupling strengths as in case of UCDP that might be responsible for violations of scaling in the long time limit.

Simulations of a 3-component model in 1d coupled by instantaneous particle production of the form (301) resulted in decay exponents for the order parameter defined as (295):

$$\delta_A = 0.280(5), \quad \delta_B = 0.190(7), \quad \delta_C = 0.120(10), \quad (306)$$

For further critical exponents see Sect.VII 1.

It would be interesting to investigate parity-conserving growth processes in higher dimensions. Since the upper critical dimension d'_c is less than 2, one expects the roughening transition – if still existing – to be described by mean-field exponents. In higher dimensions, n -mers might appear in different shapes and orientations.

1. Dimer adsorption-desorption at terraces models

Similarly to the monomer case (Sect.VI H 1) dimer adsorption-desorption models were defined [382, 411, 412]. With the restriction that desorption may only take place at the edges of a plateau the models can be mapped onto the unidirectionally coupled BARW2 (Sect.VII 1). The dynamical rules in $d = 1$ are defined in Fig. 30. The mapping onto unidirectionally

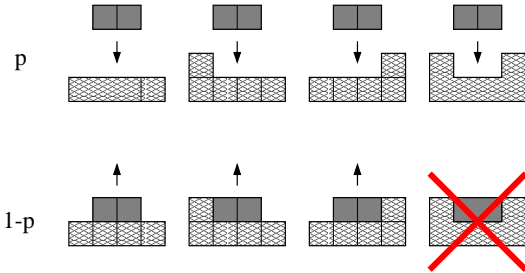


FIG. 30: Dimers are adsorbed with probability p and desorbed at the edges of terraces with probability $1 - p$. Evaporation from the middle of plateaus is not allowed [382].

coupled BARW2 can be seen on Fig.31.

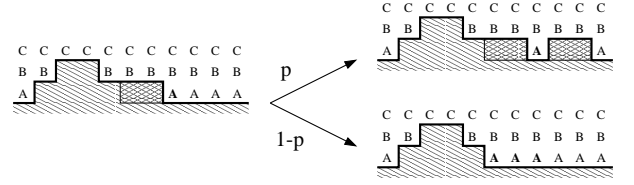


FIG. 31: Extended particle interpretation. Dimers are adsorbed ($2A \rightarrow \emptyset$) and desorbed ($A \rightarrow 3A$) at the bottom layer. Similar processes take place at higher levels [382].

Such dimer models can be defined in arbitrary spatial dimensions. In [382] four one dimensional variants were investigated:

- 1) Variant A is a restricted solid-on-solid (RSOS) model evolving by random sequential updates.
- 2) Variant B is a solid-on-solid (SOS) model evolving by random sequential updates.
- 3) Variant C is a restricted solid-on-solid (RSOS) model evolving by parallel updates.
- 4) Variant D is a solid-on-solid (SOS) model evolving by parallel updates.

Variants A and B exhibit transitions in contrast with PNG (Sect.VI H 2) and PC-PNG (Sect.VII 2) models, in which only parallel update rules permit roughening transitions. By varying the adsorption rate p the phase diagram shown in Fig.32 emerges for RSOS and SOS cases. If p is very small, only a few dimers are adsorbed at

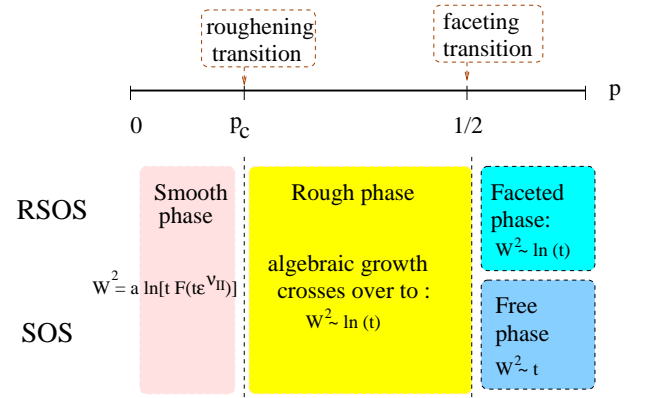


FIG. 32: Phase diagram of 1d dimer models.

the surface, staying there for a short time before they evaporate back into the gas phase. Thus, the interface is anchored to the actual bottom layer and does not propagate. In this smooth phase the interface with growths logarithmically until it saturates to a finite value (even for $L \rightarrow \infty$).

As p increases, a growing number of dimers covers the surface and large islands of several layers stacked on top

of each other are formed. Approaching a certain critical threshold p_c the mean size of the islands diverges and the interface evolves into a rough state with the finite-size scaling form

$$W^2(L, t) \simeq a \ln \left[t G(t/L^Z) \right]. \quad (307)$$

The order parameter defined on the k -th layer as (295) exhibits unidirectionally coupled BARWe critical behavior. The transition rates and exponents are summarized in Table XXXI.

variant	A	B	C	D
restriction	yes	no	yes	no
updates	random	random	parallel	parallel
p_c	0.3167(2)	0.292(1)	0.3407(1)	0.302(1)
a	0.172(5)	0.23(1)	0.162(4)	0.19(1)
Z	1.75(5)	1.75(5)	1.74(3)	1.77(5)
δ_0	0.28(2)	0.29(2)	0.275(10)	0.29(2)
δ_1	0.22(2)	0.21(2)	0.205(15)	0.21(2)
δ_2	0.14(2)	0.14(3)	0.13(2)	0.14(2)
$\tilde{\alpha}$	1.2(1)	undefined	1.25(5)	undefined
$\tilde{\beta}$	0.34(1)	0.50(1)	0.330(5)	0.49(1)

TABLE XXXI: Numerical estimates for the four variants of the dimer model at the roughening transition $p = p_c$ (upper part) and at the transition $p = 0.5$ (lower part).

Above p_c one may expect the interface to detach from the bottom layer in the same way as the interface of monomer models starts to propagate in the supercritical phase. However, since dimers are adsorbed at neighboring lattice sites, solitary unoccupied sites may emerge. These pinning centers prevent the interface from moving and lead to the formation of ‘droplets’. Due to interface fluctuations, the pinning centers can slowly diffuse to the left and to the right. When two of them meet at the same place, they annihilate and a larger droplet is formed. Thus, although the interface remains pinned, its roughness increases continuously. The width initially increases algebraically until it slowly crosses over to a logarithmic increase $W(t) \sim \sqrt{a \ln t}$.

The restricted as well as the unrestricted variants undergo a second phase transition at $p = 0.5$ [412] where the width increases *algebraically* with time as $W \sim t^{\tilde{\beta}}$. In the RSOS case ordinary *Family-Vicsek* scaling (258) occurs with the exponents given in Table XXXI. The dynamic exponent is $Z = \tilde{\alpha}/\tilde{\beta} \simeq 3$. This value stays the same if one allows dimer digging at the faceting transition but other surface exponents $\tilde{\alpha} \simeq 0.29(4)$ and $\tilde{\beta} \simeq 0.111(2)$ will be different [412]. An explanation of the latter exponents is given in [192] based on mapping to globally constrained random walks. In the SOS cases (variants B,D) large spikes are formed, the surface roughens much faster with a growth exponent of

$\tilde{\beta} \simeq 0.5$. The interface evolves into configurations with large columns of dimers separated by pinning centers. These spikes can grow or shrink almost independently. As the columns are spatially decoupled, the width does not saturate in finite systems, i.e., the dynamic exponents $\tilde{\alpha}$ and Z have no physical meaning.

For $p > 0.5$ the restricted models A and C evolve into faceted configurations. The width first increases algebraically until the pinning centers become relevant and the system crosses over to a logarithmic increase of the width. Therefore, the faceted phase may be considered as a rough phase. The unrestricted models B and D, however, evolve into spiky interface configurations. The spikes are separated and grow independently by deposition of dimers. Therefore, W^2 increases *linearly* with time, defining the *free* phase of the unrestricted models.

In the simulations mentioned by now the interface was grown from flat initial conditions. It turns out that starting with **random initial conditions** $h_i = 0, 1$ the densities n_k turn out to decay much slower. For restricted variants an algebraic decay of n_0 with an exponent

$$\delta_0 \simeq 0.13 \quad (308)$$

was observed. Similarly, the critical properties of the faceting transition at $p = 0.5$ are affected by random initial conditions. The non-universal behavior for random initial conditions is related to an *additional* parity conservation law. The dynamic rules not only conserve parity of the particle number but also conserve the parity of droplet sizes. Starting with a flat interface the lateral size of droplets is always even, allowing them to evaporate entirely. However, for a random initial configuration, droplets of odd size may be formed which have to recombine in pairs before they can evaporate, slowing down the dynamics of the system. In the language of BARW2 processes the additional parity conservation law is due to the absence of nearest-neighbor diffusion. Particles can only move by a combination of offspring production and annihilation, i.e., by steps of *two* lattice sites. Therefore, particles at even and odd lattice sites have to be distinguished. Only particles of different parity can annihilate. Starting with a fully occupied lattice all particles have alternating parity throughout the whole temporal evolution, leading to the usual critical behavior at the PC transition. For random initial conditions, however, particles of equal parity cannot annihilate, slowing down the decay of the particle density. Similar sector decomposition has been observed in diffusion of k -mer models [383].

2. Parity conserving polynuclear growth

In analogy with PNG models (Sect. VI H 2) parity conserving PNG models were introduced in [382]. The model

is defined on a one-dimensional lattice with periodic boundary conditions and evolves by sub-lattice-parallel updates. In the first half time step pairs of sites $(i, i+1)$ with even i are updated. If $h_i(t) \neq h_{i+1}(t)$, the heights are incremented by one step

$$\begin{aligned} h_i(t+1/2) &= h_i(t) + 1, \\ h_{i+1}(t+1/2) &= h_{i+1}(t) + 1. \end{aligned} \quad (309)$$

If, however, the two heights are equal, they are updated by the probabilistic rule

$$\begin{aligned} h_i(t+1/2) &= h_{i+1}(t+1/2) = \\ &= \begin{cases} m(t) + 1 & \text{with prob. } p \\ m(t) & \text{with prob. } 1 - p \end{cases} \end{aligned} \quad (310)$$

where $m(t) = \max[h_{i-1}(t), h_i(t), h_{i+1}(t), h_{i+2}(t)]$. In the second half time step the same update rule is applied to odd pairs of sites. Clearly, this model generalizes the PNG model and conserves parity at each height level in a co-moving frame. The conservation law leads to the formation of pinning centers moving at maximal velocity. Simulations showed that the critical behavior at the threshold $p_c = 0.5697(3)$ are the same as those of the unidirectionally BARW2 class in 1d.

VII. SUMMARY

In summary dynamical extensions of classical equilibrium classes were introduced in the first part of this review. New exponents, concepts, sub-classes, mixing dynamics and some unresolved problems were discussed. The common behavior of these models was the strongly fluctuating ordered state. In the second part genuine nonequilibrium dynamical classes of reaction-diffusion systems and interface growth models were overviewed. These were related to phase transitions to absorbing

CLASS ID	features	Section
DP	time reversal symmetry	IV A
DyP	long memory	IV B
VM	Z_2 symmetry	IV C
PCP	coupled frozen field	V E
NDCF	global conservation	VI
PC	Z_2 symmetry, BARW2 conservation	IV D 2
BP	DP coupled to ARW	V F
DCF	coupled diffusive, conserved field	V H
N-BARW2	N-component BARW2 conservation	V K
N-BARW2s	symmetric NBARW2 + exclusion	VL
N-BARW2a	asymmetric NBARW2 + exclusion	VL

TABLE XXXII: Summary of known absorbing state universality classes in homogeneous isotropic systems.

states of weakly fluctuating ordered states. The class behavior is usually determined by the spatial dimension,

symmetries, boundary conditions and inhomogeneities like in case of equilibrium models but in low dimensions hard-core exclusion was found to be a relevant factor too, splitting up criticality in fermionic and bosonic models. The symmetries are not so evident as in case of equilibrium models, they are expressed in terms of the relations of fields and response fields most precisely. Furthermore in recently discovered coupled systems with binary, triplet or quadruplet particle production no special symmetry seems to be responsible for a novel type of critical behavior. Perhaps a proper field theoretical analysis of the coupled DP+ARW system could shed some light on this mystery. The parity conservation in hard-core and in binary spreading models seems to be irrelevant. In Table XXXII I summarized the most well known families of absorbing phase transition classes of homogeneous, spatially isotropic systems. Those which are below the horizontal line exhibit *fluctuating absorbing states*. The necessary and sufficient conditions for these classes are usually unknown. The mean-field classes can also give a guide to distinguish classes below d_c . In Table XXXIII I collected the mean-field exponents and upper critical dimensions of the known absorbing-state model classes. Note that in the general $nA \rightarrow (n+k)A$, $mA \rightarrow (m-l)A$ type of RD systems the values of n and m determine the critical behavior.

CLASS	β	β'	Z	$\nu_{ }$	α	δ	η	d_c
DP	1	1	2	1	1	1	0	4
DyP	1	1	2	1	1	1	0	6
VM	0	1	2	1	0	1	0	2
PC	1	0	2	1	1	0	-1/2	2
BkARW	$1/(k-1)$	0	2	1	$1/(k-1)$	0	0	$2/(k-1)$
PARWs	1	0	2	n	$1/n$	0	0	
PARWa	$1/(m-n)$		2	$(m-1)/(m-n)$	$1/(m-1)$			
NDCF	1	1	2	1	1	1	0	4
NBARW2	1	0	2	1	1	0	0	2

TABLE XXXIII: Mean-field classes of known, homogeneous absorbing-state transitions

In $d > 1$ dimension the mapping of spin-systems onto RD systems of particles is not straightforward, instead one should also deal with the theory of branching interfaces [414]. Preliminary simulations found interesting critical phenomena by generalized Potts models, exhibiting absorbing states [104]. Further research should also explore the universality classes of such nonequilibrium phase transitions that occur by external current driven systems or by other models exhibiting fluctuating ordered states [153, 154]. Nonequilibrium phase transitions in quantum systems [413] or by irregular graph or network based systems are also of current interest of research. Finally, having settled the problems arisen by fundamental nonequilibrium models one should turn towards the study of more application motivated systems.

Acknowledgements

I thank H. Hinrichsen, N. Menyhárd and M. A. Muñoz for their comments to the manuscript. Support from

Hungarian research funds OTKA (No.25286), Bolyai (BO/00142/99) and IKTA (Project No.00111/2000) is acknowledged.

Abbreviations

ABC	active boundary condition	(IV A 4)
ARW	annihilating random walk ($AA \rightarrow \emptyset$)	(IV C 1)
AF	annihilation-fission process	(V F)
BARW	branching and annihilation random walk	(IV A)
BARWe	even-offspring branching and annihilation random walk	(IV D 2)
BARWo	odd-offspring branching and annihilation random walk	(IV A 3)
BARW2	two-offspring branching and annihilation random walk	(IV D 2)
BkARW	branching and k particle annihilating random walk	(IV E)
BP	binary production	(V F)
CAM	coherent anomaly method	(IV A)
CDP	compact directed percolation	(IV A 2)
DCF	diffusive conserved field	(V H)
DK	Domany-Kinzel cellular automaton	(IV A 2)
DP	directed percolation	(IV A)
DS	damage spreading	(ID 1)
DyP	dynamical percolation	(IV B)
EW	Edwards-Wilkinson	(VI B)
DMRG	density matrix renormalization group	(IV)
GEP	generalized epidemic process	(IV B)
GDK	generalized Domany-Kinzel cellular automaton	(IV D 4)
GMF	generalized mean-field approximation	(II)
IBC	inactive boundary condition	(IV A 4)
KPZ	Kardar-Parisi-Zhang	(VI D)
LIM	linear interface model	(VI C)
MF	mean-field approximation	(I E)
N-BARW	N-component branching and annihilation random walk	(V K)
N-BARW2	even-offspring, N-component branching and annihilation random walk	(V K)
NDCF	non-diffusive conserved field	(VI)
NEKIM	nonequilibrium Ising model	(IV D 3)
NEKIMA	nonequilibrium Ising model with locally broken symmetry	(V K 2)
PC	parity conserving	(IV D)
PCP	pair contact process	(V E)
PCPD	pair contact process with particle diffusion	(V F 1)
PARWs	symmetric production and m-particle annihilating random walk	(IV F)
PARWa	asymmetric production and m-particle annihilating random walk	(IV F)
RBC	reflecting boundary condition	(IV A 4)
RD	reaction-diffusion	(I E)
RG	renormalization group	(I E)
RFT	Reggeon field theory	(IV A)
RSOS	restricted solid on solid model	(VI)
SCA	stochastic cellular automaton	(IV A 2)
SOS	solid on solid model	(VI)
TTP	threshold transfer process	(V E)
UCDP	unidirectionally coupled directed percolation	(VI H)
VM	voter model	(IV C)

-
- [1] E. V. Albano, J. Phys. A **27**, L881 (1994).
- [2] T. Liggett, *Interacting particle systems* (Springer-Verlag, Berlin, 1985).
- [3] J. R. Stat. Soc B **39**, 283 (1977).
- [4] R. Ziff, E. Gulari, Y. Barshad, Phys. Rev. Lett. **56**, 2553 (1986).
- [5] S. Havlin, D. ben-Avraham, Adv. Phys. **36**, 695 (1987).
- [6] D. Chowdhury, L. Santen and A. Schadschneider, Phys. Reports, **329**, 199 (2000).
- [7] H. Berry, Phys. Rev. E **67**, 031907 (2003).
- [8] J.-P. Bouchaud, A. Georges, Phys. Rep. **195**, 127 (1990).
- [9] For references see : J. Marro and R. Dickman, *Nonequilibrium phase transitions in lattice models*, Cambridge University Press, Cambridge, 1999.
- [10] P. Grassberger, *Directed percolation: results and open problems*, preprint WUB 96-2 (1996).
- [11] H. Hinrichsen, Adv. Phys. **49**, 815 (2000).
- [12] M. E. Fisher, Rep. Prog. Phys. **30**, 615 (1967).
- [13] L. P. Kadanoff et al., Rev. Mod. Phys. **39**, 395 (1967).
- [14] H. E. Stanley, *Introduction to phase transitions and critical phenomena*, Oxford University Press, Oxford (1971).
- [15] S. K. Ma, *Modern theory of critical phenomena*, Addison-Wesley (1976).
- [16] D. J. Amit, *Field theory, the renormalization group and critical phenomena* (2nd. edn.) World Scientific, Singapore (1984).
- [17] D. Stauffer and A. Aharony, *Introduction to percolation theory*, Taylor & Francis, London (1994).
- [18] G. Grimmett, *Percolation* Springer-Verlag 1999.
- [19] C. M. Fortuin and P. W. Kasteleyn, Physica **57**, 536 (1972).
- [20] A. Coniglio and W. Klein, J. Phys. A **13**, 2775 (1980).
- [21] P. Bialas et al., Nucl. Phys. B **583**, 368 (2000).
- [22] S. Fortunato, H. Satz, Nucl. Phys. B **598**, 601 (2001); S. Fortunato, cond-mat/0204366.
- [23] P. Blanchard et al., J. Phys. A **33** 8603 (2000).
- [24] B. I. Halperin and P. C. Hohenberg, Rev. Mod. Phys. **49**, 435 (1977).
- [25] K. Binder and D. Stauffer, Phys. Rev. Lett. **33**, 1006 (1974).
- [26] J. Marro, J. Lebowitz and M. H. Kalos, Phys. Rev. Lett. **43**, 282 (1979).
- [27] B. Derrida, A. J. Bray and C. Godr che, J. Phys. A **27**, L357 (1994).
- [28] S. N. Majumdar, A. J. Bray, S. J. Cornell and C. Sire, Phys. Rev. Lett. **77**, 3704 (1996).
- [29] N. Meny rd and G.  dor, J. Phys. A **30**, 8515 (1997).
- [30] P. Grassberger, Physica A **214**, 547 (1995).
- [31] A. M. Mariz, H. J. Herrmann and L. de Arcangelis, J. Stat. Phys. **59** 1043 (1990).
- [32] N. Jan and L. de Arcangelis, Ann. Rev. Comp. Phys. **1**, 1 (ed. D. Stauffer, World Scientific, Singapore 1994).
- [33] P. Grassberger, J. Phys. A **28** L67, (1995).
- [34] H. Hinrichsen, S. Weitz and E. Domany, J. Stat. Phys. **88**, 617 (1997).
- [35] P. Grassberger, J. Stat. Phys. **79**, 13, (1995).
- [36] J. Cardy, *Scaling and Renormalization in Statistical Physics*, Cambridge lecture notes in Physics 5, ed. P. Goddard and J. Yeomans, Cambridge University Press 1996.
- [37] J. Cardy, *Renormalisation group approach to reaction-diffusion problems*, e-print: cond-mat/9607163.
- [38] U. T uber, *Scale invariance and dynamic phase transitions in diffusion-limited reactions*, e-print: cond-mat/0304065.
- [39] M. A. Munoz, G. Grinstein and Y. Tu, Phys. Rev. E **56**, (1997) 5101.
- [40] H. K. Janssen, cond-mat/0304631.
- [41] H. Hinrichsen, cond-mat/0006212.
- [42] R. J. Glauber, J. Math. Phys. **4**, 191 (1963).
- [43] N. Meny rd and G.  dor, J. Phys. A **31**, 6771 (1998).
- [44] H. K. Janssen and B. Schmittman, Z. Phys. B **64**, 503 (1986).
- [45] B. Derrida, Phys. Rep. **301**, 65 (1998).
- [46] R. Dickman and T. Tom , Phys. Rev. A **44**, 4833 (1991).
- [47] T. Tom  and M. J. de Oliveira, Phys. Rev. A **40**, 6643 (1989).
- [48] A. Szolnoki, Phys. Rev. E **62**, 7466 (2000).
- [49] A. Lipowski and M. Lopata, Phys. Rev. **60**, 1516 (1999); A. Lipowski, Phys. Rev. **60**, R6255 (1999);
- [50] H. Hinrichsen, Phys. Rev. E **63**, 16109 (2001).
- [51] G.  dor, N. Boccara, G. Szab , Phys. Rev. E **48**, 3168 (1993).
- [52] N. Meny rd and G.  dor, J. Phys. A. **28**, 4505 (1995).
- [53] G.  dor and A. Szolnoki, Phys. Rev. E **53**, 2231 (1996).
- [54] L. D. Landau and E. M. Lifshitz, *Statistical mechanics*, (Pergamon, London, 1981)
- [55] N. D. Mermin and H. Wagner, Phys. Rev. Lett. **17**, 1133 (1996).
- [56] H. K. Janssen, B. Schaub and B. Schmittman, Z. Phys. **73**, 539 (1989).
- [57] D. A. Huse, Phys. Rev. B **40**, 304 (1989).
- [58] S. A. Kauffman, J. Theor. Biol. **22**, 437 (1969).
- [59] M. Creutz, Ann. Phys. **167**, 62 (1986).
- [60] H. Stanley, D. Stauffer, J. Kert sz and H. Herrmann, Phys. Rev. Lett. **59**, 2326 (1986).
- [61] B. Derrida and G. Weisbuch, Europhys. Lett. **4**, 657 (1987)
- [62] U. Gropengiesser, Physica A **207**, 492 (1994).
- [63] F. Wang and M. Suzuki, Physica A **223**, 34 (1996).
- [64] T. Vojta, J. Phys. A **31**, 6595 (1998).
- [65] H. Hinrichsen, E. Domany and D. Stauffer, J. Stat. Phys. **91**, 807-814 (1998).
- [66] H. Hinrichsen and E. Domany, Phys. Rev. E **56**, 94 (1997).
- [67] E. Ising, Z. Phys. **31**, 253 (1925).
- [68] L. Onsager, Phys. Rev. **65**, 117 (1944).
- [69] For a review see M. Henkel, *Conformal Invariance and Critical Phenomena*, Springer 1999.
- [70] M. Suzuki, Prog. Theor. Phys. **46**, 1337 (1971).
- [71] E. Frdakin and L. Susskind, Phys. Rev. D **17**, 2637 (1978).
- [72] I. J. Alonso and M. A. Munoz, Eur. Phys. Lett. **56**, 485 (2001).
- [73] K. Kawasaki, Phys. Rev. **145**, 224 (1966).
- [74] W. Zwerger, Phys. Lett. A **84**, 269 (1981).
- [75] S. J. Cornell K. Kaski and R. B. Stinchcomb, Phys. Rev. B **44**, 12263 (1991).
- [76] B. Zheng, Int. J. Mod. Phys. **12** 1419 (1998).
- [77] D. Stauffer, Int. J. Mod. Phys. C **7**, 753 (1996).
- [78] B. Zheng, Phys. Lett. A **277**, 257 (2000); *ibid.* A **282**

- 132 (2001).
- [79] A. Jaster, J. Mainville, L. Schuelke, B. Zheng, J. Phys. A: Math. Gen. **32**, 1395 (1999).
- [80] S. Tang and D. P. Landau, Phys. Rev. B **36**, 567 (1987).
- [81] Z. Rácz, in *Nonequilibrium Statistical Mechanics in one Dimension*, Ed. by V. Privman (Cambridge University Press, 1996) *Kinetic Ising models with competing dynamics: Mappings, correlations, steady states and phase transitions*.
- [82] Grinstein G, Jayaprakash C, and Yu He, Phys. Rev. Lett. **55**, 2527 (1985),
- [83] K. E. Bassler and B. Schmittman, Phys. Rev. Lett. **73**, 3343 (1994).
- [84] U. C. Täuber and Z. Rácz, Phys. Rev. E **55**, 4120 (1997).
- [85] B. Schmittman and R. K. P. Zia, *Phase transitions and Critical Phenomena*, eds. C. Domb and J. L. Lebowitz (Academic Press, New York 1996).
- [86] B. Schmittman and R. K. P. Zia, Phys. Rev. Lett. **66**, 357 (1991).
- [87] B. Schmittman, Europhys. Lett. **24**, 109 (1993).
- [88] K. E. Bassler and Z. Rácz, Phys. Rev. Lett. **73**, 1320 (1994); Phys. Rev. E **52**, R9 (1995).
- [89] M. J. Oliveira, J. Stat. Phys. **66**, 273 (1992).
- [90] C. H. Bennett, G. Grinstein, Phys. Rev. Lett. **55**, 657 (1985).
- [91] J. M. González-Miranda, P. L. Garrido, J. Marro and J. Lebowitz, Phys. Rev. Lett. **59**, 1934 (1987).
- [92] H. W. J. Blöte, J. R. Heringa, A. Hoogland and R. K. P. Zia, J. Phys. A **23**, 3799 (1990).
- [93] M. J. Oliveira, J. F. F. Mendes, M. A. Santos, J. Phys. A **26**, 2317 (1993).
- [94] M. C. Marques, J. Phys. A **22**, 4493 (1989).
- [95] M. C. Marques, Phys. Lett. A **145**, 379 (1990).
- [96] T. Tomé, M. J. Oliveira and M. A. Santos, J. Phys. A **24**, 3677 (1991),
- [97] H. W. J. Blöte, J. R. Heringa, A. Hoogland and R. K. P. Zia, Int. J. Mod. Phys. B **5**, 685 (1990).
- [98] P. Tamayo, F. J. Alexander and R. Gupta, Phys. Rev. E **50**, 3474 (1995)
- [99] P. L. Garrido, J. Marro and J. M. Gonzalez-Miranda, Phys. Rev. A **40**, 5802 (1989).
- [100] M. A. Santos and S. Teixeira, J. Stat. Phys. **78**, 963 (1995)
- [101] J. M. Drouffe and C. Godréche, J. Phys. A **32**, 249 (1999).
- [102] I. Dornic, H. Chaté, J. Chave and H. Hinrichsen, Phys. Rev. Lett. **87** 045701 (2001).
- [103] A. Achahbar, J. J. Alonoso and M. Munoz, Phys. Rev. E **54**, 4838 (1996).
- [104] A. Lipowski and M. Droz, Phys. Rev. E **65**, 056114 (2002)
- [105] J. Zhuo, S. Redner and H. Park, J. Phys. A **26**, 4197 (1993).
- [106] K. E. Bassler and D. A. Browne, Phys. Rev. E **55**, 5225 (1997).
- [107] K. S. Brown, K. E. Bassler and D. A. Browne, Phys. Rev. E **56**, 3953 (1997).
- [108] K. E. Bassler, Dana A. Browne, J. Phys. A **31**, 6309 (1998).
- [109] H. Park, Mann Ho Kim, and H. Park, Phys. Rev. E **52**, 5664 (1995).
- [110] S. Kwon and H. Park, Phys. Rev. E **52**, 5955 (1995).
- [111] E. Praestraad et al. Europhys. Lett **25** 447 (1994); E. Praestraad, B. Schmittmann and R. K. P. Zia, cond-mat/0010053.
- [112] P. L. Garrido, J. L. Lebowitz, C. Maes and H. Spohn, Phys. Rev. A **42**, 1954 (1990).
- [113] K. Binder, Z. Phys. B **43**, 119 (1981).
- [114] A. Achahbar, Pedro L. Garrido, J. Marro, Miguel A. Munoz, Phys. Rev. Lett. **87**, 195702 (2001).
- [115] J. L. Vallés, J. Marro, J. Stat. Phys. **49**, 89 (1987).
- [116] K.-t. Leung, Phys. Rev. Lett. **66**, 453 (1991).
- [117] R.K.P. Zia, L.B.Shaw and B. Schmittman, Physica A **279**, 60 (2000).
- [118] M. Droz, Z. Rácz and T. Tartaglia, Phys. Rev. A **41**, 6621 (1990).
- [119] A. J. Bray, K. Humayun, and T. J. Newman, Phys. Rev. B **43**, 3699 (1991).
- [120] B. Bergersen and Z. Rácz, Phys. Rev. Lett. **67**, 3047 (1991).
- [121] R. B. Potts, Proc. Camb. Phil. Soc. **48**, 106 (1952).
- [122] F. Y. Wu, Rev. Mod. Phys. **54**, 235 (1982).
- [123] S. F. Edwards and P. W. Anderson, J. Phys. F **5**, 965 (1975).
- [124] R. J. Baxter, *Exactly Solved Models in Statistical Mechanics*, Academic, London, 1982.
- [125] R. de Silva, N. A. Alves and J. R. D. de Felicio, Physics Lett. A **298**, 325 (2002).
- [126] B. Derrida, V. Hakim and V. Pasquier, Phys. Rev. Lett. **75**, 751 (1995).
- [127] G. I. Menon and P. Ray, J. Phys. A **34**, L735 (2001).
- [128] A. J. Bray, B. Derrida and C. Godreche, Euro. Phys. Lett. **27**, 175 (1994).
- [129] A. Gopinathan, cond-mat/0111068.
- [130] Z. Glumac and K. Uzelac, Phys. Rev. E **58** 4372 (1998).
- [131] A. Brunstein and T. Tomé, Physica A **257**, 334 (1998).
- [132] A. Crisanti and P. Grassberger, J. Phys. A **27**, 6955 (1994).
- [133] G. Szabó and T. Czárán, Phys. Rev. E **50**, 061904 (2001).
- [134] L. da Silva, F. A. Tamarit and A. C. N. Magalhães, J. Phys. A **30**, 2329 (1997).
- [135] J. M. Kosterlitz and D. J. Thouless, J. Phys. C **6**, 1181 (1973).
- [136] C. Itzykson and J. M. Drouffe, *Statistical Field Theory*, Camb. U. Press, Cambridge 1989.
- [137] R. Guida and J. Zinn-Justin, cond-mat/9803240.
- [138] T. H. Berlin and M. Kac, Phys. Rev. **86**, 821 (1952); H. E. Stanley, Phys. Rev. **176**, 718 (1968).
- [139] A. Pelissetto, E. Vicari, cond-mat/0012164.
- [140] H. P. Ying, B. Zheng, Y. Yu and S. Trimper, Phys. Rev. E **63**, R35101 (2001)
- [141] K. E. Bassler and Z. Rácz, Phys. Rev. Lett. **73**, 1320 (1994).
- [142] T. Vicsek, A. Czirók, E. Ben-Jacob, I. Cohen and O. Shochet, Phys. Rev. Lett. **75**, 1226 (1995).
- [143] Y. Tu and J. Toner, Phys. Rev. Lett. **75**, 4326 (1995).
- [144] A. Czirók, H.E. Stanley and T. Vicsek, J. Phys. A **30**, 1375 (1997).
- [145] A. Czirók, A. Barabási and T. Vicsek, Phys. Rev. Lett. **82**, 209 (1999).
- [146] S. G. Gorishny, S. A. Larin and F.V. Tkachov, Phys. Lett. **101A**, 120 (1984).
- [147] J. Berges, N. Tetradis, C. Wetterich, hep-ph/0005122, to appear in Physics Reports
- [148] M. Hasenbuch, cond-mat/0010463.
- [149] K. Oerding, S. J. Cornell and A.J.Bray, Phys. Rev. E

- 56**, R25 (1997).
- [150] U. C. Täuber, J. E. Santos and Z. Rácz, *cond-mat/9807207*.
 - [151] M. R. Evans, D. P. Foster, C. Godrèche and D. Mukamel, *Phys. Rev. Lett.* **74**, 208 (1995).
 - [152] A. B. Kolomeisky, G. M. Schütz, E. B. Kolomeisky and J. P. Starley, *J. Phys. A* **31**, 6911 (1998).
 - [153] M. R. Evans, Y. Kafri, H. M. Koduvely and D. Mukamel, *Phys. Rev. E* **58**, 2764 (1998).
 - [154] M. R. Evans, *Braz. J. Phys.* **30**, 42 (2000).
 - [155] B. Chopard and M. Droz, *Cellular Automaton Modelling of Physical Systems*, Cambridge Univ. Press, Cambridge 1998.
 - [156] A. Bunde and S. Havlin, *Fractals and disordered systems*, eds. A. Bunde and S. Havlin, Springer Verlag, Heidelberg 1991.
 - [157] J. Benzonzi and J. L. Cardy, *J. Phys. A* **17**, 179 (1984).
 - [158] P. Grassberger, in *Fractals in physics*, eds. L. Pietronero and E. Tosatti (Elsevier, 1986).
 - [159] M. C. Marques and A. L. Ferreira, *J. Phys. A* **27**, 3389 (1994).
 - [160] H. K. Janssen, K. Oerding, F. van Wijland and H. Hilhorst, *Eur. Phys. J. B* **7**, 137 (1999).
 - [161] H. Hinrichsen and M. Howard, *Eur. Phys. J. B* **7**, 635 (1999).
 - [162] G. Zumofen and J. Klafter, *Phys. Rev. E* **50**, 5119 (1994).
 - [163] K. Oerding, *J. Phys. A* **29**, 7051 (1996).
 - [164] M. W. Deem and J.-M. Park, *Phys. Rev. E* **57**, 2681 (1998); *ibid.* 3618.
 - [165] H. Hinrichsen and G. Ódor, *Phys. Rev. E* **58**, 311 (1998).
 - [166] A. B. Harris, *J. Phys. C* **7**, 1671 (1974).
 - [167] A. J. Noest, *Phys. Rev. Lett.* **57**, 90 (1986); A. J. Noest, *Phys. Rev. B* **38**, 2715 (1988).
 - [168] H. K. Janssen, *Phys. Rev. E* **55**, 6253 (1997).
 - [169] A. G. Moreira and R. Dickman, *Phys. Rev. E* **54**, R3090 (1996).
 - [170] I. Webman, D. ben Avraham, A. Cohen, and S. Havlin, *Phil. Mag. B* **77**, 1401 (1998).
 - [171] R. Cafiero, A. Gabrielli, and M. A. Muñoz, *Phys. Rev. E* **57**, 5060 (1998).
 - [172] J. Hooyberghs, F. Iglói and C. Vanderzande, *cond-mat/0203610*.
 - [173] *Phys. Rev. Lett.* **77**, 4988 (1996).
 - [174] S. V. Buldyrev, A. L. Barabási, F. Caserta, S. Havlin, H. E. Stanley, and T. Vicsek, *Phys. Rev. A* **45**, R8313 (1992).
 - [175] F. Family and T. Vicsek, *J. Phys. A* **18**, L75 (1985).
 - [176] A.-L. Barabási and H. E. Stanley, *Fractal Concepts in Surface Growth*, Cambridge University Press, Cambridge, (1995)
 - [177] J. Krug, *Adv. Phys.* **46**, 139 (1997).
 - [178] J. Krug, *Phys. Rev. Lett.* **72**, 2907 (1994).
 - [179] M. Schroeder, *et. al.*, *Europhys. Lett.* **24**, 563 (1993).
 - [180] J.M. López and M.A. Rodríguez, *Phys. Rev. E* **54**, R2189 (1996).
 - [181] S. Das Sarma, *et. al.*, *Phys. Rev. E* **53**, 359 (1996).
 - [182] C. Dasgupta, S. Das Sarma and J.M. Kim, *Phys. Rev. E* **54**, R4552 (1996).
 - [183] J.M. López and M.A. Rodríguez, *J. Phys. I* **7**, 1191 (1997).
 - [184] M. Castro, *et. al.* *Phys. Rev. E* **57**, R2491 (1998).
 - [185] H.-Yang, G.-C. Wang and T.-M. Lu, *Phys. Rev. Lett.* **73**, 2348 (1994).
 - [186] J.H. Jeffries, J.-K. Zuo and M.M. Craig, *Phys. Rev. Lett.* **76**, 4931 (1996).
 - [187] J.M. López and J. Schmittbuhl, *Phys. Rev. E* **57**, 6405 (1998).
 - [188] S. Morel *et. al.*, *Phys. Rev. E* **58**, 6999 (1998).
 - [189] A. Bru *et. al.* *Phys. Rev. Lett.* , 1998
 - [190] J. A. Sales, M. L. Martins and J. G. Moreira, *Physica A* **245**, 461 (1997).
 - [191] R. Dickman and M. A. Munoz, *Phys. Rev. E* **62**, 7631 (2000).
 - [192] J. D. Noh, H. Park, D. Kim and M. den Nijs, *Phys. Rev. E* **64**, 046131 (2001).
 - [193] S. F. Edwards and D. R. Wilkinson, *Proc. R. Soc.* **381**, 17 (1982).
 - [194] H. Kim, K. Park and I. Kim, *Phys. Rev. E* **65**, 017104 (2001).
 - [195] T. Nattermann, S. Stepanow, L.-H. Tang and H. Leschhorn, *J. Phys. II* **2**, 1483 (1992); H. Leschhorn T. Nattermann, S. Stepanow and L.-H. Tang, *Ann. Phys.* **7**, 1 (1997).
 - [196] O. Narayan and D. S. Fisher, *Phys. Rev. B* **48**, 7030 (1993).
 - [197] M. Kardar, G. Parisi and Y.C. Zhang, *Phys. Rev. Lett.* **56**, 889 (1986).
 - [198] T. Halpin-Healy, *Phys. Rev. A* **42**, 711 (1990).
 - [199] M. Lässig, *Nucl. Phys. B* **559**, (1995); M. Lässig and H. Kinzelbach, *Phys. Rev. Lett* **78**, 906 (1997).
 - [200] K. Moser, D. E. Wolf and J. Kertész, *Physica A* **178**, 215 (1991).
 - [201] J.M. Kim and J.M. Kosterlitz, *Phys. Rev. Lett.* **62**, 2289 (1989); D.E. Wolf and J. Kertész, *Europhys. Lett.* **4**, 651 (1987); L.H. Tang, B.M. Forrest, and D.E. Wolf, *Phys. Rev. A* **45**, 7162 (1992); T. Ala-Nissila, T. Hjelt, J.M. Kosterlitz, and O. Venäläinen, *J. Stat. Phys.* **72**, 207 (1993).
 - [202] E. Marinari, A. Pagnani, and G. Parisi, *J. Phys. A* **33**, 8181 (2000).
 - [203] C. Castellano, M. Marsili, and L. Pietronero, *Phys. Rev. Lett.* **80**, 3527 (1998); C. Castellano, A. Gabrielli, M. Marsili, M.A. Munoz, and L. Pietronero, *Phys. Rev. E* **58**, R5209 (1998); C. Castellano, M. Marsili, M.A. Munoz, and L. Pietronero, *Phys. Rev. E* **59**, 6460 (1999).
 - [204] Y. Tu, *Phys. Rev. Lett.* **73**, 3109 (1994).
 - [205] E. Marinari, A. Pagnani G. Parisi and Z. Rácz, *Phys. Rev. E* **65**, 026136 (2002).
 - [206] H. Leschhorn, *Phys. Rev. E* **54**, 1313 (1996).
 - [207] S. V. Buldrev, S. Havlin and H. E. Stanley, *Physica A* **200**, 200 (1993)
 - [208] L. Tang and H. Leschhorn, *Phys. Rev. A* **45**, R8309 (1992).
 - [209] A. L. Barabási, G. Grinstein and M. A. Munoz, *Phys. Rev. Lett* **76**, 1481 (1996).
 - [210] W. Kinzel, in *Percolation Structures and Processes*, ed. G. Deutscher, R. Zallen, and J. Adler, *Ann. Isr. Phys. Soc.* **5** (Hilger, Bristol, 1983).
 - [211] H. K. Janssen, *Z. Phys. B* **42**, 151 (1981); P. Grassberger, *Z. Phys. B* **47**, 365 (1982); G. Grinstein, Z.-W. Lai and D. A. Browne, *Phys. Rev. A* **40**, 4820 (1989).
 - [212] H. Hinrichsen, *Braz. J. Phys.* **30**, 69-82 (2000).
 - [213] H. Takayasu and A. Yu. Tretyakov, *Phys. Rev. Lett.* **68**, 3060, (1992).
 - [214] I. Jensen, *Phys. Rev. E* **50**, 3623 (1994).

- [215] J. L. Cardy and U. C. Täuber, Phys. Rev. Lett. **77**, 4780 (1996); J. L. Cardy and U. C. Täuber, J. Stat. Phys. **90**, 1 (1998).
- [216] P. Grassberger, F. Krause and T. von der Twer, J. Phys. A:Math.Gen., **17**, L105 (1984).
- [217] N. Menyhárd, J.Phys.A **27**, 6139 (1994).
- [218] N. Menyhárd and G. Ódor, J.Phys.A **29**, 7739 (1996).
- [219] M. H. Kim and H. Park, Phys. Rev. Lett. **73**, 2579, (1994).
- [220] K. E. Bassler and D. A. Browne, Phys. Rev. Lett. **77**, 4094 (1996).
- [221] H. Hinrichsen, Phys. Rev. **E 55**, 219 (1997).
- [222] I. Jensen, J. Phys. A, **30**, 8471 (1997).
- [223] G. Ódor, Phys. Rev. E **63**, 021113 (2001).
- [224] G. Ódor, Phys. Rev E **65** 026121 (2002).
- [225] J. Hooyberghs, E. Carlon and C. Vanderzande, Phys. Rev. E **64**, 036124 (2001).
- [226] J. W. Essam, J. Phys. A **22**, 4927 (1989).
- [227] E. Domany, W. Kinzel, Phys. Rev. Lett. **53**, 311 (1984).
- [228] J. W. Essam and D. TanlaKishani, J. Phys. A **27**, 3743 (1994).
- [229] J. W. Essam and A. J. Guttmann, J. Phys. A **28**, 3591 (1995).
- [230] M. Rossi, R. Pastor-Satorras and A. Vespagnani, Phys. Rev. Lett. **85**, 1803 (2000).
- [231] M. A. Munoz, R. Dickman, A. Vespagnani and S. Zapperi, Phys. Rev. **59**, 6175 (1999).
- [232] R. Pastor-Satorras and A. Vespagnani, Phys. Rev. E **62**, 5875 (2000).
- [233] H. J. Jensen, *Self-Organized Criticality*, Cambridge Univ. Press, Cambridge England 1998.
- [234] S. S. Manna, J. Phys. A **24**, L363 (1991), D. Dhar, Physica A **263**, 4 (1999).
- [235] R. Dickman, A. Vespagnani and S. Zapperi, Phys. Rev. E **57**, 5095 (1998).
- [236] M. A. Muñoz, R. Dickman, R. P-Satorras, A. Vespagnani and S. Zapperi, in *Modeling Complex Systems, Proceedings of the 6th Granada Seminar on Computational Physics*, eds. J. Marro and P. L. Garrido, AIP Conference Proceedings, v. 574 (2001).
- [237] M. Alava and M. A. Munoz, Phys. Rev. E **65**, 026145 (2001).
- [238] R. Dickman, M. Alava, M. A. Munoz, J. Peltola, A. Vespagnani, S. Zapperi, Phys. Rev. E **64** 056104 (2001).
- [239] J. Kockelkoren and H. Chaté, cond-mat/0306039.
- [240] T. Halpin-Healy and Y.-C. Zhang, Phys. Rep. **254**, 215 (1995).
- [241] M. Marsili, J. Stat. Phys. **77**, 733 (1994).
- [242] S. Lübeck and A. Hucht, J. Phys. A **35**, 4853 (2002).
- [243] S. Lübeck, Phys. Rev. E **64** 016123 (2001); Phys. Rev. E **65** 046150 (2002);
- [244] R. Dickman, T. Tomé and M. J. de Oliveira, cond-mat/0203565.
- [245] R. Dickman, cond-mat/0204608.
- [246] P. Grassberger, Z. Phys. B **47**, 365 (1982).
- [247] M. J. Howard and U. C. Täuber, J. Phys. A **30**, 7721 (1997).
- [248] G. Ódor, Phys. Rev. E **62**, R3027 (2000).
- [249] E. Carlon, M. Henkel and U. Schollwöck, Phys. Rev. E **63**, 036101-1 (2001).
- [250] H. Hinrichsen, Phys. Rev. E **63**, 036102-1 (2001).
- [251] G. Ódor, Phys. Rev. E **63**, 067104 (2001).
- [252] H. Hinrichsen, Physica A **291**, 275 (2001).
- [253] M. Henkel and H. Hinrichsen, J. Phys. A **34**, 1561 (2001).
- [254] K. Park, H. Hinrichsen, and In-mook Kim, Phys. Rev. E **63**, 065103(R) (2001).
- [255] G. Ódor, Phys. Rev E **67**, 016111 (2003).
- [256] K. Park and I. Kim, Phys. Rev E **66**, 027106 (2002).
- [257] R. Dickman and M. A. F. de Meneses, Phys. Rev. E **66**, 045101 (2002).
- [258] H. Hinrichsen, cond-mat/0208345.
- [259] M.C. Marques and J.F.Mendes, Eur. Phys. B **12**, 123 (1999).
- [260] H. S. Park and H. Park, J. of Korean Phys. Soc. **38**, 494 (2001).
- [261] R. Kree, B. Schaub and B. Schmitmann, Phys. Rev. A **39**, 2214 (1989).
- [262] F. van Wijland, K. Oerding and H. J. Hilhorst, Physica A **251**, 179 (1998).
- [263] J. E. de Freitas, L. S. Lucena, L. R. da Silva and H. J. Hilhorst, Phys. Rev. E **61**, 6330 (2000).
- [264] U. L. Fulco, D. N. Messias and M. L. Lyra, Phys. Rev. E **63**, 066118 (2001).
- [265] K. Oerding, F. van Wijland, J.P. Leroy and H. J. Hilhorst, J. Stat. Phys. **99**, 1365 (2000).
- [266] S. Kwon, J. Lee and H. Park, Phys. Rev. Lett. **85**, 1682 (2000).
- [267] G. Ódor, Phys. Rev. E **63**, 056108 (2001).
- [268] H. S. Park and H. Park, J. of Korean Phys. Soc. **38**, 494 (2001).
- [269] S. Park, D. Kim and J. Park, Phys. Rev. E **62**, 7642 (2000).
- [270] F. Wijland, Phys. Rev. E **63**, 022101 (2001)
- [271] P. L. Krapivsky and E. Ben-Naim, Phys. Rev. E **56**, 3788 (1997).
- [272] D. ben-Avraham, M. A. Burschka and C.R. Doring, J. Stat. Phys. **60**, 695 (1990).
- [273] S. R. Broadbent and J. M. Hammersley, Proc. Camb. Phil. Soc. **53**, 629 (1957).
- [274] I. Jensen and R. Dickman, Phys. Rev. E **48**, 1710 (1993).
- [275] J. F. F. Mendes, R. Dickman, M. Henkel and M. C. Marques, J. Phys. A **27**, 3019 (1994).
- [276] H. Park and H. Park, Physica A **221**, 97 (1995).
- [277] K. B. Lauritsen, P. Fröjd, and M. Howard, Phys. Rev. Lett. **81**, (1998).
- [278] P. Fröjd, M. Howard, K. B. Lauritsen, Int. J. Mod. Phys. B **15**, 1761 (2001).
- [279] N. Menyhárd and G. Ódor, J. Phys. A. **29**, 7739 (1996).
- [280] G. Ódor, A. Krikelis, G. Vesztergombi and F. Rohrbach: Proceedings of the 7-th Euromicro workshop on parallel and distributed process Funchal (Portugal) Feb. 3-5 1999, IEEE Computer society press, Los Alamitos, ed.: B. Werner; e-print: physics/9909054
- [281] G. Ódor and N. Menyhárd, Phys. Rev. E **57**, 5168 (1998).
- [282] H. K. Janssen, Z. Phys. B **23**, 377 (1976).
- [283] J. L. Cardy and R. L. Sugar, J. Phys. A **13**, L423 (1980).
- [284] H. D. I. Abarbanel, J. B. Bronzan, R. L. Sugar and A. R. White, Phys. Rep. **21**, 119 (1975); R. Brower, M. A. Furman and M. Moshe, Phys. Lett. B **76**, 213 (1978).
- [285] P. Grassberger and A. de la Torre, Ann. Phys. **122**, 373 (1979).
- [286] E. Ben-Naim and P. L. Krapivsky, J. Phys. A **27**, L481 (1994).

- [287] G. Ódor, Phys. Rev. E **51**, 6261 (1995).
- [288] R. Dickman, Phys. Rev. E **50**, 4404 (1994).
- [289] H. Hinrichsen and H. M. Koduvely, Eur. Phys. J. B **5**, 257 (1998).
- [290] K. Oerding and F. van Wijland, J. Phys. A **31**, 7011 (1998).
- [291] I. Jensen, J. Phys. A **32**, 5233 (1999).
- [292] C. A. Voigt and R. M. Ziff, Phys. Rev. E **56**, R6241 (1997).
- [293] I. Jensen, Phys. Rev. E **45**, R563 (1992).
- [294] J. B. Bronzan and J. W. Dash, Phys. Lett. B **51**, 496 (1974).
- [295] P. Grassberger, J. Phys. A **22**, 3673 (1989).
- [296] P. Grassberger, J. Phys. A **25**, 5867 (1992).
- [297] R. Dickman and I. Jensen, Phys. Rev. Lett. **67**, 2391 (1991).
- [298] K. De'Bell and J. W. Essam, J. Phys. A **16**, 385 (1983). J. W. Essam, A. Guttmann and K. De'Bell, *ibid.* **21**, 3815 (1988). I. Jensen and R. Dickman, J. Stat. Phys. **71**, 89 (1993); I. Jensen, Phys. Rev. Lett. **77**, 4988 (1996); I. Jensen and R. Dickman, J. Phys. A **26**, L151 (1993). I. Jensen and A. J. Guttmann, *ibid.* **28**, 4813 (1995). I. Jensen and A. J. Guttmann, Nucl. Phys. B **47**, 835 (1996).
- [299] T. E. Harris, *Ann. Prob.* **2**, 969 (1974); P. Grassberger and A. de la Torre, *Ann. Phys. (NY)* **122**, 373 (1979).
- [300] R. Dickman and J. K. de Silva, Phys. Rev. E **58**, 4266 (1998).
- [301] N. Boccara and M. Roger, in *Instabilities and Nonequilibrium Structures IV*, edited by E. Tirapegui and W. Zeller (Kluwer Academic, Dordrecht, 1993), p. 109.
- [302] S. Wolfram, Rev. Mod. Phys. **55**, 601 (1983).
- [303] G. Ódor et al, CERN-OPEN-97-034.
- [304] G. Szabó and G. Ódor, Phys. Rev. E **49**, 2764 (1994).
- [305] K. Eloranta and E. Nummelin, J. Stat. Phys. **69**, 1131 (1992).
- [306] R. Bidaux, N. Boccara, H. Chate, Phys. Rev. A **39**, 3094 (1989).
- [307] I. Jensen, Phys. Rev. A **43**, 3187 (1991).
- [308] Y. Hieida, J. Phys. Soc. Jpn. **67**, 369 (1998); E. Carlon, M. Henkel, and U. Schollwöck, Euro. Phys. J. B **12**, 99 (1999);
- [309] E. Frey, U. C. Täuber and F. Schwabl, Phys. Rev. E **49**, 5058 (1993).
- [310] P. Fröjdh and M. den Nijs, Phys. Rev. Lett. **78**, 1850 (1997).
- [311] V. Brunel, K. Oerding and F. van Wijland, J. Phys. A **33**, 1085 (2000).
- [312] O. Deloubrière and F. van Wijland, Phys. Rev. E **65**, 046104 (2002).
- [313] G. Ódor and N. Menyhard, cond-mat/0109399, Physica D **168**, 305 (2002).
- [314] I. Jensen, Phys. Rev. E **47**, R1 (1993).
- [315] F. Iglói, I. Peschel, and L. Turban, Adv. Phys. **42**, 683 (1993).
- [316] J. L. Cardy, J. Phys. A **16**, 3617 (1983).
- [317] J. W. Essam, A. J. Guttmann, I. Jensen and D. Talla-Kishani, J. Phys. A **29**, 1619 (1996).
- [318] K. B. Lauritsen, K. Sneppen K, M. Markošová and M. H. Jensen M H, Physica A **247**, 1 (1997).
- [319] H. K. Janssen, B. Schaub and B. Schmittmann, Z. Phys. B **72**, 111 (1988).
- [320] I. Jensen, J. Phys. A **32**, 6055 (1999).
- [321] P. Fröjdh, M. Howard, and K. B. Lauritsen, J. Phys. A **31**, 2311 (1998).
- [322] M. Howard, P. Fröjdh, and K. B. Lauritsen, Phys. Rev. E **61**, 167 (2000).
- [323] E. V. Albano, Phys. Rev. E **55**, 7144 (1997).
- [324] C. Kaiser and L. Turban, J. Phys. A **27**, L579 (1994); C. Kaiser and L. Turban, J. Phys. A **28**, 351 (1995).
- [325] P. Grassberger, H. Chaté and G. Rousseau, Phys. Rev. E **55**, 2488 (1997).
- [326] D. Mollison, J. R. Stat. Soc. B **39**, 238 (1977).
- [327] P. Grassberger, Math. Biosci. **63**, 157 (1982).
- [328] J. L. Cardy, J. Phys. A **16**, L709 (1983).
- [329] J. L. Cardy and P. Grassberger, J. Phys. A **18**, L267 (1985).
- [330] H. K. Janssen, Z. Phys. B **58**, 311 (1985).
- [331] M. A. Munoz, R. Dickman, G. Grinstein and R. Livi, Phys. Rev. Lett. **76**, 451 (1996).
- [332] M. A. Munoz, G. Grinstein and R. Dickman, J. Stat. Phys. **91**, 541 (1998).
- [333] F. van Wijland, Phys. Rev. Lett. **89**, 190602 (2002).
- [334] A. J.-Dalmaroni, H. Hinrichsen, cond-mat/0304113.
- [335] G. Ódor, J. F. Mendes, M. A. Santos and M. C. Marques, Phys. Rev. E **58**, 7020 (1998).
- [336] M. C. Marques, M. A. Santos and J. F. Mendes, Phys. Rev. E **65**, 016111 (2001).
- [337] M. A. Munoz, G. A. da S. Santos and M. A. Santos, cond-mat/0202244.
- [338] C. López and M. A. Muñoz, Phys. Rev. E **56**, 4864 (1997).
- [339] R. Dickman and J. Kamphorst Leal da Silva, Phys. Rev. E **58**, 4266 (1998).
- [340] R. Dickman, cond-mat/9909347
- [341] R. Dickman, W. R. M. Rabelo and G. Ódor, Phys. Rev. E **65**, 016118 (2001).
- [342] J. Kamphorst Leal da Silva and R. Dickman, Phys. Rev. E **60**, 5126 (1999).
- [343] M. A. Munoz, R. Dickman, A. Vespignani and S. Zapperi, Phys. Rev. E **59**, 6175 (1999).
- [344] H. Drossel and F. Schwabl, Physica A **199**, 183 (1993).
- [345] T. Antal, M. Droz, A. Lipowski and G. Ódor, Phys. Rev. E **64**, 036118 (2001).
- [346] P. Grassberger, J. Phys. A **25**, 5867 (1992).
- [347] R. Dickman and A. Yu. Tretyakov, Phys. Rev. E **52**, 3218 (1995).
- [348] R. Durrett, *Lecture Notes on Particle Systems and Percolation*, (Wadsworth, Pacific Grove, CA 1988).
- [349] M. Scheucher and H. Spohn, J. Stat. Phys. **53**, 279 (1988).
- [350] P. L. Krapivsky, Phys. Rev. A **45**, 1067 (1992); L. Frachebourg and P. L. Krapivsky, Phys. Rev. E **53**, R 3009 (1996).
- [351] H. K. Janssen, J Stat. Phys. **103**, 801 (2001).
- [352] K. Park, H. Hinrichsen and I. Kim, Phys. Rev. E **66**, 025101 (2002).
- [353] J. Kockelkoren and H. Chaté, Phys. Rev. Lett. **90**, 125701 (2003).
- [354] G. Ódor, cond-mat/0210615, Phys. Rev. E **67**, 056114 (2003).
- [355] V. Privman, *Nonequilibrium Statistical Mechanics in one Dimension* Cambridge University Press, 1996.
- [356] B. P. Lee, J. Phys. A **27**, 2633 (1994).
- [357] Z. Rácz, Phys. Rev. Lett. **55**, 1707 (1985).
- [358] A. A. Lushnikov, Phys. Lett. A **120**, 135 (1987)

- [359] L. Peliti, J. Phys. A: Math. Gen. **19**, L365 (1986).
- [360] A. A. Ovchinnikov and Ya. B. Zel'dovich, Chem. Phys. **28**, 215 (1978); S. F. Burlatskii and A. A. Ovchinnikov, Russ. J. Phys. Chem. **52**, 1635 (1978); D. Toussaint and F. Wilczek, J. Chem. Phys. **78**, 2642 (1983); K. Kang and S. Redner, Phys. Rev. A **32**, 435 (1985); M. Bramson and J. Lebowitz, Phys. Rev. Lett. **61**, 2397 (1988).
- [361] B. P. Lee and J. Cardy, J. Stat. Phys. **7**, 971 (1995).
- [362] S. J. O'Donoghue and A. J. Bray, Phys. Rev. E **64**, 041105 (2001).
- [363] G. Ódor and N. Menyhárd, Phys. Rev. E **61**, 6404 (2000).
- [364] R. Dickman and D. ben-Avraham, Phys. Rev. E **64**, 020102 (2001).
- [365] P. L. Krapivsky and S. Redner, private communication.
- [366] S. N. Majumdar, D. S. Dean and P. Grassberger, Phys. Rev. Lett. **86**, 2301 (2001).
- [367] O. Deloubrière, H. J. Hilhorst and U. C. Täuber, Phys. Rev. Lett. **89**, 250601 (2002).
- [368] I. Jensen and R. Dickman, Phys. Rev. E **48**, 1710 (1993); I. Jensen, Phys. Rev. Lett. **70**, 1465 (1993).
- [369] U.C. Täuber, M.J. Howard, and H. Hinrichsen, Phys. Rev. Lett. **80**, 2165 (1998);
- [370] A. Lipowski and M. Droz, Phys. Rev. E **64**, 031107 (2001).
- [371] N. Inui, A. Y. Tretyakov and H. Takayasu, J. Phys. A **28**, 1145 (1995).
- [372] K. Park, H. Hinrichsen and I. Kim, Phys. Rev. E **63**, 065103(R) (2001).
- [373] G. Ódor, M.A. Santos, M.C. Marques, Phys. Rev. E **65**, 056113 (2002).
- [374] U. Täuber, private communication.
- [375] G. Ódor, Phys. Rev. E **63**, 056108 (2001).
- [376] H. Park and H. Park, Physica A **221**, 97 (1995).
- [377] W. Hwang, S. Kwon, H. Park, H. Park, Phys. Rev. E **57**, 6438 (1998).
- [378] W. Hwang and H. Park, Phys. Rev. E **59**, 4683 (1999).
- [379] N. Menyhárd and G. Ódor, Brazilian J. of Physics, **30**, 113 (2000).
- [380] K. Mussawisade, J. E. Santos and G. M. Schütz, J. Phys. A **31**, 4381 (1998).
- [381] A. Sudbury, Ann. Prob. **18**, 581 (1990).
- [382] H. Hinrichsen and G. Ódor, Phys. Rev. E **60**, 3842 (1999).
- [383] M. Barma, M. D. Grynberg and R. B. Stinchcomb, Phys. Rev. Lett. **70**, 1033 (1993); M. Barma and D. Dhar, *ibid.* **73**, 2135 (1994).
- [384] P. Grassberger, J. Phys. A **22** L1103, (1989).
- [385] D. Zhong and D. ben Avraham, Phys. Lett. A **209**, 333 (1999).
- [386] A. Lipowski, J. Phys. A **29**, L355, (1996).
- [387] H. K. Janssen, Phys. Rev. Lett. **78**, 2890 (1997).
- [388] D. ben Avraham, F. Leyvraz and S. Redner, Phys. Rev. E **50**, 1843 (1994).
- [389] I. Jensen, J. Phys. A **26**, 3921 (1993).
- [390] A. DeMasi, P. A. Ferrari, J. L. and Lebowitz, Phys. Rev. Lett. **55**, 1947 (1985); J. Stat. Phys. **44**, 589 (1986).
- [391] J. S. Wang and J. L. Lebowitz, J. Stat. Phys. **51**, 893 (1988).
- [392] M. Droz, Z. Rácz and J. Schmidt, Phys. Rev. A **39**, 2141 (1989).
- [393] N. Menyhárd and G. Ódor, Phys. Rev. E **66**, 016127 (2002); cond-mat/0203419.
- [394] A. Lipowski and M. Droz, cond-mat/0110404, Phys. Rev. E **66**, 016106 (2002).
- [395] Grinstein G., Muñoz M.A., and Tu Y., Phys. Rev. Lett. **76**, 4376 (1996); Tu Y., Grinstein G., and Muñoz M.A. Phys. Rev. Lett. **78**, 274 (1997).
- [396] P. Bak, C. Tang and K. Wiesenfeld, Phys. Rev. Lett. **59**, 381 (1987).
- [397] S. N. Majumdar, S. Krishnamurthy, and M. Barma, Phys. Rev. Lett. **81**, 3691 (1998).
- [398] S. N. Majumdar, S. Krishnamurthy, and M. Barma, J. Stat. Phys. **99**, 1 (2000).
- [399] H. Takayasu, I. Nishikawa and H. Tasaki, Phys. Rev. A **37**, 3110 (1988); M. Takayasu and H. Takayasu in *Nonequilibrium Statistical Mechanics in One Dimension* ed. V. Privman (Cambridge Univ. Press, Cambridge, 1997).
- [400] S. N. Majumdar, S. Krishnamurthy, and M. Barma, Phys. Rev. E **61**, 6337 (2000).
- [401] R. Rajesh and S. N. Majumdar, Phys. Rev. E **63**, 036114 (2001).
- [402] U. C. Täuber, M. J. Howard, and H. Hinrichsen, Phys. Rev. Lett. **80**, 2165 (1998).
- [403] Y. Y. Goldschmidt, H. Hinrichsen, M. Howard, and U. C. Täuber, Phys. Rev. E **59**, 6381 (1999).
- [404] U. Alon, M. Evans, H. Hinrichsen, and D. Mukamel, Phys. Rev. E **57**, 4997 (1998).
- [405] U. Alon, M. Evans, H. Hinrichsen, and D. Mukamel, Phys. Rev. Lett. **76**, 2746 (1996).
- [406] H. Hinrichsen, and D. Mukamel, Phys. Rev. E **67**, 016110 (2003).
- [407] Y. Y. Goldschmidt, Phys. Rev. Lett. **81**, 2178 (1998).
- [408] J. Kertész and D. E. Wolf, Phys. Rev. Lett. **62**, 2571 (1989).
- [409] C. Lehner, N. Rajewsky, D. Wolf, and J. Kertész, Physica A **164**, 81 (1990).
- [410] A. Toom, J. Stat. Phys. **74**, 91 (1994); A. Toom, J. Stat. Phys. **74**, 111 (1994).
- [411] H. Hinrichsen and G. Ódor, Phys. Rev. Lett. **82**, 1205 (1999).
- [412] J. D. Noh, H. Park, M. den Nijs, Phys. Rev. Lett. **84**, 3891 (2000).
- [413] Z. Rácz, *Nonequilibrium Phase Transitions*, Lecture Notes, Les Houches, July 2002, cond-mat/0210435.
- [414] J. Cardy, *Renormalisation group theory of branching pots interfaces*, eprint cond-mat/9806098.